Abstract

Di Wu. THE SIGNIFICANCE OF MIRNA PATHWAY IN PERIPHERAL NERVE REGENERATION FOLLOWING SCIATIC NERVE INJURY (under the direction of Dr. Alexander Murashov) Department of Physiology,

microRNAs (miRNAs) are small (21-23 nucleotides) single-stranded RNAs that play important roles in post-transcriptional regulation of gene expression. The binding of miRNA to its specific target mRNAs at 3' UTR causes either degradation of the mRNAs or inhibition of protein translation. Increasing evidence suggests that miRNA participate in the regulation of almost every cellular process investigated and changes of their expressions are observed in human pathologies. In neurons, the functions of miRNA pathway are just beginning to emerge. Recent studies have elucidated that miRNAs are dysregulated in neurological disorders and that they serve important roles in neural development. Subcellular localization of miRNA and miRNA machinery has also been identified in axons, which suggests its involvement in axonal functions. In the current study, we tested the hypothesis that miRNA pathway is involved in the post-transcriptional regulation of gene expression in sciatic nerve after injury, and that it plays a critical role for peripheral nerve regeneration. We performed sciatic nerve crush as our injury model on adult mice. A corresponding injury-regulated expression of miRNA machinery, including components of RNA induced silencing complex (RISC) and Processing bodies (P-bodies) were observed in both western blot analysis and immuofluorescent staining. Microarray analysis followed by RT-qPCR confirmation revealed a group of miRNAs following injury-regulated expression patterns as well. The physiological importance of miRNA pathway in peripheral nerve regeneration was evaluated in inducible Dicer knockout mice. Blocking Dicer-dependent miRNA biogenesis significantly delayed peripheral nerve regeneration in behavioral

tests, electrophysiological studies, and histological evaluations. The detrimental effect of Dicer ablation on regenerative axon growth was also shown in dissociated dorsal root ganglion (DRG) neurons. A significant decrease in axon length and arborization was observed in vitro. To find the specific miRNAs involved in mediating axon growth, 19 miRNAs differentially expressed after nerve injury were identified with miRNA array analyses. Functional analysis for injury-induced miRNAs has shown that miR-431 promoted axon growth in DRG neurons. Bioinformatics prediction followed by experimental approaches proved *Kremen1* as a target gene for miR-431. A negative correlation between miR-431 and *Kremen1* expression was confirmed at both mRNA and protein levels. Since *Kremen1* inhibits the Wnt signaling, enhanced axon growth after overexpressing miR-431 might be mediated through Wnt signaling. The findings of this study improve our understanding of the significant role that miRNA pathway plays in regenerative axon growth.

THE SIGNIFICANCE OF THE MIRNA PATHWAY IN PERIPHERAL NERVE REGENERATION FOLLOWING SCIATIC NERVE INJURY

A Dissertation

Presented to

the Faculty of the Department of Physiology

Brody School of Medicine at East Carolina University

In Partial Fulfillment

Of the Requirement for the Degree

Doctor of Philosophy in Physiology

by

Di Wu

May 3rd, 2012

THE SIGNIFICANCE OF MIRNA PATHWAY IN PERIPHERAL NERVE REGENERATION FOLLOWING SCIATIC NERVE INJURY

by

Di Wu

APPROVED BY:

DIRECTOR OF DISSERATION _____

Alexander Murashov, M.D. Ph.D.

COMMITTEE MEMBER _____

Kori Brewer, Ph.D.

COMMITTEE MEMBER _____

Stefan Clemens, Ph.D.

COMMITTEE MEMBER _____

Qun Lu, Ph.D.

COMMITTEE MEMBER _____

Baohong Zhang, Ph.D.

CHAIR OF THE DEPARTMENT OF PHYSIOLOGY _____

Robert M. Lust, Ph.D.

DEAN OF THE GRADUATE SCHOOL_____

Paul J. Gemperline, Ph.D.

I would like to dedicate this work to my wonderful family.

I would not trade your love for anything in this world.

Acknowledgements

I take this opportunity to thank the many people who have made this dissertation possible.

First, I want to express my deepest appreciation to my advisor, Dr. Alexander Murashov, for the continuous support throughout the process of pursuing my Ph.D. degree, for his patience, enthusiasm, encouragement, and faith in my abilities.

Of course this work would not have been possible without the help of my committee. I thank Dr. Kori Brewer for getting me through the orientation in her lab and infecting me with a passion for neurosciences. I also express my gratitude to Dr. Stefan Clemens for his invaluable suggestions, constructive advice, and helping with all the electrophysiological experiments in this study. I appreciate Dr. Qun Lu and Dr. Baohong Zhang for their encouraging words, critiques, and insightful comments at different stages of my research.

I have been especially fortunate to know and work with the faculty in Department of Physiology. I thank each of them for the advice and support they have provided during the past five years. I express my sincere thanks to Dr. Robert Carroll for always having an open door and great advice to share. I also thank Dr. Robert Lust for his constant encouragement and helping me decide the next step in my career. I appreciate Dr. Randall Renegar and Joani Zary for their help in completing experiment in my second specific aim.

I have to thank graduate students of the department. They have provided a congenial atmosphere for scientific thinking and helped me with my presentation skills. I shall always cherish their friendship

Special thanks to the administrative staff of Physiology department: Laura Frye, Crystal Stallings, Cheryl Smith, and Marsha Hall for taking care of all the administrative work.

Lastly, I also gratefully acknowledge the members in Dr. Murashov's lab. I thank Elena Pak for always being encouraging and understanding.

Table of Contents

LIST OF FIGURES

LIST OF TABLES

LIST OF ABBREVIATIONS

AD	Alzheimer's disease
AGO	argonaute protein
ALS	amyotrophic lateral sclerosis
AP-1	activating protein1
APT-1	acyl protein thioesterase 1
Arac	Cytosin β-D-arabinofuranoside
ATF-3	Cyclic AMP-dependent transcription factor 3
BACE1	β-amyloid precursor protein converting enzyme1
BLC2	B-cell lymphoma 2
CAP	compound action potential
CAP-23	cortical cytoskeleton-associated protein 23
CLIP	Cross-Linked Immunoprecipitation
CMAK2	calcium/calmodulin dependent kinase 2
CNS	central nervous system
CREB	cAMP responsive element binding protein
DCP 1/2	decapping protein 1/2
Dkk1	Dickkopf1
DLG2	disks large homolog2
DMEM	Dulbecco's modified Eagle's medium
DRB	5,6-dichlorobenzimidazole riboside
DRG	dorsal root ganglion
dsRNA	double-stranded RNA
eIF	eukaryotic translation initiation factor
ERK	extracellular-signal-regulated kinases

FISH	fluorescent in situ hybridization
FMRP	fragile X mental retardation protein
FXS	fragile X syndrome
GAP	GTPase –activating protein
GAP-43	growth associated protein 43
GWB	GW bodies
HD	Huntington's disease
JNK	c-jun N-terminal kinase
Limk1	LIM domain kinase 1
LRP5/6	Lipoprotein-receptor-related protein 5 and 6
NCV	nerve conduction velocity
NeuroD2	neurogenic differentiation factor 2
NGF	nerve growth factor
MAPK	mitogen-activated protein kinase
miRNA	microRNA
mRNA	messenger RNA
NC	neural crest
P-bodies	mRNA-processing bodies
PD	Parkinson’s disease
Pitx3	pituitary homeobox 3
PKA	protein kinase A
PKC	protein kinase C
PNS	peripheral nervous system
Pre-miRNA	precursor microRNA
Pri-miRNA	primary microRNA

REST	RE1 induced silencing factor
RGC	retinal ganglion cell
RISC	RNA induced silencing complex
RNAi	RNA interference
SCG	superior cervical sympathetic ganglia
SFI	sciatic functional index
SGs	stress granules
siRNA	small interfering RNAs
SMN	survival of motor neurons
SNL	spinal nerve ligation
TRBP	TAR RNA binding protein
Trk	tyrosine kinase receptors

CHAPTER I: Introduction

Peripheral Nerve Injury

Nerve injuries induce severe disability and greatly compromise the quality of life. Injuries to peripheral nerves, occurring in approximately 2.8% of trauma patients, cause partial or total loss of motor, sensory and autonomic functions (Noble et al., 1998). Peripheral nerve injury leads to axon discontinuity and degeneration of myelinated fibers, which may finally result in eventual death of axotomized neurons (Navarro et al., 2007, Schuning et al., 2009). After peripheral nerve injury, the severed axons have the capability to regenerate and recover functional connections. However a number of clinical reports and experimental studies in recent years also indicate that the rate of axonal regeneration is far from satisfactory, especially after severe injuries (Navarro et al., 2007). When the lesion creates a laceration with an associated tissue gap longer than 4 cm, or the injury is left unrepaired, the probability of effective recovery is rare (Krarup et al., 2002, Navarro et al., 2007).

The first detailed description on the repair of transected nerve trunks was recorded by Gabriele Ferrara in the 16th century (Ferrara, 1596). He described applying gentle traction to the retracted nerve stumps, suturing using an alcohol disinfected needle, and finally, insulating the sutured segment with a mixture of oils. The injured limb was later immobilized to prevent damaging the suture (Artico et al., 1996, Ngeow, 2010). The whole procedure closely resembles modern surgical protocol, which includes disinfection, appropriate identification of injured nerve trunk, correct suturing technique, and wound immobilization (Artico et al., 1996, Ngeow, 2010). Over the years, different procedures have been developed to boost intrinsic neuronal growth

properties. Physical therapies, such as treadmill training, resistance training, and swimming help maintain muscle strength, relieve pain and enhance functional recovery (Bonetti et al., 2011). Electrical stimulations have been reported to facilitate rehabilitation after nerve injuries, in rats and human patients. One hour of low-frequency (2 Hz) or 20 Hz electrical stimulation after surgical repair can accelerate axon outgrowth at the site of injury and lead to earlier reinnervation of denervated muscles (Nix and Hopf, 1983, Ahlborn et al., 2007, Gordon et al., 2009b). In animal models, pharmacological elevation of cAMP and overexpression of neuronal growth-associated genes such as GAP-43 or CAP-23 also accelerates axon outgrowth and promotes efficient regeneration (Caroni et al., 1997, Bomze et al., 2001, Cai et al., 2001).

Despite the technological advances and extensive research on nerve regeneration, the functional outcome after nerve injury and repair are generally still insufficient, particularly when sensory functions are considered (Dahlin et al., 2009). The failure of functional recovery after peripheral nerve injuries can be explained by various factors. It can result from the damage to the neuronal cell body due to axotomy and retrograde degeneration (Krarup et al., 2002, Schmidhammer et al., 2007). The success of nerve regeneration and functional reinnervation of targets are based on the capacity of neuron to survive and shift from maintaining structure and supporting synaptic transmission toward a regenerative phenotype. Loss of neuron excludes the possibility of regeneration (Witzel et al., 2005, Navarro et al., 2007). The failure of functional recovery may also stem from the slow rate for axonal growth. At an average rate of 1-3mm/day for axonal regeneration in mammals, weeks or even months would have been anticipated for signs of functional recovery (Gordon et al., 2009a). Moreover, the progressive outgrowth of axons across the surgical repair site is surprisingly slow, probably due to a lack of organization of the extracellular matrix and the supports from Schwann cells (Gordon et al., 2009a). Since

peripheral nerve injuries always involve connective tissue scarring, regenerative attempts over long distance are always impeded by scar tissue (Deumens et al., 2010, Ngeow, 2010). Underlying diseases, such as diabetic generalized neuropathy, may impede axonal regeneration (Stoll and Muller, 1999). The failure of functional recovery may also result from the poor specificity of reinnervation. The selectivity of axon-target reconnection plays an important role in the recovery of function after nerve injury and regeneration. During the process of nerve regeneration, several sprouts emerge from each parent axon (Witzel et al., 2005). When axons reconnect the appropriate peripheral tissue, misdirected axonal sprouts are withdrawn gradually. The pruning of supernumerary axonal sprouts helps refine the selectivity of axon-target reconnection. However, the later refinement of distal reconnection and the reinnervation of targets are often far from adequate. When inappropriate distal reconnection is established, disturbed sensory localization or limited fine motor control are expected to occur (English et al., 2011). Denervation atrophy also contributes to the failure of functional recovery. The progressive elapse of time during the slow regeneration is responsible for relentless atrophy of denervated target tissue (Gordon et al., 2009a). If the denervated skeletal muscles are replaced by adipose tissue, despite the fact that peripheral axons can regenerate through the injury site and reconnect the skeletal muscles, functional recovery is only limited.

Currently, no medical treatment can overcome the limitations in axonal regeneration, and ensure the recovery of normal sensory and motor functions following severe nerve trauma, and it is generally considered that the gold standard treatment by surgical repair has reached a plateau (Navarro et al., 2007). Therefore, new therapeutic intervention strategies for peripheral nerve repair are needed. A fundamental understanding of the multiple mechanisms involved in

successful axon regeneration and appropriate target re-innervation would facilitate the development of potentially therapeutic methods.

Endogenous Mechanisms that Support Peripheral Axon Regeneration

Cellular bases of peripheral nerve regeneration

Nerve injuries are powerful stimuli that lead to profound cellular responses. Following injury, axons and myelin sheaths distal to the lesion site are degraded by a process of Wallerian degeneration (Glass, 2004, Makwana and Raivich, 2005). Myelin breaks down to vesicles, resulting in the collapse of the myelin sheath (Ngeow, 2010). Schwann cell cytoplasm withdraws from the myelin vesicles and significantly decreases the synthesis of myelin lipid and protein between 12 and 48 hours of injury (Ngeow, 2010). Injuries increase the permeability of the blood-nerve barrier, and the increased permeability allows the recruitment of macrophages to the site of the injured nerve. Infiltrating macrophages and injury-activated Schwann cells phagocyte the degenerative end products (Stoll and Muller, 1999). Wallerian degeneration takes place during the first few days. During this stage, elimination of myelin sheaths is important, because it clears the regeneration-inhibitory factors associated with myelin (Skaper, 2005, Raivich and Makwana, 2007). At the same time, degeneration also takes place retrogradely at a short segment of the proximal nerve stump. The remaining axons in the proximal nerve also exhibit a reduction in diameter, and chromatolysis at the neuron soma and dendritic arbor retraction occur (Hanz and Fainzilber, 2006, Navarro et al., 2007). Chromatolysis reflects a reactive alteration in neuronal biochemistry and function. The neuronal cells shift their functions from the synthesis of proteins required for neurotransmission to those required for regenerative axon growth (Deumens et al., 2010).

Next, Schwann cells in the distal nerve dedifferentiate and proliferate, stimulated by the loss of axonal contact (Karanth et al., 2006, Navarro et al., 2007). Proliferated Schwann cells line up in bands of Bungner, which later provide support for regenerating axons (Geuna et al., 2009). Schwann cells not only pave a path for the regenerating axons to grow along, they also are able to attract injured neurons by secreting neurotrophic factors, such as nerve growth factor (NGF), that stimulate axon elongation (Ngeow, 2010). Proximal to the lesion, fine sprouts emerge from the severed axons and elongate (Witzel et al., 2005). In the absence of a guiding structure, regenerating axons make a tortuous course and form a neuroma, composed of immature axonal sprouts and connective tissue. If regenerating axons gain the distal endoneurial tube as a guiding structure, they elongate in association with the Schwann cells toward correct targets (Stoll and Muller, 1999, Navarro et al., 2007).

Finally, regenerated axons reconnect with target peripheral tissue. Because several sprouts emerge from each parent axon, supernumerary axonal sprouts will be withdrawn gradually during the maturation of the nerve fiber (Witzel et al., 2005, Navarro et al., 2007). The regenerated axons will have smaller caliber and with shorter internodes than normal nerve structures (Geuna et al., 2009). For a successful regeneration, the regenerated axons are expected to replace the distal nerve segment lost during degeneration and perform a normal function. However, more often than not, the regenerated axons do not innervate target tissues adequately or relay information from sensory receptor accurately, which lead to a loss of complete recovery of motor and sensory function, especially when the lesion is severe (Choi et al., 2005, Bannerman and James, 2009). Usually, after nerve injury and repair, the diameter of regenerated axons, their conduction velocity and excitability remain below normal levels for a long time,

which consequently result in incomplete and inadequate functional recovery of reinnervated organs (van Meeteren et al., 1997, Xiao et al., 2007).

Molecular bases of peripheral nerve regeneration

Previous studies have demonstrated that to initiate a regenerative response to injury in the peripheral nerve system (PNS), the neuron must shift its physiology from synaptic transmission and maintenance of structure to the growth of the axon (Benowitz and Yin, 2007). A sequence of molecular responses would take place in response to injury for the successful nerve regeneration and recovery of function (Figure1.1). After nerve lesion, calcium and sodium ions influx into axoplasm through the ruptured plasmatic membrane, generating high frequency burst of action potentials at the lesioned site (Makwana and Raivich, 2005, Navarro et al., 2007). This first signal promotes an influx of calcium through voltage-dependent ion channels and leads to the activation of several protein kinase pathways, including calcium/calmodulin dependent kinase 2 (CMAK2), protein kinase A (PKA), protein kinase C (PKC), and mitogen-activated protein kinase (MAPK), such as Erk1 and Erk2, c-jun N-terminal kinase (JNK) and P38 kinase (Makwana and Raivich, 2005, Raivich and Makwana, 2007). During the second phase of signaling, these activated proteins, termed “positive injury signals”, will incorporate to the retrograde transport system for trafficking back to cell body from the injured site and induce several signaling pathways genes in cell bodies (Hanz and Fainzilber, 2006). Several transcription factors have been demonstrated as the mediators in the regulation of gene expression. The modification in the activity of transcription factors is considered the downstream event influenced by axotomy-activated protein kinases (Dahlin et al., 2009). The activation of transcription factor cAMP responsive element binding protein (CREB) has been demonstrated in early stages after injury (Miletic et al., 2004). Phosphorylation of CREB can be mediated by

multiple protein kinase pathways through activation of tyrosine kinase receptors (Trk) (Miletic et al., 2004). Two other transcription factors induced by nerve injury are ATF-3 and c-Jun. c-Jun up-regulation and phosphorylation is induced by activated JNK, leading to the formation of activating protein1 (AP-1) complexes. JNK pathways and the Erk1/2 pathways also show cross-talk coordinated by MEKK1in PC12 cells (Waetzig and Herdegen, 2005). ATF-3 is induced in all DRG neurons after peripheral axotomy, which makes it a reliable nerve injury marker. Inhibition of JNK reduces ATF-3 expression, which impairs nerve regeneration (Dahlin et al., 2009). The modifications in the activity of transcription factors result in characteristic changes of gene expression. Hundreds of genes have been found differentially expressed after nerve injury, including genes encoding for transcription factors, cytoskeletal proteins, cell adhesion and guidance molecules, trophic factors and receptors, cytokines, neuropeptides and neurotransmitter synthesizing enzymes, ion channels, and membrane transporters (Navarro et al., 2007, Raivich and Makwana, 2007, Dziennis and Alkayed, 2008, Hou et al., 2008). The changes in gene expression support the formation of new growth cones and elongation of the regenerating axon, leading to nerve regeneration.

Figure1.1. Signal transduction in neuronal cells after nerve injury.

The schematic diagram depicts several important signaling pathways activated by axon injury. Cellular injury induces sodium and calcium influx, which lead to depolarization. Among many other processes, the elevated intracellular calcium concentration leads to the activation of protein kinase pathways such as the MAPK Erk1 and Erk2, JNK and P38 kinase. Downstream events influenced by axotomy-activated kinases include up-regulation or activation of several transcription factors. The modifications in the activity of transcription factors result in characteristic changes of gene expression in the injured and regenerating neurons.

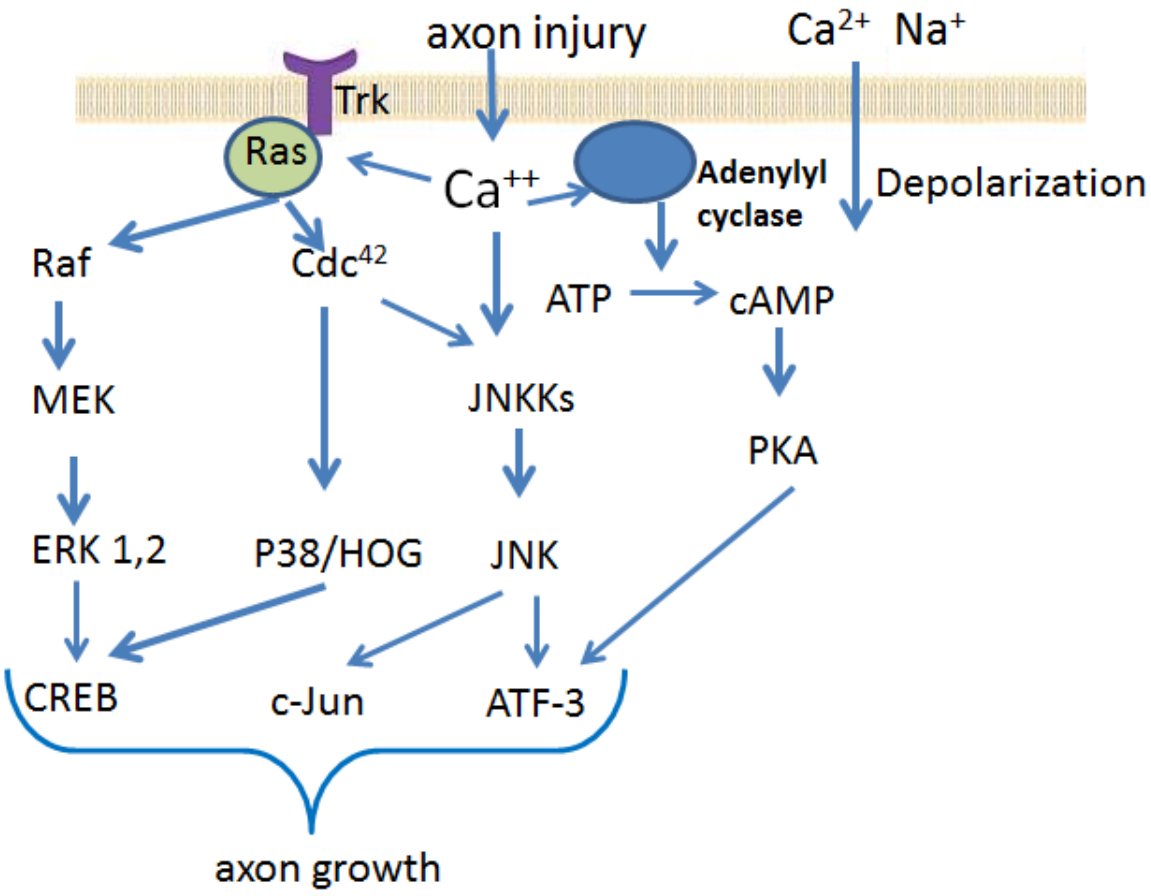
axon injury
Ca2+ Na+
Trk
Ras
Ca++
Adenylyl cyclase
Depolarization
Raf
Cdc42
ATP
cAMP
MEK
JNKKs
PKA
ERK 1,2
P38/HOG
JNK
CREB
c-Jun
ATF-3
axon growth

Post-transcriptional Regulation of Gene Expression

In the last decades, enormous efforts have been made in extending our understanding of the cellular and molecular requirement for successful peripheral axon regeneration. While previous studies gave an insight on regulation of expression at the transcriptional level, very little is known about the regulation of gene expression at the post-transcriptional level after peripheral nerve injury.

Post-transcriptional regulation of gene expression by small RNAs was first observed in petunia. When an exogenous RNA sequence was introduced into petunia, instead of being translated into protein, it 'silenced' endogenous homologous gene's expression (Napoli et al., 1990). This gene-silencing phenomenon was then characterized in *Caenorhabditis elegans* by Andrew Fire and Craig Mello, which they termed 'RNA interference' (RNAi) (Fire et al., 1998). Subsequent studies also showed that long double-stranded RNAs (dsRNAs) can induce a sequence-specific inhibition of gene expression in a number of invertebrates whereas shorter double-stranded RNA, termed small interfering RNAs (siRNAs), are required to induce highly specific gene silencing in mammalian cells (Elbashir et al., 2001).

RNAi is an evolutionary conserved mechanism to selectively suppress gene expression (Filipowicz et al., 2008). It is originally recognized as a defensive response to foreign nucleic acids. Eukaryotic cells infected by viruses can process the dsRNA carried by viruses into siRNAs, which bind to and cause degradation of matched messenger RNA (mRNA), preventing the synthesis of protein necessary for viral replication. RNAi also protect the eukaryotic genome from endogenous transposable elements and it was later demonstrated that RNAi is required for normal development. Endogenous small RNAs, such as Let-7 and Lin-4, were initially identified

in *C. elegans*, whose expressions play an important role for development (Saugstad, 2010). The term ‘microRNA (miRNA)’ was then introduced in a series of subsequent studies. Both exogenous double-stranded siRNA and endogenous single-stranded miRNA can initiate RNAi utilizing the same RNAi machinery to produce gene silencing (Rana, 2007) .

miRNA biogenesis and RISC assembly

miRNAs, by definition, are endogenous, non-coding 21to 23 nucleotide small RNA molecules that regulate gene expression by binding to the 3’-untranslated region of target mRNAs, leading to their translational inhibition or degradation (Filipowicz et al., 2008, Carthew and Sontheimer, 2009). As showing in Figure 1.2, miRNAs are encoded in genomic DNA, located either in the introns of protein-coding genes or as independent entities. miRNA genes are first transcribed via RNA polymerase II into primary miRNA (pri-miRNAs). A single pri-miRNAs often contains sequences for several different miRNAs and they fold into hairpin structures containing imperfect base-paired steam. Primary miRNAs are cleaved by enzymes including Drosha and DGCR8 in mammals (or Pasha in *Drosophila*) into ~70 nucleotide hairpins known as precursor miRNAs (pre-miRNAs), which are transported into the cytoplasm by Exportin-5. In the alternative way, when miRNA transcription occurs from introns of protein-coding genes, it bypasses the Drosha/DGCR8 enzyme complex. This subclass of miRNAs is named ‘mirtron’ or ‘mitron’, and mitrons are spliced out from premature mRNA to form pre-miRNAs (Sibley et al., 2012). Pre-miRNAs are further processed by *Dicer*, an endoribonuclease, which works with its cofactors in the cytoplasm. In mammals, *Dicer* forms complex with TAR RNA binding protein (TRBP) and in *D. melanogaster Dicer* complexes with Loquacious. (Bernstein et al., 2001, Lee et al., 2003, Filipowicz et al., 2008). The products of *Dicer* processing form miRNA duplexes with protruding 2-nucleotide 3’ end. The strand with the 5’

terminus located at the thermodynamically less-stable end of the duplex are usually selected to function as the mature miRNA, while the other strand is degraded. Occasionally, both strands of the duplexes give rise to mature miRNA (Filipowicz et al., 2008). They are designated as miR-X and miR-X*, with the less predominately expressed transcript indicated by an asterisk (Saugstad, 2010).

The mature miRNA target specific mRNAs to either cause degradation of the mRNA or inhibit protein translation via RNA induced silencing complex (RISC), a ribonucleoprotein complex associated with miRNA. Although the assembly of RISC is a very dynamic process and its details are not well understood, proteins of Argonaute (AGO) family are considered the most important components of RISC (Peters and Meister, 2007, Filipowicz et al., 2008). The number of Ago proteins differs among species. For example, humans have eight Ago proteins, *Drosophila* has five, and *C. elegans* expresses 27 Ago proteins (Sasaki et al., 2003, Peters and Meister, 2007). In mammals, only Ago2 can cleave mRNA at the center of the siRNA-mRNA duplex. The significance of Ago2 in RNAi pathway is also evidenced by the pronounced reduction in RNAi function after Ago2 knockdown (Hammond et al., 2001).

Apart from Ago proteins, RISC contains further regulatory factors and effectors mediating inhibitory function. The fragile X mental retardation protein (FMRP) is one of the conclusively identified subunit. Both miRNA and siRNA can co-immunoprecipitate with FMRP. The FMRP belongs to the fragile X gene family, which encodes three different proteins: FMRP, FXR1, and FXR2. The loss-of-function mutations in the FMRP gene results in fragile X syndrome (FXS), whereas the function of FXR1 and FXR2 remains unknown. However, it is suspected that all three fragile X protein functions similarly in regulating mRNA stability by binding with ribosomes, and FXR1 and FXR2 has the potential to associate with RISC as well

(Siomi et al., 2004). Other well identified components of RISC include Gemin3 and Gemin4, which are also components of the survival of motor neurons (SMN) complex. The SMN complex plays a critical role in the assembly of diverse ribonucleoprotein complexes in the nervous system. The functions of Gemin3 and Gemin4 are speculated to be involved in target mRNA recognition and translational repression (Dostie et al., 2003, Battle et al., 2007). RISC also recruits P-100. P-100 may be a nuclease in RISC since it showed ribonuclease activity in some studies (Sundstrom et al., 2009).

Figure 1.2 Biogenesis of miRNAs

miRNAs are processed from precursor molecules, which are either transcripts from independent miRNA genes (pri-miRNA) or are a portion of introns of protein coding transcripts (mitron). The precursor molecules are excised into pre-miRNA with a hairpin structure. The final processing of pre-miRNA by *Dicer* yields miRNA duplex. One strand of the duplex is degraded and the remaining mature miRNA binds to Argonaute proteins to form RNA-induced silencing complexes (RISCs). miRNAs target sequences within messenger RNAs, causing repression of translation and subsequent degradation or storage of mRNAs in P bodies.

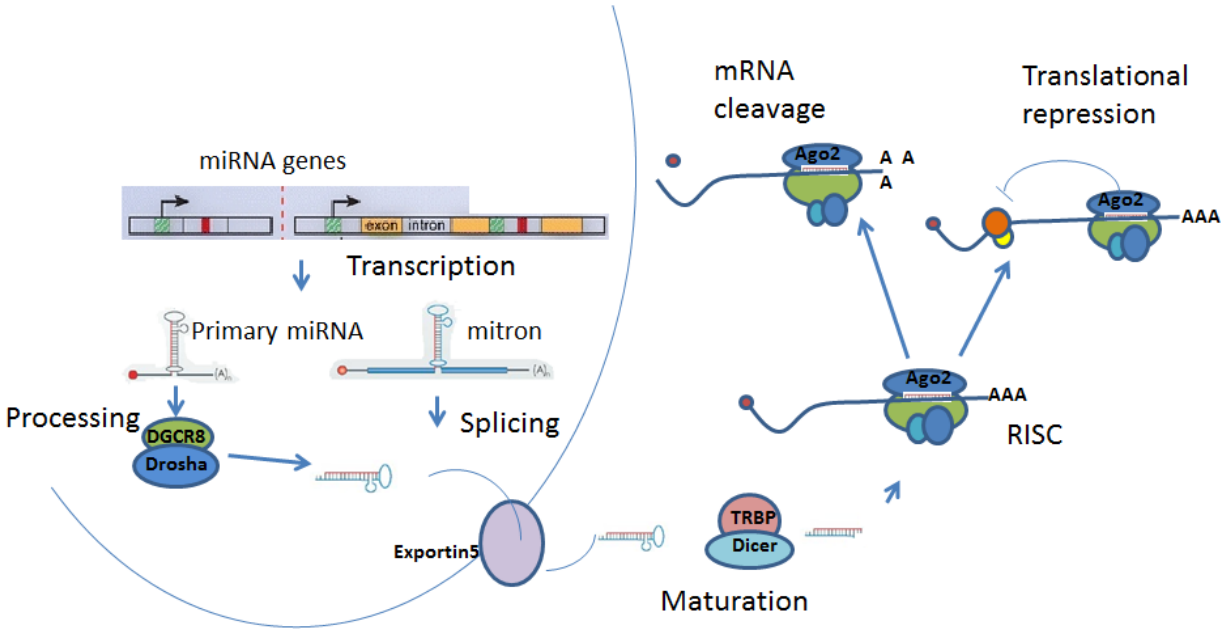
miRNA genes
exon
intron
Transcription
Primary miRNA
mitron
Processing
DGCR8
Drosha
Splicing
Exportin5
TRBP
Dicer
Maturation
RISC
Ago2
AAA
mRNA
cleavage
Translational
repression

The miRNA / target mRNA interaction

miRNAs in RISC form complementary base pairs with mRNAs within their 3'- UTR, leading to their translational inhibition or degradation (Carthew and Sontheimer, 2009). The primary rule for mRNA targeting is the perfect base pairing of the 'seed region', which locates at the miRNA nucleotides 2 to 8. Perfect and contiguous Watson-Crick base pairing at this limited region associates miRNA with target mRNA (Filipowicz et al., 2008). The second rule requires a mismatch to be present in the central region of the miRNA-mRNA duplex. The bulge generated by the mismatch precludes the Ago-2 mediated endonucleolytic cleavage of mRNA (Filipowicz et al., 2008). Some base pairing at the other half side of miRNAs, especially the 13-16 nucleotides would stabilize the binding between miRNA and mRNA as well (Grimson et al., 2007). Multiple miRNA binding sites within the mRNA 3' UTR can improve the silencing efficiency (Doench and Sharp, 2004). A position of binding site close to the poly(A) tail or the termination codon increases the accessibility of mRNA to RISC (Grimson et al., 2007). Interactions between proteins bound to miRNA or mRNAs can also influence target selection and efficiency of repression. In addition, exceptions always exist in the target selection, which makes the prediction of targets for miRNAs by bioinformatics analyses alone insufficient (Ritchie et al., 2009).

miRNA mediated translational repression and degradation

The cytoplasmic foci termed P-bodies serve as the sites where miRNAs are believed to exert the majority of their function (Ding and Han, 2007). Several independent studies showed that Argonaute proteins interact with the RNA-binding protein GW182 proteins (Sen and Blau, 2005, Eulalio et al., 2009b, Takimoto et al., 2009). Subsequent studies showed that GW182-

containing foci, known as GW bodies (GWBs) coincide with mRNA-processing bodies or P-bodies (Sen and Blau, 2005, Eulalio et al., 2009b, Takimoto et al., 2009). Studies also showed that depleting GW182 suppresses repression of miRNA targets, irrespective of whether they are directed to a translational repression or degradation, leading to an upregulation of many mRNAs (Ding and Han, 2007, Eulalio et al., 2009b). Furthermore, when GW182 is directly tethered to an mRNA reporter, reporter expression is silenced independently of Argonaute proteins (Behm-Ansmant et al., 2006). These observations suggested that once miRNA and their associated proteins are bound to an mRNA target, Ago2 together with mRNA are sequestered into P-bodies (Saugstad, 2010). The first proteins found in P-bodies are those functioning in the degradation of mRNA (Eulalio et al., 2007b). In eukaryotes, mRNA degradation can follow two pathways, and both are initiated by a gradual shortening of the mRNA poly(A) tail with deadenylases. Following deadenylation, mRNAs are exonucleolytically digested from 3' to 5', which is catalysed by the exosome (Eulalio et al., 2007b, Filipowicz et al., 2008). Alternatively, the cap structures at 5' end are removed by decapping enzymes after deadenylation, followed by 5' to 3' degradation catalysed by exonuclease. The decapping enzymes and decapping coactivator, including DCP1 and DCP2, as well as exonuclease XRN1 colocalize in P-bodies. They form the decay machinery and destabilize mRNAs in P-bodies (Eulalio et al., 2007a). Consistent with its role in mediating mRNA degradation, the knockdown of the decay machinery component prevents miRNA- mediated degradation, but leads to an accumulation of deadenylated mRNAs (Filipowicz et al., 2008). Additional P-bodies components include decapping activators RCK/p54 and Pat1, translational repressor eIF4E-transporter (4E-T), and RAP55. RAP55 responds to stress and has a putative role in translation regulation (Eulalio et al., 2007b).

In addition to mRNA degradation, an alternative mechanism to repress the expression of target mRNAs is through translation inhibition. Translation requires the participation of several initiation factors, many of which are multiprotein complexes. Initiation of translation starts with the binding between mRNA 7-methylguanosine cap and eukaryotic translation initiation factor (eIF) 4E. When miRNA is bound to the mRNA 3' UTR, Ago proteins interact with the 7-methylguanosine cap of the mRNA. The association of Ago instead of eIF4E with 7-methylguanosine cap prevents effective recruitment of ribosomes and blocks the initiation of translation (Kiriakidou et al., 2007). Further studies also showed that multiple miRNA binding site at the 3' UTR increase the likelihood of Ago association with 7-methylguanosine cap, therefore enhancing the translational repression (Filipowicz et al., 2008). Association of Ago with 7-methylguanosine cap has another function. The association disrupts the 3D structure of the mRNA, and possibly makes the poly (A) tail more vulnerable to exonucleolytic activity (Eulalio et al., 2007b).

Targeting translation initiation is not the only mechanism by which miRNAs inhibit mRNA translation. The inhibition of translation occurs at post-initiation phase as well. Studies showed that mRNAs targeted by miRNAs remain associated with polysomes, despite a strong reduction in their protein expression level (Filipowicz et al., 2008). miRNA are speculated to be able to slow elongation and result in ribosome preferentially drop off from mRNA. How miRNA could modulate the elongation or terminate the translation of mRNA remains unclear.

Recent findings indicate that under certain conditions, mRNAs sequestered into P-bodies can be freed when cells respond to a subsequent stress. The mRNAs released from P-bodies are recruited to the polysome and translation can resume (Saugstad, 2010). The ability of miRNA to disengage from repressed mRNA makes miRNA regulation more dynamic and wide-ranging.

One example in neuronal cell is the miR-134 mediated repression of LIMK1, a protein kinase that is important for the development of dendritic spine. In response to extracellular stimuli, miR-134 mediated repression of LIMK1 expression will be released at dendritic spines (Schratt et al., 2006). This observation also suggests that miRNA regulated mRNA translation is probably an important regulator of gene expression in response to synaptic activity.

Functional Significance of miRNAs

Bioinformatic predictions indicate that mammalian miRNAs can regulate at least 30% of all protein coding genes (Filipowicz et al., 2008). Therefore, it is no surprise that miRNA based regulations are involved in many cellular process. miRNA plays diverse roles in cell differentiation, proliferation (Stefani and Slack, 2008), metabolism (Wang et al., 2011), and signal transduction (McCoy, 2012).

miRNAs in development

Early studies interrupted miRNA processing by *Dicer* gene ablation. Decreasing miRNA production in the entire organism induced embryonic lethality, suggesting miRNAs are necessary for normal fetal development (Bernstein et al., 2003). To better reveal the functions of miRNAs in different tissues at different developmental phases, conditional *Dicer* knockout mice were created. For example, *Dicer* was ablated from cardiac myocytes in early embryonic mouse heart by *NKX2.5*-Cre, in neonatal mouse heart by *MYH6*-Cre, and in adult mouse heart by *MYH6* driven tamoxifen activated *Cre*. Embryonic cardiac *Dicer* ablation caused intrauterine cardiac hypoplasia, a lethal cardiomyopathology. Postnatal hearts with *Dicer* ablation exhibited cardiomyocyte hypertrophy, cardiomyocyte apoptosis, and abnormal sarcomeric structure (Huang et al., 2011). The importance of *Dicer* in germ cell differentiation and maturation has

been demonstrated. When *Dicer* was deleted specifically in postnatal male germ cells, it resulted in abnormal spermatozoa and eventual male infertility (Korhonen et al., 2011). Smooth muscle cell specific knockout of *Dicer* developed severe dilation of the intestinal tract associated with destruction of smooth muscle layers, suggesting the role of miRNA pathway in the development of the gastrointestinal tract (Park et al., 2011). *Dicer* dependent miRNA pathway also regulated the development of nephrogenic and ureteric compartments in kidney, white adipose tissue, and skin (Yi et al., 2006, Mudhasani et al., 2011, Nagalakshmi et al., 2011). miRNA pathway is required for neural development as well. *Dicer* is essential for cellular and tissue morphogenesis in cortex and hippocampus. *Dicer* ablation in hippocampus at different embryonic time points resulted in abnormal hippocampal morphology and affected the number of hippocampal progenitors due to altered proliferation and increased apoptosis (Li et al., 2011). *Dicer* knockout in neocortex disrupted differentiation of newborn neurons and results in neuronal cell death (De Pietri Tonelli et al., 2008). *Dicer*-null neural stem cells were incapable of generating either glial or neuronal progeny, which blocked the differentiation (Andersson et al., 2010). Conditional knockout also resulted in the malformation of the midbrain and cerebellum and failure of neural crest and dopaminergic differentiation in mice (Huang et al., 2010).

miRNA modulation of the cellular stress response

Studies on cellular stress found crucial roles for specific miRNAs in modulating the stress response. For instance, recent studies have established that the regulation of miRNAs is a feature of the hypoxic response (Crosby et al., 2009). The hypoxic microenvironment induces the up-regulation of miR-210 and miR-373. Thus, miR-210 and miR-373 can serve as a marker of solid cancer, which is linked to an *in vivo* hypoxic signature. Mir-210 also participates in endothelial and neuronal cell responses to oxygen deprivation (Crosby et al., 2009). In addition,

specific miRNAs have been identified as key regulators of the response to ischemia, suggesting miRNA pathway plays a role in different components of tissue response to ischemia (Fasanaro et al., 2009). Other studies have shown the importance of miRNAs on immune system development and response, and miRNAs are found to be involved in the regulation of immunity (Aldrich et al., 2009, Bi et al., 2009). Therefore, miRNAs can be considered as one of the key regulators mediating the shift of gene expression in response to injury, which is also a response to cellular stress.

miRNAs in pathological events

Dysregulation of miRNA has been documented in developmental defects and diseases, therefore miRNA may also play a role as diagnostic or prognostic biomarker. For instance, miR-1, a muscle-enriched miRNA has increased expression level in both experiential acute myocardial infarction animal models as well as patients with acute myocardial infarction (Fichtlscherer et al., 2011). miR-423-5P increases circulating level in the plasma samples from patients with heart failure (Tijsen et al., 2010). Extensive studies have documented profound alteration of miRNA expression in all major human cancers. For example, miR-15a and miR-16 are severely down-regulated in 70% of patients with chronic lymphocytic leukemia. B-cell lymphoma 2 (BLC2), an anti-apoptotic factor was found to be the target gene of miR-15 and miR-16. Loss of miR-15 and miR-16 is responsible for the overexpression of BLC2 in chronic lymphocytic leukemia specimens (Ofir et al., 2011). Alternatively, some miRNAs are overexpressed in cancer specimens. These miRNAs are defined as oncomiR and the most characterized oncomiR is miR-21. miR-21 act as an oncogene by regulating the tumor-suppressor genes PTEN an PDCD, and the upregulation of miRNA has been found in over 15 different cancers (Koturbash et al., 2011). A number of miRNAs can work as both oncogene and

tumor suppressor. For example, miR-220 is up-regulated in pancreatic and thyroid cancer, but significantly down-regulated in lung cancer (Bloomston et al., 2007). The tumor type-selective miRNA dysregulation may be useful for diagnostic and prognostic purpose. miRNA expression profile can help distinguish tumor histopathological subtypes, determine the stage of carcinogenic process, determine tumor's aggressiveness, modulate drug resistance, and predict overall survival and recurrent rates (Koturbash et al., 2011).

miRNAs as effectors in neurological disorder

A number of studies have shown the correlation between neurological diseases and the alteration of miRNA biogenesis. Although no conclusion can be made that the altered expression of miRNAs is a consequence or the cause of neurological disorders, some studies showed the change in miRNA expression prior to the onset of the disease. This raises the possibility that restoring the expressing level of specific miRNAs can prevent the pathological development of the diseases.

Mouse models and human samples have both implicated altered miRNAs in the pathology of Alzheimer's disease (AD), particularly with respect to the regulation of β-amyloid precursor protein converting enzyme1 (BACE1) (Hutchison et al., 2009). BACE1 was shown to be targeted by miR-458-5p, and an endogenous natural BACE-antisense competes with miR-485-5p for the binding on BACE1 mRNAs. In AD patients, BACE-antisense appeared to be up-regulated while miR-485-5p was down-regulated in cortex and hippocampus. Therefore the down-regulation of BACE1 translation was blocked, and the increased expression of BACE1 stimulated the formation of amyloid-β-peptide plaques in the brain region (Faghihi et al., 2010). miR-29 was found to regulate BACE1 expression *in vitro* and decreased expression of miR-29a

and miR-29b was observed in AD patients (Hebert and De Strooper, 2007, Hebert et al., 2008). In addition, miR-107 significantly decreases at early stage of AD, and it has multiple predicted binding sites on BACE1 (Wang et al., 2008c). In mouse models, miR-298 and miR-328 can also target BACE1 mRNA, and *in vitro* studies confirm the regulation of BACE1 protein expression by these miRNAs (Boissonneault et al., 2009). Increased expression of miRNAs, such as miR-9, miR-125b, miR-138, and miR-146a has also been observed in AD brains (Saugstad, 2010, Olde Loohuis et al., 2012).

The pathological development of Parkinson's disease (PD) is under the control of miRNAs as well. Conditional knockout of *Dicer* in dopaminergic neurons results in loss of dopaminergic neurons and impaired locomotion, which mimics the phenotype of PD patients (Olde Loohuis et al., 2012). Gene screen of PD patients identified a disruption in the binding site of miR-433 in the 3'UTR of the fibroblast growth factor 20 (FGF20) gene. This disruption leads to an increased expression of FGF20 and subsequent increase of α-synuclein expression, which is correlated with cytotoxicity associated with PD (Wang et al., 2008a). Increased expression of α-synuclein may also result from insufficient expression of miR-7 in neurotoxin model of PD (Junn et al., 2009). Another report found a significant decrease of miR-133b expression in PD patient. Further studies revealed that miR-133b is specifically expressed in midbrain dopaminergic neurons and targets the transcription factor pituitary homeobox 3 (Pitx3) in a feedback loop. Lack of miR-133 disrupted midbrain dopaminergic maturation and function (Kim et al., 2007).

Studies on miRNA expression in Huntington's disease brains revealed dysregulated expression of several miRNAs in both mouse models of HD (Huntington's disease) and in human patients (Hutchison et al., 2009). Huntington's disease is related to abnormal activation of

transcription factor REST. When Huntington protein can not bind to REST, REST can freely translocate to the nucleus and represses neuronal gene expression. Studies showed that several miRNAs with REST binding sites or REST cofactor binding sites are decreased in human HD, including miR-9 and miR-9*, which target REST and co-REST respectively (Packer et al., 2008). Decreased miR-124 is also observed in HD and miR-124 plays a role in maintaining neuronal identity through targeting PtBP-1 (Cao et al., 2007).

Intellectual disability syndromes and mental diseases also appear to be influenced by miRNA expression. The studies in schizophrenia patients revealed a significant schizophrenia-associated increase in global miRNA expression (Beveridge et al., 2010). miR-160b, 30b and 181b are significantly upregulated in the frontal cortex of schizophrenia patients (Kim et al., 2010, Santarelli et al., 2011). NMDA-regulated miRNA miR-132 was significantly down-regulated in the prefrontal cortical tissue from schizophrenia patients (Miller et al., 2012). Twenty-eight miRNAs are differently expressed in the brains of autistic patients, and the predicted targets of dysregulated miRNAS included Neurexin and SHANK3, which are known genetic causes of autism (Abu-Elneel et al., 2008). In another study, differential expressions of 9 miRNAs were observed in 6 autism samples in growing lymphoblastoid cell lines (Talebizadeh et al., 2008). These analyses revealed a subset of brain-related microRNAs implicated in schizophrenia and autism.

miRNAs located in neurons

In neurons, the functions of individual miRNAs are just beginning to emerge. To date, seven miRNAs have been identified to be specifically expressed in mammalian brain, which includes miR-9, miR-124a, miR-124b, miR-135, miR-153, miR-183, and miR-219, suggesting

their unique regulatory roles in brain function (Sempere et al., 2004). Functional analysis showed that transfection of brain-specific 124 into HeLa cells is sufficient to change the gene expression profile and shift it toward neuronal-like phenotype. The overexpression of miR-124 down-regulated hundreds of nonneuronal transcripts, and allows the transition from nonneuronal to neuronal phenotypes during development (Lim et al., 2005). One direct target of miR-124 is small c-terminal domain phosphatase 1, an antineural factor of REST/SCP1 pathway. Suppression of small c-terminal domain phosphatase 1 induces neurogenesis during brain development (Visvanathan et al., 2007). MiR-124 also repressed the expression of SRY-box transcription factor Sox9. This repression promotes the adult neurogenesis in the subventricular zone stem cell niche (Cheng et al., 2009). MiR-124 also regulates early neurogenesis in forebrain and optic vesicle by targeting NeuroD1 (Liu et al., 2011). More recently, miRNA expression profiles within more specific brain regions, such as the cortex and hippocampus, have been identified. It was found that the expression of let-7g, miR-92b, miR-146b, miR-330*, and miR-394 were significantly higher in rat hippocampus than in cortex (Olde Loohuis et al., 2012). The specificity in miRNA expression further suggested the cell or tissue specific functions of miRNAs. For example, miR-449 has been identified in choroid plexus, the area in the brain ventricle that is responsible for the production of cerebrospinal fluid. Transcription factor E2f5 which regulates cerebrospinal fluid production is targeted by miR-449 (Redshaw et al., 2009).

miRNAs in axons and dendrites

Subcellular localization of miRNAs within neuronal dendrites and axons has been shown in recent studies. With laser capture microdissection, RNA populations from dendrites and cell bodies were acquired. RT-qPCR analysis revealed that most miRNAs distributed with a gradient decrease from soma into the dendrites. A few miRNAs, such as miR-26a, miR-26b, and miR-

292-5p, are enriched in dendrites (Kye et al., 2007). Enrichment of precursor miRNAs has been observed in dendrites as well. These dendritically enriched precursor miRNAs show a distinct structure which may allow them to bind to proteins that mediate dendritic transport (Smalheiser, 2008). The significant correlation between precursor and mature miRNAs enrichments suggests precursor miRNAs may be processed locally in dendrites. The identification of *Dicer* at postsynaptic densities further supported this hypothesis (Lugli et al., 2005, Lugli et al., 2008). It has been widely accepted that local protein synthesis in distal domains of neuron has a key role in synaptic formation, synaptic plasticity, and axonal regeneration (Schacher and Wu, 2002, Hanz et al., 2003). Regulation of local mRNA translation can alter the synaptic protein expression upon stimulations. One theory for miRNA based regulation of local protein synthesis suggests that precursor miRNAs are predominantly associated with postsynaptic densities. Upon stimulations, neuronal-mediated calcium influxes activate proteases such as calpain, resulting in release of *Dicer* from the postsynaptic density. The newly freed *Dicer* processes precursor miRNAs into mature miRNAs, which then incorporate into RISC and inhibit target mRNA translation. Meanwhile, activated protease can also degrade components of RISC. mRNA that are important for synaptic plasticity can be released from RISC and selectively enter the polysome compartment, where they will resume the initiation of translation. This local translational regulatory model provides a mechanism that meets the requirement for both increased and decreased protein synthesis (Saugstad, 2010).

A small number of miRNAs involved in synaptic morphogenesis and plasticity have been identified through recent functional analysis. miR-138 is localized in dendrites of rat hippocampal neurons and it inhibits dendrite spine growth through activating the Rho signaling pathway. miR-138 targets acyl protein thioesterase 1 (APT1), which in turn catalyze membrane

association of Gα12/13. The membrane association of small G protein subunit Gα13 has been shown to be involved in the activation of RhoA signaling pathway (Siegel et al., 2009). In contrary, miR-132 expression enhances dendrite morphogenesis in hippocampal neurons. miR-132 represses the expression of the Rho GTPase –activating protein (GAP) p250. p250GAP regulates spine formation through modulating Rac1 and RhoA activities. Therefore, miR-132 expression is conversely related to P250GAP. Introduction of miR-132 showed the same effect on dendritic spine phenotype as p250GAP knockout, which results in increased spine density and spine size (Olde Loohuis et al., 2012). miR-134 is an example for neurotrophic control of dendritic spine plasticity through miRNA mechanism. miR-134 localized to dendrites negatively regulate the size of dendritic spine by inhibiting the expression of LIM domain kinase 1 (Limk1), neurogenic differentiation factor 2 (NeuroD2), and disks large homolog2 (DLG2). Exposure to brain-derived neurotrophic factor relieves the inhibition in spine development by miR-134, and increases the expression of Limk1 protein. Limk1 regulates actin filament dynamics, thereby controlling cytoskeletal reorganization, promoting spine outgrowth (Schratt et al., 2006). The involvement of miRNAs in synaptic plasticity is further confirmed with the changes of miRNA expressions after long-term potentiation.

Compared with the studies in dendritic miRNAs, there is less understanding in the role of miRNA in axonal functions. However, the studies in axonal miRNA pathway are growing. Pure axonal miRNAs have been obtained from superior cervical ganglia neurons cultured in compartmentalized Campenot cell culture chambers. Totally, 130 matured miRNAs have been detected in distal axon, and a few miRNAs, including miR-15b, miR-16, and miR-221, are highly enriched in axons (Natera-Naranjo et al., 2010). miRNA machinery components, such as *Dicer*, argonaute proteins, fragile-X mental retardation protein (FMRP) have been found to be

localized in developing axons and growth cones in RNA granule-like structure (Hengst et al., 2006). Although direct evidence for miRNA-mediated suppression of axonal mRNA translation has not been demonstrated, the involvement of the miRNA pathway in the regulation of axonal function is suggested by the functional activity of miRNA machinery in axons (Hengst et al., 2006).

Studies from our laboratory have shown that sciatic nerve axons contain functional miRNA biogenesis proteins (Murashov et al., 2007). They are functional when exogenous siRNAs are applied. Based on the fact the siRNA pathway and miRNA pathway share the same important functional enzymes, we presume that endogenous miRNAs may regulate translation in peripheral nerve axon and might play a role in regenerative axon growth during peripheral nerve regeneration.

Objective of Current Study

In the current study, we investigated the involvement of miRNA pathway in regulation of gene expression after sciatic nerve injury. To prove our hypothesis that miRNA pathway plays a critical role in peripheral nerve regeneration, the following three specific aims were devised:

(1) Determine the expression of the miRNA biosynthetic machinery and miRNAs in regulation of response to nerve injury. We hypothesized that there will be injury-regulated expression of miRNA biosynthetic enzymes, including components of RISC and P-body, and injury regulated expression of miRNAs

(2) Determine the role of *Dicer*-dependent miRNA pathway in regulation of regenerative nerve growth. We hypothesized that the deletion of *Dicer* will disrupt production of *Dicer*-dependent small RNAs and will negatively impact peripheral nerve regeneration.

(3) Determine the specific miRNAs involved in regenerative axonogenesis. We hypothesized that some of the miRNAs may be the key regulatory switches for peripheral axonal regeneration.

CHAPTER II: Methods

Animals and Surgeries

Animals

The animal use protocol was approved by the institutional Animal Care and Use Committee of East Carolina University, an AAALAC-accredited facility. Animals were housed individually under standard laboratory conditions, with a 12 h light/dark schedule and unlimited access to food and water. In the approved animal use protocol, we included a detailed description of the research being conducted, minimized the number of animals being used in the study, minimized pain and distress to animals in the study, and proved there is no an alternative model to the use of a living animal.

CD-1 mice: 8-wk-old CD-1 mice were obtained from Charles River laboratories (Wilmington, MA).

Dicer mice: Breeding pairs of *CAG-CreERt* and *Dicer*$^{fl/fl}$ mice were provided by Dr. Tatsuya Kobayashi as a generous gift (Kobayashi et al., 2008). The offspring, *CAG-CreERt:Dicer*$^{fl/fl}$ mice carried an homozygous allele of floxed *Dicer* gene (*Dicer*$^{fl/fl}$) and heterozygous *Cre* gene with an inducible estrogen promoter. By breeding *CAG-CreERt:Dicer*$^{fl/fl}$ mice, we obtained *CAG-CreERt:Dicer*$^{fl/fl}$ mice and *Dicer*$^{fl/fl}$ littermates. Genotypes were determined by PCR using genomic DNA derived from tail biopsies.

To induce the deletion of *Dicer*, 8-wk-old *CAG-CreERt:Dicer*$^{fl/fl}$ mice received intraperitoneal (i.p.) injections of tamoxifen (Sigma, St. Louis, MO) at the dose of 0.1mg/g body

weight for five consecutive days (Kobayashi et al., 2008). These animals were hereafter called *Dicer KO* (*Dicer* KO) mice in this study. Sesame oil (Sigma) with ethanol (EMD Chemicals Inc., Gibbstown, NJ) (3.75%) solution was used as vehicle to dissolve tamoxifen. *CAG-CreERt:Dicer*$^{fl/fl}$ mice with vehicle treatment (hereafter called vehicle treated group) and *Dicer*$^{fl/fl}$ littermates with tamoxifen treatment (hereafter called no-*Cre* group) were used as controls in this study (Fig 2.1.). All animals were normal at birth, exhibiting normal weight and weaning behavior as compared with control littermates. At 8 weeks, (beginning of tamoxifen treatment) heterozygous mutant mice were viable, normal in size, and did not display any physical or behavioral abnormalities.

Conditioning nerve lesion

Before surgery, anesthesia was induced using intraperitoneal Ketamine (18/mg/ml)-Xylazine (2 mg/ml) mixture (0.05 ml/10 g of body weight, i.p). The procedure followed a protocol described previously (Islamov et al., 2004). Exposure of the right sciatic nerve was performed with sterile surgical instruments through an incision on the middle thigh of the right hind limb. Approximately 5 mm of nerve was exposed from the sciatic notch to the trifurcation of the nerve. The exposed sciatic nerve was crushed in the mid-thigh for 15 sec with a fine hemostat. The wounds were closed with 3M™ Vetbond™ Tissue Adhesive (3M, St. Paul, MN) and the recovery of sciatic nerve was monitored until the day we euthanized animals.

In the following experiments, the injured ipsilateral nerves were called injured nerves and the ipsilateral DRGs were called injured DRGs. The contralateral nerves were called naïve nerves and DRGs from contralateral side were called naïve DRGs. Nerves and DRG from intact animals were called intact nerves and intact DRGs.

Figure 2.1 Inducible *Dicer* knock out models.

3 groups of animals were generated for the studies in specific aim 2. *CAG-CreERt:Dicer*$^{fl/fl}$ mice received intraperitoneal (i.p.) injections of tamoxifen at the dose of 0.1mg/g body weight for five consecutive days were called *Dicer KO* (*Dicer* KO) mice in this study. Tamoxifen treatment induced *Cre* activation and results in the deletion of *Dicer*. Sesame oil solution was used as vehicle to dissolve tamoxifen. *CAG-CreERt:Dicer*$^{fl/fl}$ mice with vehicle treatment were called vehicle treated group. *Cre* was not activated in this group and *Dicer* was normally expressed. *Dicer*$^{fl/fl}$ littermates with tamoxifen treatment were used as another control in this study. Since this group did not carry *Cre* gene, treatment of tamoxifen could not induce the deletion of Cre, and they are called no-Cre group in this study.

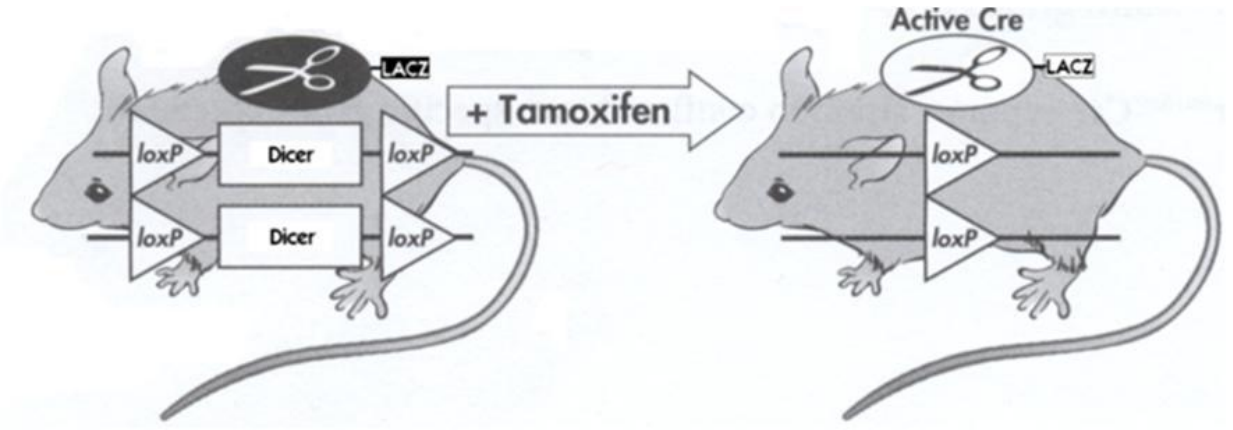

Cre(Tg/-):Dicer(fl/fl)

① Tamoxifen → **Induced activation of *Cre***
***Dicer* deletion**
Interrupted miRNA synthesis

② Vehicle

or

Cre(-/-):Dicer(fl/fl)

③ Tamoxifen → **Lacking activation of *Cre***
No *Dicer* deletion
Normal miRNAs Synthesis

Tissue Collection

After specified time periods, animals were euthanized by exposure to isofluorane (Webster Veterinary, Devens, MA). Sciatic nerves were quickly dissected out, snap frozen in liquid nitrogen and stored at -80ºC for molecular analyses. The naïve nerve was taken from the contralateral side (sciatic nerve from left side). The excised crush sample was taken from the injury side approximately 5 mm in both directions from the point of injury. The intact nerve sample was taken from mice at the matched age without sciatic nerve crush surgery. Ipsilateral and contralateral L4-L5 DRGs were collected under dissecting microscope for RNA and protein analyses.

X-gal staining of Sciatic Nerves

For *Dicer* mice, 5 days after tamoxifen or vehicle treatment, 5 mice were randomly selected from each group, and around 1 cm of sciatic nerve was dissected from 3 groups of mice. Sciatic nerves were first fixed in 0.5% glutaraldehyde in PBS with Magnesium Chloride (2mM) on ice for 30 minutes, and then rinsed in 3 changes of PBS. X-gal stock (Sigma) was diluted into X-gal reaction buffer and was incubated with the tissue for 2-4 hours at 37° C. The sciatic nerves were rinsed in PBS until the solution ran clear. The activity of β-galactosidase was checked under bright-field optics.

Analyses of Functional Recovery

Functional motor recovery

Functional recovery of motor function after sciatic nerve crush was analyzed using a walking track assessment, and quantified with the sciatic functional index (SFI). Paw prints were recorded by painting the hind paws with black ink and having the animals walk along an 8x40 cm corridor lined with a white paper. The toe spread and the paw length were measured from those prints to calculate SFI (McMurray et al., 2003). The resulting SFI was calculated according to the formula described as:

SFI=118.9 (ETS – NTS)/NTS – 51.2(EPL – NPL)/NPL-7.5

where ETS represented experimental toe spread, NTS represented normal toe spread, EPL represented experimental paw length, and NPL represented normal paw length. The value of SFI ranges from -100 to 0. A SFI close to zero suggests normal nerve function or completely recovery of nerve function, and a value of 100 indicates total loss of function. The walking corridor analysis was performed on animals before crush injury as baseline tests, and at 2, 4, 7, 14, and 21 days after injury.

Mechanical sensitivity test

Mechanical sensitivity (allodynia) was studied with the von Frey test. Filaments with stimulus intensities ranging from 0.08-10 grams were applied to the glabrous skin of each hind paw eight times while the animal stood on an elevated screen. Before testing, a 15 min quiescent period was allowed. Filaments were applied to the point of bending, at which time substantiation of response or non-response was determined. Responses included hind paw withdrawal and

orientation toward the stimulus. During each test session, the filament that produced a threshold response (response to over 4 out of 8 stimuli) in each animal was documented for both the left and right hind paws (Okada et al., 2002). Raw data measurements were recorded as stimulus intensities required to elicit a threshold response and subsequently normalized to baseline values.

Electrophysiological analyses on isolated sciatic nerves

Electrophysiological approaches were used to assess the effects of *Dicer* deletion on nerve conduction velocity (NCV) and compound action potential (CAP) amplitude of the regenerating sciatic nerve, at 14 and 21 d after injury. Mice were euthanized by decapitation under deep anesthesia with ketamine (18 mg/ml)-xylazine (2 mg/ml), and sciatic nerves from injured and contralateral uninjured side were dissected from the ankle to the spinal column at a length of ~ 20 mm and immediately placed in Locke solution (154 mM NaCl, 5.6 mM KCl, 2.2 mM $CaCl_2$, 5 mM dextrose, 2 mM HEPES, pH 7.2), equilibrated to room temperature. Nerve segments were straightened and fixed in a slightly stretched position by pinning the two ends to the bottom of a Sylgard-lined dissecting dish. After removing all connective tissues from the nerves, glass suction electrodes were gently attached to the nerves, proximal and distal to the site of the injury, usually ~ 2 cm apart and bracketing the injury site by ~ 1cm. The proximal site was stimulated with a series of 10 constant-current pulses of 500 μA and 100 μs, at intervals of 2 s, to achieve a maximal and stable peak CAP response recorded at the distal side. To minimize the size of the stimulus artifact and maximize the size of the CAP signal, the diameters of the suction electrode were fabricated to match the diameter of the sciatic nerve. Signals were recorded, amplified with a 4-channel extracellular amplifier (AM Systems, Model 1700, Sequim, WA), and digitized with a Digidata 1322A using pClamp 10 software (both: Molecular Devices, Sunnyvale, CA, USA). Data were subsequently analyzed off-line with pClamp and SigmaPlot

(Version 11, Systat, San Jose, CA) software. In short, signal responses from injured nerves were rectified and the calculated integrals of these responses were measured against control epochs of identical duration from intact controls. Comparisons were made between the averaged amplitudes of ten consecutive responses measured between injured and un-injured sides at each time point.

Histological Evaluation of Re-myelinated Axons

Semi-thin sections of sciatic nerves were prepared to visualize the re-myelinated axons. The lesioned portions of the sciatic nerves were fixed with cold 2.5% glutaraldehyde, post-fixed with 1% osmium tetraoxide solution, dehydrated stepwise in increasing concentrations of ethanol, embedded with Low Viscosity Embedding Media Spurr's Kit (EMS, Hatfield, PA), and cut into transverse sections. Transverse semi-thin sections (1 μm thick) were stained with Richardson's solution. The number of myelinated axons was counted under bright field microscope at magnification of 40X. The myelinated axon area was quantified at 40X magnification using the NIH ImageJ software package, as described previously (McMurray et al., 2003).

Cell Cultures and Transfection

Dissociated DRG cultures

Mouse L4/5 dorsal root ganglion (DRG) neurons were collected 5 days after a conditioning sciatic nerve crush from both the intact side and injured side. DRGs were dissociated with collagenase and 0.25% trypsin in Dulbecco’s modified Eagle’s medium (DMEM) (GIBCO, Carlsbad, CA). The dissociated DRGs were plated on Poly-L-Lysine and

Laminin (Invitrogen, Carlsbad, CA), coated plates. DRGs were grown in DMEM/F12 containing 10% horse serum, L-glutamine and N2 supplement (Gemini Bio-product, West Sacramento, CA) at 37º C for 18hrs. To inhibit glial cell growth Cytosin β-D-arabinofuranoside (Arac, 10 μM) and 5,6-dichlorobenzimidazole riboside (DRB, 80 μM) (Sigma, Saint Louis, Missouri) or 50 nM 5-Fluoro-2'-deoxyuridine (Sigma) were added in the growth medium.

Administration of 4-hydroxytamixifen in cell cultures

To induce *Cre*-mediate *Dicer* knockout in neuronal cell cultures instead of in whole animals, DRGs were collected from *CAG-CreERt:Dicer*$^{fl/fl}$ mice and *Dicer*$^{fl/fl}$ mice without any treatments. DRG neuronal cells were dissociated and plated as describe previously. 4-hydroxytamoxifen (Sigma-Aldrich, St Louis, MO, USA) was dissolved in DMSO with sonication to obtain 1 μM stock solution and applied to DRG cultures in a final concentration of 1 nM. DRGs collected from *Dicer*$^{fl/fl}$ mice were cultured with either 4-hydroxytamoxifen or DMSO, corresponding to no-*Cre* group and vehicle treated group in other studies. DRG neurons collected from *CAG-CreERt:Dicer*$^{fl/fl}$ mice with 4-hydroxytamoxifen in culture media corresponded to *Dicer* knockout group.

PC12 cell cultures

PC12 cells were cultured in Dulbeccos' modified Eagle's medium (DMEM) containing 10% horse serum, 5% fetal bovine serum 2mM glutamine, and penicillin and streptomycin (100unitl/ml). The cells were plated on collagen-coated cell culture dishes. For NGF-induced differentiation of PC12 cells, NGF (50 ng/ml) was added to cell culture medium to initiate neurite outgrowth. Medium was refreshed every 2-3 days.

Transfection of miRNA mimics and inhibitors

In order to determine the biological effects of each individual miRNA on regenerative axon growth, we performed functional analyses for injured induced miRNAs. Gain-of-function experiments were performed with Ambion® Pre-miR™ miRNA Precursor Molecules, which are also called miRNA mimics. With transfection reagent, these small, chemically modified double-stranded RNA molecules can be introduced into cells and be taken up into the RNA-induced silencing complex, mimicking endogenous mature miRNAs activity. Loss of function analyses were performed with Ambion® Anti-miR™ miRNA Inhibitors. The miRNA inhibitors are chemically modified, single stranded nucleic acids designed to specifically bind to complementary miRNAs. The bindings between endogenous miRNA and miRNA inhibitors down-regulate endogenous miRNAs activity.

miRNA precursors and miRNA inhibitors were obtained from Ambion (Austin, TX). Transient transfections of DRGs were performed using Lipofectamine™ LTX and Plus Reagent (Invitrogen, Grand Island, NY) according to the manufacturer's protocol. To extend the time window for effective transfection of miRNA precursors and inhibitors, as well as, initiation of miRNA machinery, we incubated DRG neurons with 20 μM of SP600125 for the first 24 hours. SP600125 is a specific inhibitor of JNK and reversibly inhibits axonogenesis (Davare et al., 2009). We then released the block on axonogenesis from the SP600125 by washing out SP600125 and change culture media. DRG neurons were then cultured for an additional 24 hours to allow axon formation.

Immunofluorescent Staining and Image Analysis

After culturing lumbar DRGs on coverslips overnight, the cells were fixed with 4% paraformaldehyde for 5 min and washed with PBST. After blocking with 10% goat serum for 1 hour at room temperature, the samples were incubated with the indicated primary antibodies diluted at optimized concentrations at 4º C overnight. This was followed by incubation with secondary antibodies conjugated with FITC- , TX Red-, AMCA- or Alexa Fluor® (Invitrogen). Negative controls included samples processed in parallel with nonimmune serum or without primary antibodies. After mounting the slides with antifading media (Invitrogen), images were viewed with an Olympus IMT-2 fluorescent microscope and recorded using the Spot digital camera system (Diagnostic Instruments, Sterling Heights, MI), or viewed and captured with Leica DMI6000 B Imaging System powered by MetaMorph, or viewed with an Olympus IX81 fluorescent microscope and captured with CellSens Dimension software. The images we acquired were all single plane fluorescent images. For high magnification images and Z-stacks, images were taken with Olympus FluoView™ FV1000 confocal microscope at UNC Neuroscience Center (Chapel Hill, NC, USA).

Quantification of axon length and measurement of axon branches were performed following previously described lab protocol (Murashov et al., 2005). For each coverslip, 30 images were taken, and from each, 10-15 neurons, which were completely distinguishable from neighboring cells, were chosen for further analysis. The axon length was quantified by tracing the image of neurites with the ImageJ software. The longest axon for each neuron was measured and recorded. The number of neurite branches per neuron was also determined from each

neuronal population manually. Only branches longer than one cell body in length were counted (Liu et al., 2002).

Protein Lysates

Proteins were extracted from the sciatic nerves collected at specific time points. To obtain adequate proteins for these experiments, at least 5 animals were pooled per time-point. Samples of sciatic nerves were homogenized in ice-cold homogenization buffer, containing protease inhibitor cocktail (Sigma, St. Louis, MO), 1 mM PMSF, 20 mM Tris, 2 mM EGTA, 2 mM EDTA, 6 mM ß-mercaptoethanol and 10% Triton and centrifuged at 10,000g for 10 min at 4º C. The supernatant was transferred to a fresh tube and stored at -20º C until ready for use.

Immunoblotting Analysis

Tissue samples were homogenized in ice-cold homogenization buffer (20 mM Tris, 2 mM EGTA, 2 mM EDTA, 6 mM β-mercaptoethanol, 1 mM PMSF, and 10% Triton) containing protease inhibitor cocktail (Sigma, St. Louis, MO), and centrifuged at 10,000 g for 10 min at 4° C. The supernatants were collected in fresh tubes and stored at -20 °C. Proteins concentrations were quantified using the BioRad reagent (BioRad, Hercules, CA) and samples for western blot analysis were prepared by boiling with standard stop buffer for 5 min. Equal amounts of solubilized proteins were loaded per lane on sodium dodecyl sulfate gels and separated by electrophoresis. The separated proteins were then transferred to immobilon P membranes (Millipore Corporation; Bedford, MA).

Two types of secondary antibodies were used. When experiments were performed with horseradish peroxidase (HRP) conjugated secondary antibodies, membranes were blocked in 5%

non-fat milk/PBST for 1 hr at room temperature on a shaker, and then probed with primary antibody against FMRP (Darnell et al., 2005), Ago2 (Ikeda et al., 2006), P-100 (Keenan et al., 2000), DCP-1 (Lykke-Andersen, 2002) (Abnova; Walnut, CA), DCP-2 (Lykke-Andersen, 2002, Wang et al., 2002b), Rap55 (Yang et al., 2006), Ro52 and GWB IC-6 (Pauley et al., 2006) in 5% non-fat milk/PBST at 4º C overnight. For negative control groups, membranes were incubated with pre-immune serum. The membranes were washed three times with TBS, and then incubated with secondary antibody in 5% milk/PBST for two hours at room temperature. After incubation with horseradish peroxidase (HRP) conjugated secondary antibodies, bound antibodies were detected using a chemiluminescence detection system (ECL plus Western blotting detection reagent, Amersham; Arlington Heights, IL, USA). Densitometry was performed using Kodak 1D Image Analysis software.

When infrared dye (IRDye®) conjugated secondary antibodies were used, membranes were blocked in Odyssey blocking buffer (LI-COR, Nebraska, USA) for 1 hour at room temperature on a shaker, and then probed with primary antibody against *Dicer* (Abcam, MA, USA) at 4° C overnight. After washing, membranes were incubated in IRDye® conjugated secondary antibodies for one hour at room temperature with gentle shaking. The fluorescence signals on membrane were detected with the Odyssey® Infrared Imaging System (LI-COR).

Band values were normalized to alpha-tubulin, to obtain the relative signal intensity. One-way ANOVA were performed on injured, naive versus intact relative densitometric intensity for each antibody tested.

List of Antibodies

Primary antibodies

Rabbit polyclonal anti-AGO2- specific antibody (Tom Hobman, University of Alberta, Canada)

Guinea pig polyclonal anti-P100 antibody (Tom Keenan, VA Polytechnic Institute and State University, Blacksburg, VA)

Rabbit polyclonal primary antibody against DCP-1, DCP-2 (Jens Lykke-Anderson, University of Colorado, Colorado)

Rabbit polyclonal anti-DCP2 primary antibody (M. Kilejian, Rutgers University, New Jersey)

Human anti-Rap55 antibody (Donald Bloch, Harvard University, MA)

Antibody against GWB IC6 (Marvin Fritzler, University of Calgary, Alberta, Canada)

The specificities of the antibodies, provided by individual investigators, have been validated by original research groups and the corresponding data have been published elsewhere.

Mouse Anti-Human DCP1A Monoclonal Antibody from Abnova (Walnut, CA)

Rabbit anti-Ro52 polyclonal antibody from Millipore Corporation (Bedford, MA)

Mouse monoclonal neuro-specific beta III tubulin antibody (TUJ-1) from Covance Research Products, Inc. (Denver, PA)

Mouse monoclonal anti-FMRP antibody was purchased from Developmental Studies Hybridoma Bank (Iowa City, Iowa).

Rabbit polyclonal antibodies against *Dicer* (Abcam, MA, USA)

Goat polyclonal antibodies against *Kremen1* (R&D Systems, Minneapolis, MN)

Rabbit anti-GAP-43 polyclonal antibodies (Millipore, Billerica, MA)

Mouse monoclonal anti-α-Tubulin antibodies from ZYMED (ZYMED laboratories, Carlsbad, CA)

Secondary antibodies

HRP conjugated anti-rabbit IgG and HRP conjugated anti-mouse IgG from R&D system (Minneapolis, MN).

IRDye 800CW goat anti-Mouse IgG, IRDye 680LT goat anti-Rabbit IgG, and IRDye 800CW donkey anti-goat IgG secondary antibodies, (LI-COR Corporate, Nebraska USA).

For fluorescence studies, secondary FITC-, TX Red-, Cy-3, or Cy5-conjugated IgG (Jackson ImmunoResearch Laboratories, Inc; West Grove, PA) or Alexa Fluor 350 donkey anti-mouse IgG, Alexa Fluor 594 goat anti-human IgG, Alexa Fluor 594 donkey anti-goat from Invitrogen (Eugene, Oregon, USA) were applied.

Microarray Analyses

miRNA microarray analyses for sciatic nerve RNA

Total RNA for the microarray expression analysis was isolated from sciatic nerves, pooled from 10 mice, at 4 and 7 days after the sciatic nerve crush. 5 micrograms of total RNA were labeled with RNA ligase and a Cy3-conjugated dinucleotide, and hybridized to custom

oligonucleotide microarrays as described previously. Cy3 median intensity values were filtered to remove data points that did not exceed background levels by two fold. Values were log_2-transfomed and median centered by array. Clustering was performed with Cluster (Stanford University, CA, USA), using values that were median-centered by gene. Dendrograms and expression maps were generated using Treeview (Stanford). Some pooled samples were sent to UNC Lineberger Comprehensive Cancer Center Genomics Core. After a quality check, they were hybridized to an 8x15K miRNA one color arrays (Agilent, Santa Clara, CA, USA). Both custom and Agilent arrays were done in duplicates and repeated two times. Normalization and analyses were performed with GeneSpring software (Agilent). The GeneSpring analysis software was used for the identification of statistically significant upregulated or downregulated miRNAs at selected time points. The analysis also allowed for identification of a different temporal pattern of expression in the crushed groups compared with the control groups at the chosen points. For further analyses, we selected three miRNAs that were significantly upregulated and on that was significantly downregulated in both custom array as well as Agilent arrays.

miRNA and gene expression array analyses for DRG RNA

Total RNA for the microarray expression analysis was isolated from L4-L5 DRGs, pooled from 10 mice at 4 days after sciatic nerve crush. Total RNA extraction was performed with miRVANA^{TM} miRNA isolation kit following the manufacturer's instruction (Ambion). These pooled RNA samples were sent to UNC Lineberger Comprehensive Cancer Center Genomics Core for microarray analysis. After a quality control, they were hybridized to an 8x15 miRNA one color arrays (Agilent, Santa Clara, CA, USA). The same RNA samples were also hybridized to 4x44K mouse gene expression microarrays (Agilent) at the same Genomics Core. All microarray experiments were performed in duplicate and repeated twice. Normalization and

further analyses of microarray data were performed with GeneSpring software (Agilent). The analysis with GeneSpring allowed for identification of a different expression pattern of miRNAs in the crushed groups compared with the control groups. Statistically significant upregulated or downregulated miRNAs were then selected for further analysis.

Real-time RT-PCR

Total RNA was isolated from pooled sciatic nerves (n=6) for each group at each time points or from L4-L5 DRGs using *mir*Vana^{TM} miRNA Isolation Kit (Ambion, Austin, TX). Total RNAs from DRG neuronal cell cultures was purified with RNAqueous Micro Scale RNA Isolation Kit (Ambion, Austin, Texas, USA). RNA was quantified with a NanoDrop ND-1000 spectrophotometer (Thermo Scientific, Wilmington, DE). Reverse transcription was performed with NCode$^{\mathbf{TM}}$ VILO$^{\mathbf{TM}}$ miRNA cDNA Synthesis Kit and SuperScript VILO cDNA Synthesis Kit (Invitrogen, Life Technologies, Town, CA) for miRNA expression analysis and mRNA expression analysis respectively. The real-time PCR reactions were carried out using EXPRESS SYBER® GreenER™ qPCR SuperMix Universal (Invitrogen) in triplicates for each cDNA sample on Applied Biosystems 7500 Real-Time PCR System (Applied Biosystems, Life Technologies, Carlsbad, CA). Primers specific for each miRNA and mRNA were obtained from Invitrogen (Grand Island, NY). As an internal control, primers for S12 were added for RNA template normalization, and the relative quantification of gene and miRNA expressions were calculated against S12 using a $2^{-\Delta\Delta CT}$ method. All experiments were carried out three times independently.

List of primers

miR124a: 5’-TAAGGCACGCGGTGAATGCC-3’

miR221: 5’-AGCTACATTGTCTGCTGGGTTTC-3’

miR-199a: 5’-ACAGTAGTCTGCACATTGGTTA-3’

miR9: 5’-TCTTTGGTTATCTAGCTGTATGA-3’

miR21: 5’-TAGCTTATCAGACTGATGTTGA-3’

miR142-5p: 5’-CATAAAGTAGAAAGCACTACTAAAA-3’

miR-431: 5’-CAGGCCGTCATGCAAA-3’

miR-744: 5’-GGGCTAGGGCTAACAGCA-3’

miR-124: 5’-GCGGTGAATGCCAAAAA-3’

miR-29a: 5’-TAGCACCATCTGAAATCGGTTA-3’

Dicer: 5’-AGTGTAGCCTTAGCCATTTGC-3’ and 5’-CTGGTGGCTTGAGGACAAGAC-3’

Kremen1: 5’-ACAGCCAACGGTGCAGATTAC-3’ and 5’-TGTTGTACGGATGCTGGAAAG-3’

GAP-43: 5’TGGTGTCAAGCCGGAAGATAA-3’ and 5’-GCTGGTGCATCACCCTTCT-3’

PTK-9: 5’-AATGAGCAACTGGTGGTTGG-3’ and 5’-GGGCATTCTGAGAGTCTAACCT-3’

S-12: 5-’TGGCCCGGCCTTCTTTATG-3’ and 5’-CCTAAGCGGTGCATCTGGTT-3’

Negative control U6 was obtained from Ambion, mirVana™ qRT-PCR Primer Sets, catalog #30303.

Bioinformatic Prediction and Selection of Target Genes

Prediction for miR-431 target genes were conducted by 2 web-based miRNA target prediction programs: Targetscan (www.targetscan.org) and microRNA.org (www.microrna.org). Potential targets were chosen from genes predicted by both program, and the list of genes was compared with gene expression profile from gene expression array.

Since miR-431 was overexpressed in DRG after sciatic nerve injury, the expression of its target genes should be suppressed after injury. Therefore, selected genes had to meet the following criteria for the experimental analysis (Fig 2.2). First, they had to have a potential complementary binding site for miR-431 in their 3'UTR, as predicted by bioinformatics algorithms. Second, their expression level had to be downregulated in DRG after sciatic nerve crush in our gene expression array analysis. The changes in the expression of selected potential targets with transient transfection of miR-431 mimics in cell cultures were examined with RT-qPCR.

Figure 2.2. Selecting of potential target genes for miR-431

The list of genes with potential binding sites for miR-431 at their 3' UTR were generated by 2 web-based miRNA target prediction programs: Targetscan (www.targetscan.org) and microRNA.org (www.microrna.org). The list of genes significantly downregulated in DRG with overexpression of miR-431 after sciatic nerve injury was generated by gene expression array analyses. 24 genes that were on both lists were selected as potential target genes for further experimental validation.

miR-431 was first overexpressed transiently with miR-431 mimic in neuronal cells derived from PC12 cells. 8 out of 24 potential target genes showed downregulated expression. We further tested the expression of these 8 genes in DRG neuronal cell cultures with overexpression of miR-431. The 3 downregulated genes were selected for the following cross-linked immunoprecipitation (CLIP) experiments and western blot analysis.

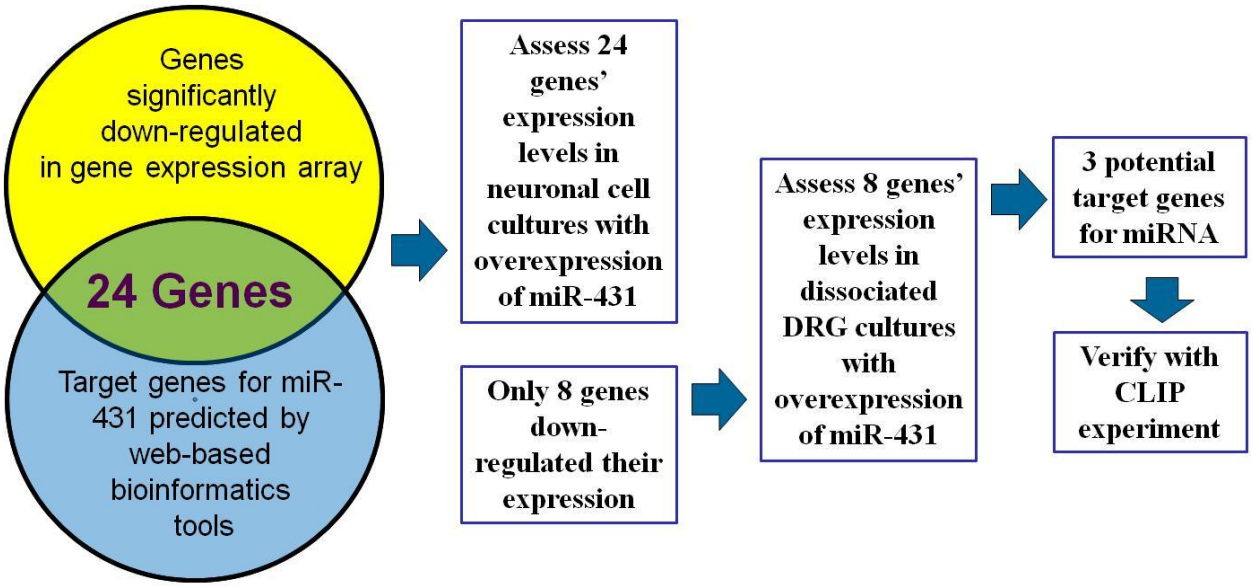
Genes significantly down-regulated in gene expression array
24 Genes
Target genes for miR-431 predicted by web-based bioinformatics tools
Assess 24 genes' expression levels in neuronal cell cultures with overexpression of miR-431
Only 8 genes down-regulated their expression
Assess 8 genes' expression levels in dissociated DRG cultures with overexpression of miR-431
3 potential target genes for miRNA
Verify with CLIP experiment

In Situ Hybridization

Similar to the immunofluorescence protocol described above, dissociated DRG cultures were postfixed in 4% paraformaldehyde solution in PBS at room temperature for 5 min, washed in PBS twice for 5 min and incubated in 100% methanol + 0.3% hydrogen peroxide solution for 10 min at 4° C. After two washes in PBS for 10 min, cell cultures were prehybridized at 42°C for 1 hour in hybridization buffer, containing 600 mM sodium chloride, 50mM sodium phosphate buffer (PH 7.0), 5.0 mM EDTA, 0.02% Ficoll (Sigma), 0.02% BSA (Sigma), 0.02% polyvinylpyrrolidone (Sigma), 200ng/ml sheared and denatured salmon sperm DNA (Sigma), and 40% formamide (Fisher Scientific, Pittsburgh, PA, USA). Hybridization was performed at 42° C in the same buffer with the addition of dextran sulfate to 7%, tRNA(baker's yeast) to 0.1 mg/ml, poly-A to 10µg/ml, and LNA antisense or sense oligonucleotide probes against miR-21, miR-142-5p and U6 to a final concentration of 1 ng/µl. Mir-21 FITC –labeled LNA antisense and sense probes were obtained from RiboTask (Odense, Denmark). Mir-142-5p FITC –labeled LNA antisense and scrambled probes, and a U6 LNA probe were obtained from Exiqon (Woburn, MA). After hybridization coverslips were incubated for 1 hour with primary antibodies against FITC, neuronal β-tubulin and GWB. To visualize the signal, FITC-, TX Red-, and AMCA- labeled secondary antibodies (Invitrogen) were applied for 1 hour in 1:100 dilution. Slides were viewed on an Olympus IMT-2 fluorescent microscope.

Cross-Linked Immunoprecipitation Analysis

DRG neuronal cell cultures were transfected with 100 nM of miR-431 mimic or a scrambled miRNA mimic negative control. Two days post-transfection, the cells were rinsed once in PBS and then placed in Crosslinker with the cover off. Cells were irradiated once for 400

mJ/cm^2 and once more for 200 mJ/cm^2 to establish protein-RNA reversible crosslinking. Cell were lysed in cell lysis buffer (100 mM KCL, 5 mM MgCl2, 10 mM HEPEs, PH 7.0, 0.5% NP-40, 1 mM DTT, 100 U/ml RNasin RNase inhibitor (Promega), 2 mM vanadyl ribonucleoside complexes solution (Sigma),) supplemented with a mixture of protease inhibitors (Invitrogen, Grand Island, NY). Cells were then detached with a cell scraper and lysate was transferred to a tube on ice. Cell lysates were centrifuged at 16,000g for 15 min at 4º C. Prior to the immunoprecipitation, protein G agarose beads (Sigma, St. Louis, MO) were equilibrated by washing twice with a wash buffer (0.5% NP-40, 150 mM NaCl, 2 mM MgCl2, 2 mM Cacl2, 20 mM Tris, pH. 7.5, 5 mM DTT, with protease inhibitor) containing 1 mg/mL yeast tRNA and 1mg/mL BSA. After pre-clearing the lysate with equilibrated protein G-agarose beads, 5 μl of each sample was saved as an input fraction. The protein lysate was immunoprecipitated with specific mouse monoclonal antibodies against Ago2 (Wako, Richmond, VA) or control serum and bounded by protein G agarose beads with agitation at 4° C overnight. After precipitation, the beads were washed 3 times with washing buffer. Afterwards, the bonds between RNA and protein were disrupted by heating at 50° C for 30 minutes. RNA was then extracted and purified using Trizol (Invitrogen).

Statistical Analysis

Data from multiple independent experiments were analyzed with GraphPad Prism version 5 for Windows (GraphPad Software; San Diego, CA, USA). The results were expressed as mean ± standard error of the mean in graphic and text representations. For comparing injured groups, naïve group, and intact group, statistical analysis was performed with one-way ANOVA and

Newman-Keuls Multiple Comparison Test using Prism (GraphPad Prism version 3.00 for Windows, GraphPad Software; San Diego, CA, USA). The difference between 3 groups (*CAG-CreERt:Dicer*$^{fl/fl}$ mice with tamoxifen treatment, *CAG-CreERt:Dicer*$^{fl/fl}$ mice with vehicle treatment, and *Dicer*$^{fl/fl}$ littermates with tamoxifen treatment) at each time point were evaluated with one-way ANOVA followed by Bonferroni's multiple comparison test using GraphPad Prism version 5 for Windows (GraphPad Software; San Diego, CA, USA). In the last specific aim, to determine the difference between three or more groups, one-way ANOVA followed by Bonferroni's multiple comparison tests was utilized. For the analysis of two independent groups, student's t-test was used. A p-value of less than 0.05 was considered statistically significant.

CHAPTER III: MicroRNA Machinery Responds to Peripheral Nerve Lesion in an Injury-regulated Pattern.

Summary

Recently, functional and potent RNA interference (RNAi) has been reported in peripheral nerve axons transfected with short-interfering RNA (siRNA). In addition, components of RNA-induced silencing complex (RISC) have been identified in axotomized sciatic nerve fibers as well as in regenerating dorsal root ganglia (DRG) neurons *in vitro*. Based on these observations, and on the fact that siRNA and microRNAs (miRNA) share the same effector enzymes, we hypothesized that the endogenous miRNA biosynthetic pathway would respond to peripheral nerve injury. To answer this question, we investigated changes in the expression of miRNA biosynthetic enzymes following peripheral nerve crush injury in mice. Here we show that several pivotal miRNA biosynthetic enzymes are expressed in an injury-regulated pattern in sciatic nerve *in vivo*, and in DRG axons *in vitro*. Moreover, the sciatic nerve lesion induced expression of mRNA-processing bodies (P-bodies), which are the local foci of mRNA degradation in DRG axons. In addition, a group of injury-regulated miRNAs was identified by miRNA microarray and validated by qPCR and in situ hybridization analyses. Taken together, our data support the hypothesis the peripheral nerve regeneration processes may be regulated by miRNA pathway.

Introduction

One of the unique features of the peripheral nervous system (PNS) is its ability to regenerate axons after injury (Yoo et al., 2009). To initiate a regenerative response, the PNS neuron must shift its physiology from synaptic transmission and maintenance of structure to the growth of the axon (Benowitz and Yin, 2007). Shifting to the growth phenotype requires both activation of a growth program via gene transcription as well as activation of local signaling cascades that regulate axon assembly (Snider et al., 2002, Vogelaar et al., 2009). Recent observations suggest that the microRNA (miRNA) pathway may be involved in regulation of these processes (Hengst et al., 2006, Murashov et al., 2007).

The miRNA pathway is an important layer of post-transcriptional gene regulation (Jackson et al., 2010). MiRNAs are initially processed in the nucleus by biosynthetic enzymes, Drosha and DGCR8/Pasha, while in cytoplasm *Dicer* cleaves them into the mature miRNAs (Bernstein et al., 2001, Lee et al., 2003). MiRNAs then trigger formation of RNA-induced silencing complex (RISC), which is implicated in a sequence-specific translational repression called RNA interference (RNAi) (Bagga et al., 2005, Tan et al., 2009). Several subunits of RISC have been conclusively identified to date: Argonaute2 (Ago2) nuclease (Hammond et al., 2001, Meister and Tuschl, 2004), fragile X mental retardation protein (FMRP) (Ishizuka et al., 2002), p100 (Caudy et al., 2003), TRBP (Chendrimada et al., 2005), PACT (Lee et al., 2006), and RCK/p54 (Chu and Rana, 2006). Recent studies showed that Argonaute proteins interact with the RNA-binding protein GW182 (Sen and Blau, 2005, Eulalio et al., 2009a, Eulalio et al., 2009b, Takimoto et al., 2009). Observations revealed that GW182-containing foci, known as GW bodies (GWBs), coincide with mRNA-processing bodies (P-bodies) where GW182 co-localizes with the

de-capping complex (Dcp1, Dcp2), Rap55 and Ro52 (Sen and Blau, 2005, Bhanji et al., 2007, Eulalio et al., 2009a, Eulalio et al., 2009b, Takimoto et al., 2009). Importantly, depleting GW182 suppressed silencing of miRNA targets. Therefore, these observations suggest that in addition to RISC, target silencing by miRNAs is regulated by P-bodies.

Recent studies revealed the differential expression of a number of miRNAs following traumatic injury in CNS, including the brain and spinal cord (Lei et al., 2009). Reduction in the expression of several sensory organ-specific miRNAs was also observed in the injured ipsilateral dorsal root ganglion (DRG) following spinal nerve ligation (SNL) (Aldrich et al., 2009). These evidences suggest that miRNAs are likely to be important mediators of plasticity. Functional RNAi machinery has been reported in axons of PNS neurons (Yoo et al., 2009). Components of RISC were observed in severed sciatic nerve fibers and cultured DRG axons (Hengst et al., 2006, Murashov et al., 2007). Based on these observations and on the fact that siRNA and miRNA share the same effector enzymes, it is logical to presume that the endogenous miRNAs machinery could be involved in the regulation of molecular response to peripheral nerve injury.

In the current study, we asked whether miRNA might be one of the pathways that respond to peripheral nerve injury. Here we show an injury-regulated expression of several pivotal miRNA biosynthetic enzymes in murine sciatic nerve *in vivo*, and in DRG axons *in vitro*. In addition, a group of miRNAs, which were expressed in an injury-regulated pattern in regenerating sciatic nerve and DRG was identified by miRNA microarrays, qPCR and *in situ* hybridization. These data provide further evidence in support of the hypothesis that the peripheral nerve regeneration processes may be regulated by miRNA pathway.

Results

Levels of miRNA biosynthetic proteins in sciatic nerve are regulated by injury

To investigate whether the expression of miRNA biosynthetic proteins was correlated with injury, we first determined the expression of protein components of RISC (FMRP, Ago2 and P-100) and P-body (DCP-1, DCP-2, Rap55, Ro52 and GWB IC-6) at 4 and 7 days post-crush. In a mouse, the process of nerve regeneration has been shown to be active over this period, justifying the time-points for these experiments (Garbay et al., 2000, McMurray et al., 2003). Previous studies in our lab already showed the existence of the components of RISC in peripheral nerve axon *in vivo* and vitro (Murashov et al., 2007). Here we used immunoblot analyses to determine the injury-regulated expression of biosynthetic components of RISC and P-body. Immunoblot analysis revealed the expression of the components of these multiprotein complexes in response to injury, indicating the potential role of miRNA biosynthetic machinery in peripheral nerve regeneration. Figure 3.1 indicates that the expressions of the RISC components, including FMRP, Ago-2, and P-100 were induced in response to injury, when compared to intact nerve. The densitometry showed significantly elevated levels of Ago2, FMRP, and P-100 respectively at 4 days (Fig. 3.1A) and 7 days (Fig. 3.1B) after injury. The contralateral naïve side of the nerve had the comparable expression level of RISC components as the intact nerve. The results indicated the induction of RISC in sciatic nerve upon injury. In addition, the injury differentially affected levels of P-body proteins, another miRNA-associated multiprotein complex (Fig. 3.2). We observed upregulation of DCP-1 and GWB IC-6 at 4 days following sciatic nerves injury (Fig. 3.2 A) and downregulation of DCP-2 and Ro2 respectively, in response to 4 day post injury (Fig. 3.2 A). In contrast, the expression of Rap55 was not

affected by the injury. Therefore, the results indicated that injury to sciatic nerve selectively affected the expression of the P-body components.

Components of miRNA machinery are differentially expressed in dissociated DRG neurons after injury

In the previous experiments we showed that miRNA machinery was present and induced in peripheral nerve after injury. In the next experiment we asked whether the source of the differentially expressed miRNA biogenesis enzymes might be of axonal origin. To answer this question, we performed immunofluorescence staining on murine dissociated DRG neurons to visualize the presence of P-body proteins in axons. The DRG neurons plated at a low density were stained with FITC conjugated antibodies against DCP-1 (Fig. 3.3B) and Alexa 594-conjugated antibodies against GWB IC-6 (Fig. 3.3C). The human polyclonal serum against GWB was used previously to detect P-bodies. Since the polyclonal antibodies could detect other proteins associated with GW182 protein in GWB, antibodies against DCP-1, another major component in P-bodies was used to further confirm the localization of P-bodies in axon. AMCA staining against TUJ1, a neuronal marker indicated the location of neuronal soma and axons (Fig. 3.3A). Confocal immunofluorescence showed colocalization of GWB IC-6 with DCP-1 in the varicosities along axons (Fig. 3.3D). A Z-scanning showed a complete overlap of immunoreactivities against DCP-1 and GWB in axons.

These results clearly demonstrated the colocalization of P-bodies proteins in the varicosities along axons. By comparing the images of DRG neurons collected from the injured side (Fig. 3.4A) and the DRG neurons collected from the naïve side (Fig. 3.4B), we revealed that preconditioning by crush injury not only induces more robust axon regenerative growth but also

induces the formation of P-bodies in regenerating axons. Quantifications of the mean number of the varicosities containing P-bodies per neuron in naïve versus regenerating DRG cultures revealed that the average number of varicosities containing P-bodies per neuron increased over ~2.4 fold, from around 3 (n=30) to around 8 (n=30) following injury (Fig. 3.4 C). These findings were consistent with the Western Blot results, which indicated that the expression of miRNA biogenesis enzymes followed an injury-regulated pattern.

MiRNAs and genes are expressed in an injury-regulated pattern after conditioning nerve lesion

Since we observed an injury-regulated expression of miRNA biosynthetic enzymes after the sciatic nerve crush, we asked if the pattern of miRNA expression could be also injury-regulated. Total RNA was isolated from pooled crushed and contralateral intact sciatic nerves and subjected to custom and Agilent miRNA expression arrays. Genespring analysis of array data revealed a set of differentially expressed miRNAs. The miRNAs that were following injury-regulated expression pattern at both 4 and 7 days post-crush were selected for subsequent analyses. Three most high upregulated miRNAs, that is, miR-21, miR-142-5p, and miR-221 as well as brain-specific miR-124a, which was significantly downregulated were selected for further analyses (Table 1 and 2).

qPCR confirms injury-regulated expression of miR-21, miR-142-5p, miR-221, and miR-124a

To verify the result of miRNA array, we next determined the expression of selected miRNAs in the same total RNA samples that were used for arrays. Real-time RT-PCR demonstrated the same pattern of expression of miR-124a, miR-221, miR-142-5p, and miR-21,

after sciatic nerve crush (Fig. 3.5). In agreement with the microarray data, the real time RT-PCR demonstrated that miR-124a is significantly down-regulated after nerve injury. At the same time, we observed an up-regulation of miR-221, miR-142-5p, and miR-21 expression. These data provided further evidence that miRNAs expression could be injury-regulated.

In situ hybridization analysis localized injury-regulated miRNAs miR-21 and miR-142-5p to regenerating DRG axons

In the previous experiments we have shown that several miRNAs are induced in an injury-regulated pattern in peripheral nerve. The potential sources of miRNAs in crushed nerve samples could include glial cells, connective tissue, macrophages, and axons. In the next experiment we asked whether the identified differentially expressed miRNAs might be present in regenerating DRG neurons. To answer this question, we performed fluorescent in situ hybridization (FISH) on murine dissociated DRG neurons plated at a low density to visualize the presence of miRNAs in cell bodies and axons. For this experiment, we selected miR-21 and miR-142-5p, which showed an upregulation by injury in the miRNA arrays. After FISH, DRG preparations were immunostained with TUJ1 antibody against neuron-specific β-tubulin. The localization of P-bodies was visualized by immunostaining against GWB IC-6. Analyses of these immunofluorescent images revealed presentation of miR-21 and miR-142-5p in DRG cells and axons (Fig. 3.6). Interestingly, the distribution of miRNAs in the axon was overlapping with P-bodies immunostaining included in axon VR. These results demonstrate an interesting possibility that miRNAs could be induced in cell body on crush and subsequently translocated into the axon.

Table 3.1. Regulation of miRNAs at 4 days after nerve crush.

Total RNA for the microarray expression analysis was isolated from sciatic nerves, pooled from 10 mice, at 4d and 7d after the sciatic nerve crush. Both custom and Agilent arrays were done in duplicates and repeated two times. Normalization and analyses were performed with GeneSpring software (Agilent). Data from custom and Agilent arrays were $\log_2$-transformed and median-center by array. The GeneSpring analysis software was used for the identification of statistically significant upregulated or downregulated miRNAs at selected time points. The analysis also allowed for identification of a different temporal pattern of expression in the crushed groups compared with the control groups at the chosen time. For further analyses we selected three miRNAs that were significantly upregulated and on that was significantly downregulated in both custom arrays as well as in Agilent arrays.

Note the similarities in the expressions of miRNAs between 4 d (Table 3.1) and 7 d (Table 3.2) post sciatic nerve injury.

Custom array	Fold difference regulation	Agilent array	Fold difference regulation	Average of both arrays	Fold difference regulation
miR-424	2.05 up	miR-29b	2.14 up	miR-29b	2.26 up
miR-223	2.22 up	miR-142-5p	2.27 up	miR-142-5p	2.42 up
miR-29b	2.38 up	miR-221	2.63 up	miR-424	2.43 up
miR-142-5p	2.56 up	miR-223	2.70 up	miR-223	2.46 up
miR-221	2.77 up	miR-424	2.81 up	miR-221	2.70 up
miR-142-3p	5.21 up	miR-142-3p	4.56 up	miR-142-3p	4.88 up
miR-21	13.67 up	miR-21	13.04 up	miR-21	13.36 up
miR-133b	1.23 down	miR-99a	2.02 down	miR-99a	1.67 down
miR-99a	1.32 down	miR-124a	2.04 down	miR-30d	1.77 down
miR-30d	1.39 down	miR-125b	2.08 down	miR-143	1.86 down
miR-143	1.60 down	miR-100	2.09 down	miR-124a	1.92 down
miR-9*	1.66 down	miR-422b	2.11 down	miR-9*	1.94 down
miR-9	1.72 down	miR-143	2.12 down	miR-100	1.95 down
miR-124a	1.79 down	miR-30d	2.15 down	miR-422b	1.98 down
miR-100	1.81 down	miR-9*	2.22 down	miR-125b	2.03 down
miR-30a-3p	1.82 down	miR-138	2.40 down	miR-9	2.13 down
miR-422b	1.84 down	miR-338	2.44 down	miR-30a-3p	2.18 down
miR-150	1.95 down	miR-9	2.54 down	miR-338	2.24 down
miR-125b	1.98 down	miR-30a-3p	2.55 down	miR-138	2.26 down
miR-338	2.04 down	miR-145	2.75 down	miR-150	2.52 down
miR-182	2.07 down	miR-150	3.08 down	miR-145	2.64 down
miR-138	2.11 down	miR-183	3.23 down	miR-204	2.78 down
miR-204	2.32 down	miR-204	3.23 down	miR-182	2.79 down
miR-183	2.44 down	miR-182	3.51 down	miR-183	2.83 down
miR-145	2.53 down	miR-133b	4.47 down	miR-133b	2.85 down

Table 3.2. Regulation of miRNAs at 7 d after nerve crush.

Custom array	Fold difference regulation	Agilent array	Fold difference regulation	Average of both arrays	Fold difference regulation
miR-29b	1.13 up	miR-29b	2.17 up	miR-29b	1.13 up
miR-223	1.49 up	miR-142-5p	2.30 up	miR-223	1.49 up
miR-221	1.87 up	miR-221	2.72 up	miR-221	1.87 up
miR-142-5p	1.94 up	miR-223	2.75 up	miR-142-5p	1.94 up
miR-424	2.11 up	miR-424	2.79 up	miR-424	2.11 up
miR-142-3p	3.06 up	miR-142-3p	4.55 up	miR-142-3p	3.06 up
miR-21	8.80 up	miR-21	13.75 up	miR-21	8.80 up
miR-30d	2.01 down	miR-143	1.94 down	miR-30d	2.01 down
miR-183	2.04 down	miR-9*	1.97 down	miR-183	2.04 down
miR-150	2.04 down	miR-125b	1.98 down	miR-150	2.04 down
miR-99a	2.05 down	miR-422b	1.98 down	miR-99a	2.05 down
miR-133b	2.05 down	miR-30d	2.11 down	miR-133b	2.05 down
miR-9*	2.06 down	miR-124a	2.18 down	miR-9*	2.06 down
miR-422b	2.07 down	miR-99a	2.21 down	miR-422b	2.07 down
miR-30a-3p	2.18 down	miR-338	2.23 down	miR-30a-3p	2.18 down
miR-100	2.18 down	miR-138	2.28 down	miR-100	2.18 down
miR-182	2.25 down	miR-100	2.33 down	miR-182	2.25 down
miR-124a	2.34 down	miR-9	2.59 down	miR-124a	2.34 down
miR-204	2.35 down	miR-30a-3p	2.75 down	miR-204	2.35 down
miR-138	2.36 down	miR-145	2.93 down	miR-138	2.36 down
miR-125b	2.47 down	miR-204	3.23 down	miR-125b	2.47 down
miR-338	2.47 down	miR-182	3.28 down	miR-338	2.47 down
miR-9	2.50 down	miR-183	3.32 down	miR-9	2.50 down
miR-143	2.81 down	miR-150	3.84 down	miR-143	2.81 down
miR-145	3.23 down	miR-133b	4.26 down	miR-145	3.23 down

Figure 3.1. Immunoblot analyses for FMRP, Ago2, and p-100 protein in sciatic nerve.

Proteins were extracted from 3 groups of pooled samples (intact sciatic nerves, the contralateral naive nerve and the injured sciatic nerve) at 4 days or 7 days after a conditioning nerve lesion. Immunoblot analyses were conducted with primary antibodies against FMRP, AGO2, and p-100. Using the expression level in intact nerve as a control, relative densitometry were normalized to alpha-tubulin. Quantified bands densitometry showed a more abundant expression of RISC component (FMRP, Ago2, p-100) in injured sciatic nerve at both 4 days (A) and 7 days (B) after injury (N=3, * indicate $P<0.05$, ** indicate $P<0.01$). Representative immunoblot of FMRP, Ago2, and p-100 protein in sciatic nerve from 3 independent experiments were shown in C.

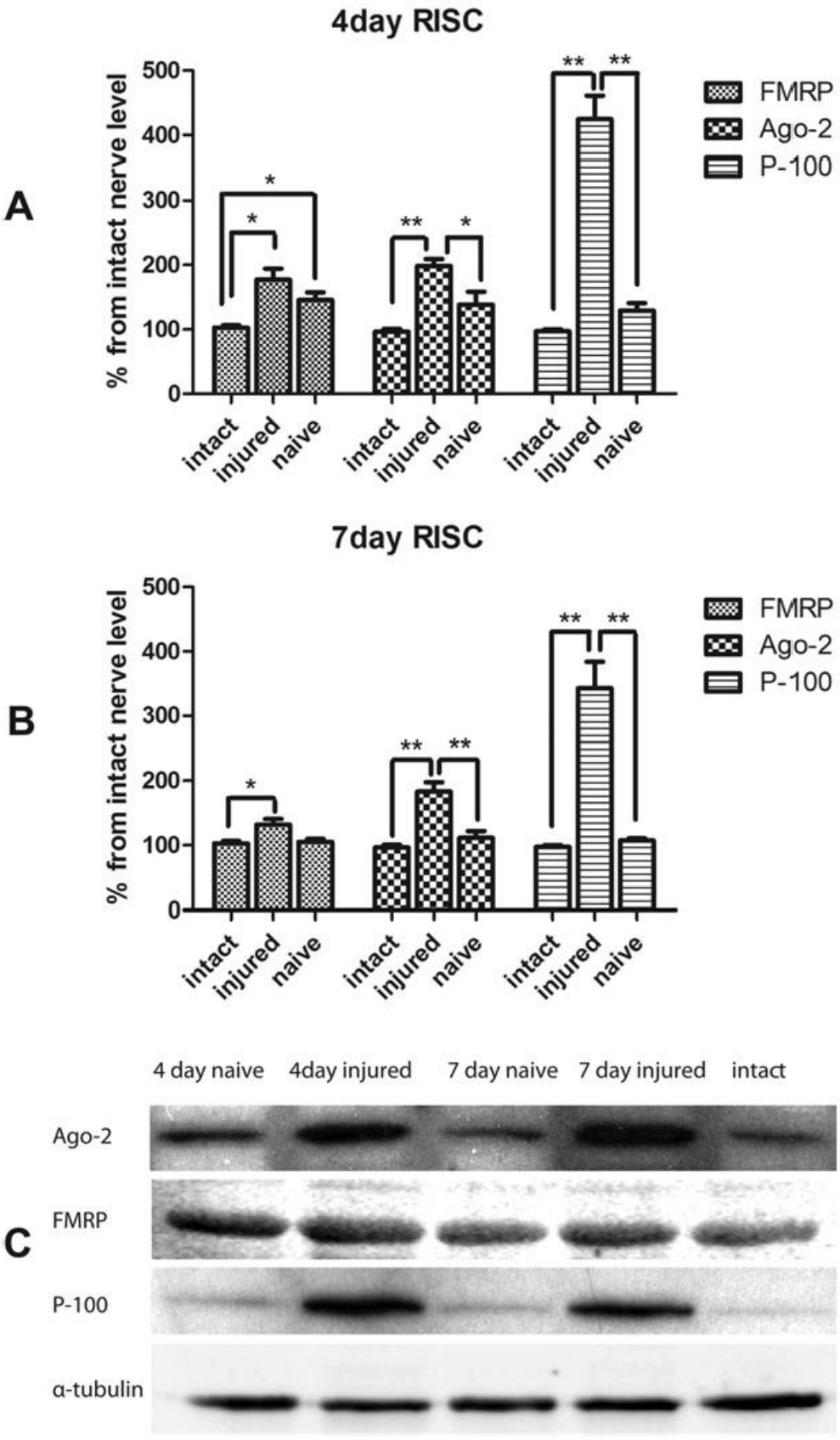
A
4day RISC
% from intact nerve level
500
400
300
200
100
0
FMRP
Ago-2
P-100
intact
injured
naive
B
7day RISC
C
4 day naive
4day injured
7 day naive
7 day injured
intact
Ago-2
FMRP
P-100
α-tubulin

Figure 3.2. Western Blot analyses of P-body components in the sciatic nerve after injury.

Western Blot analysis of P-body components in the sciatic nerve utilized the primary antibody against DCP-1, DCP-2, Rap55, Ro52, and GWB IC6. Pooled samples (6 nerves each sample) were extracted from intact sciatic nerves, the contralateral naive nerve and the injured sciatic nerve at 4 days or 7 days after a conditioning nerve lesion. Protein levels were quantified by band densitometry and normalized to alpha-tubulin at 4 days (A) and 7 days (B) after conditional lesion. Immunostaining for DCP-1, the catalytic factor for DCP-2, showed an increase in expression in response to injury, whereas the expression of DCP-2, the decapping enzyme in P-body, decreased after injury at both time points. Immunostaining for GWB IC-6 showed much higher GWB IC-6 expression at 4 days and 7 days after injury, while Rap-55 showed no change in expression in response to injury. Ro52 expression level was significantly decreased following injury. (N=3, * indicates $P<0.05$, ** indicates $P<0.01$) Representative immunoblot of protein DCP-1, DCP-2, Rap55, Ro52, and GWB IC6in sciatic nerve were shown in (C).

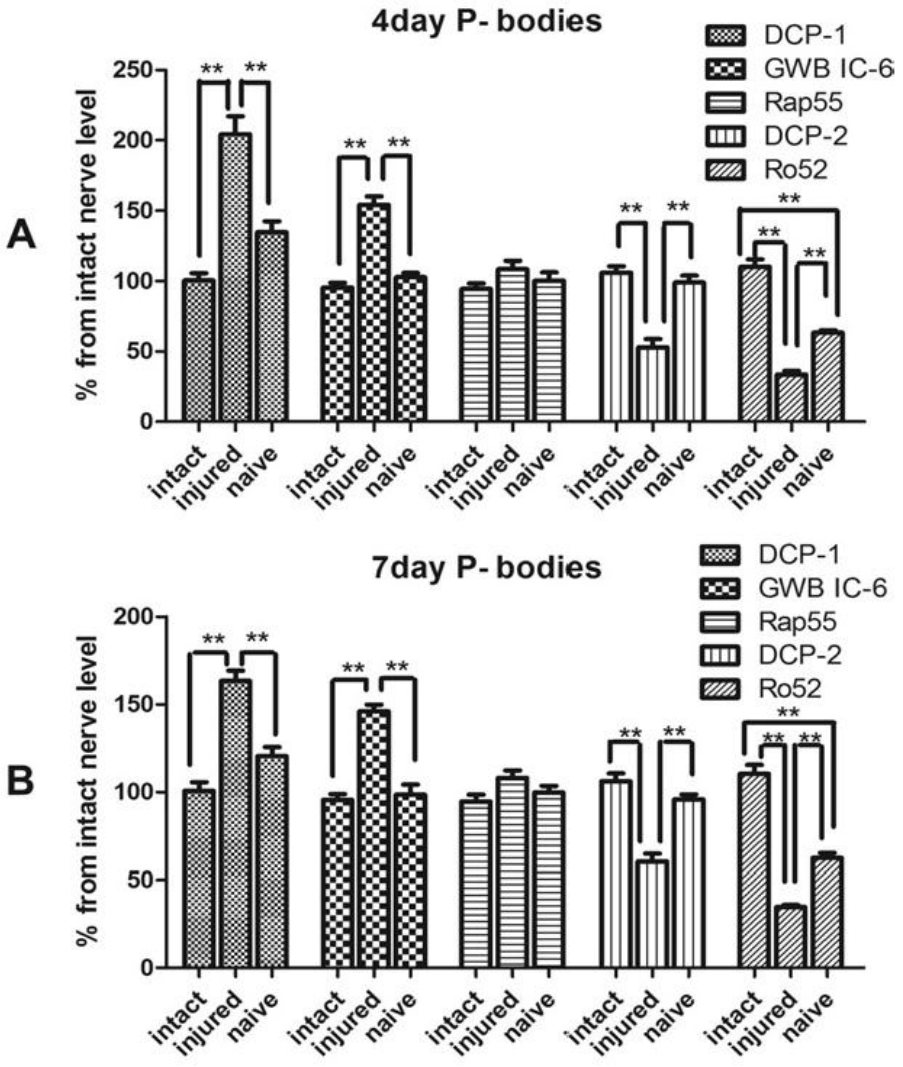
A
4day P- bodies
DCP-1
GWB IC-6
Rap55
DCP-2
Ro52
% from intact nerve level
250
200
150
100
50
0
**
intact
injured
naive
B
7day P- bodies
DCP-1
GWB IC-6
Rap55
DCP-2
Ro52
% from intact nerve level
200
150
100
50
0
intact
injured
naive

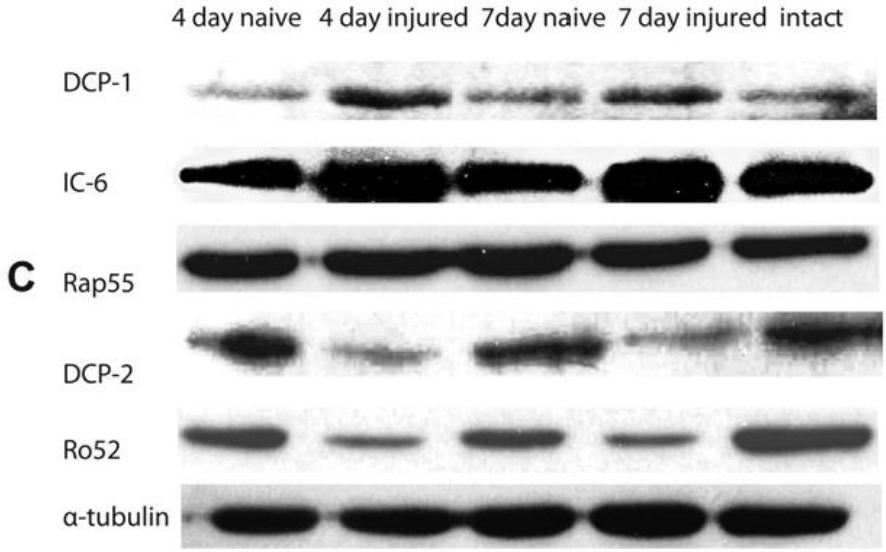
4 day naive
4 day injured
7day naive
7 day injured
intact
C
DCP-1
IC-6
Rap55
DCP-2
Ro52
α-tubulin

Figure 3.3. Colocalization of P-body proteins in regenerating DRG axons.

Dissociated cultures of mouse DRG neurons collected 5 days after a conditioning lesion were co-labeled with FITC (green) conjugated antibodies to DCP1 (B) and Alexia 594 (red) conjugated antibodies to GWB IC-6 (C). TUJ1 (Blue) staining indicated the location of the axon (A). The merged images revealed co-localizations of investigated proteins in regenerating axons (D). The Z-scanning further confirmed their co-localization on the same level in the axon (E). White arrows in Image (D) indicated P-bodies in the VR.

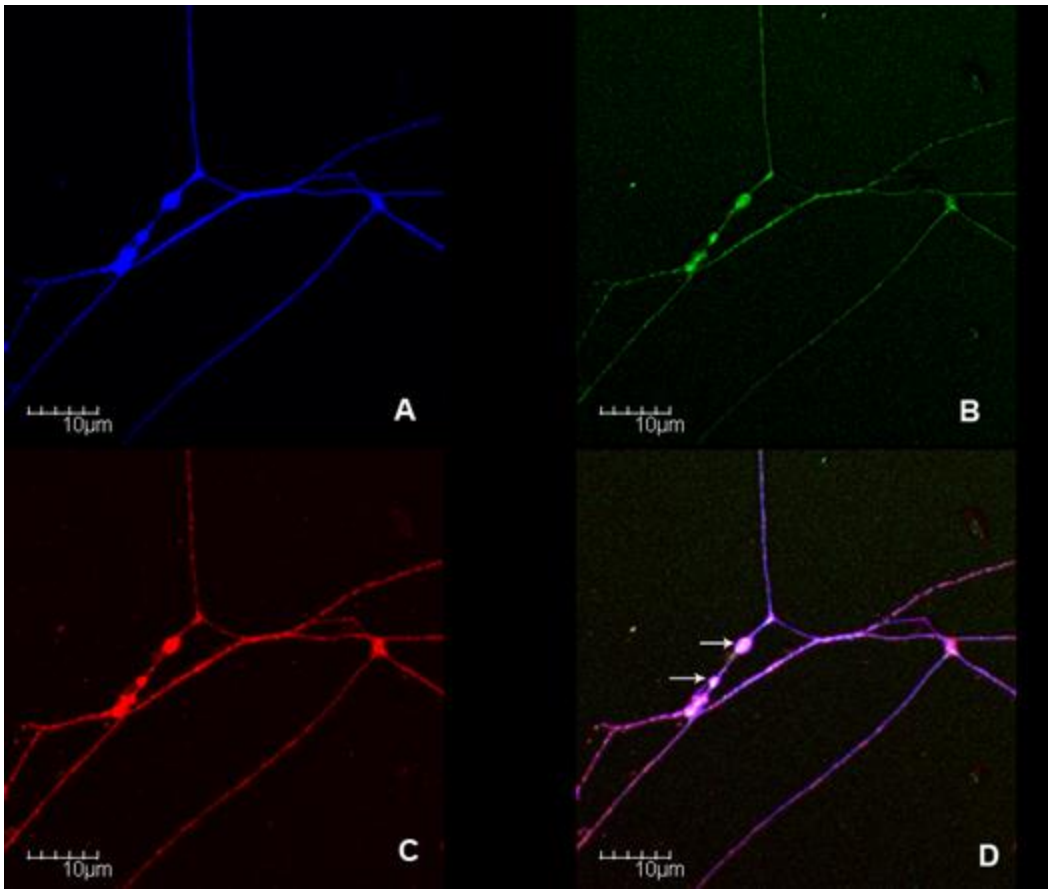
10µm
A
10µm
B
10µm
C
10µm
D

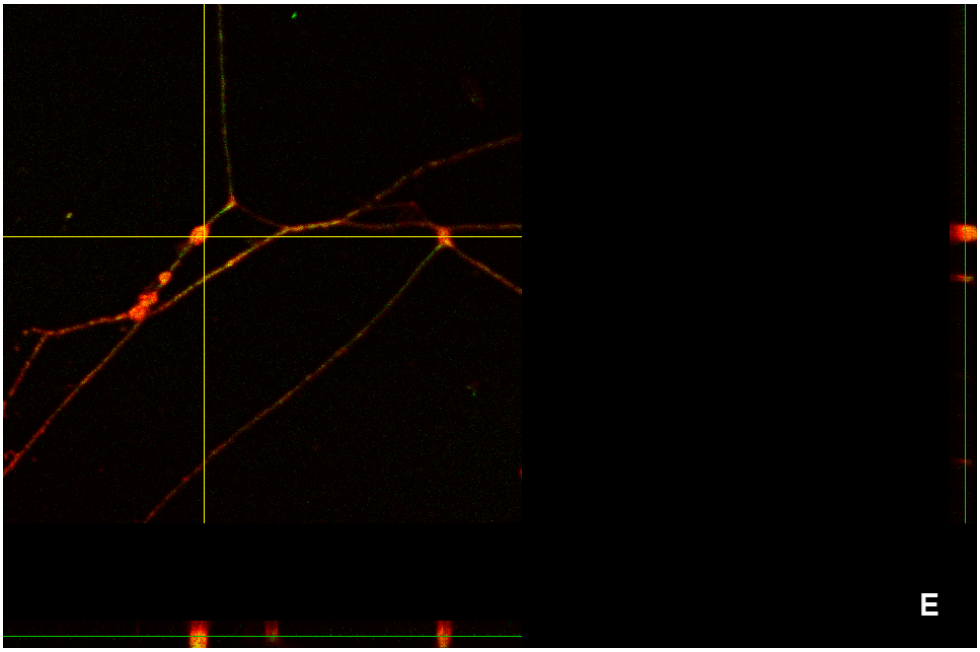
E

Figure 3.4. Number of varicosities along the axon containing P-bodies markedly increases after conditioning lesion.

Low density dissociated DRG cultures were labeled with antibodies to neuronal maker TUJ1 (Blue), DCP-1 (Green) and GWB IC-6 (Red). Merges of the images revealed the localization of the P-bodies in soma and axon. The appearance of P-bodies was limited to varicosities along the axon. The fluorescent images in upper panel showed neurons cultures after sciatic nerve crush pre-conditioning (A). The images in lower panel showed neurons from naïve side (B). After injury, the average number of VR containing P-bodies (white arrows) per neuron has significantly increased (C). Scale bar on microphotographs is 100μm.

A

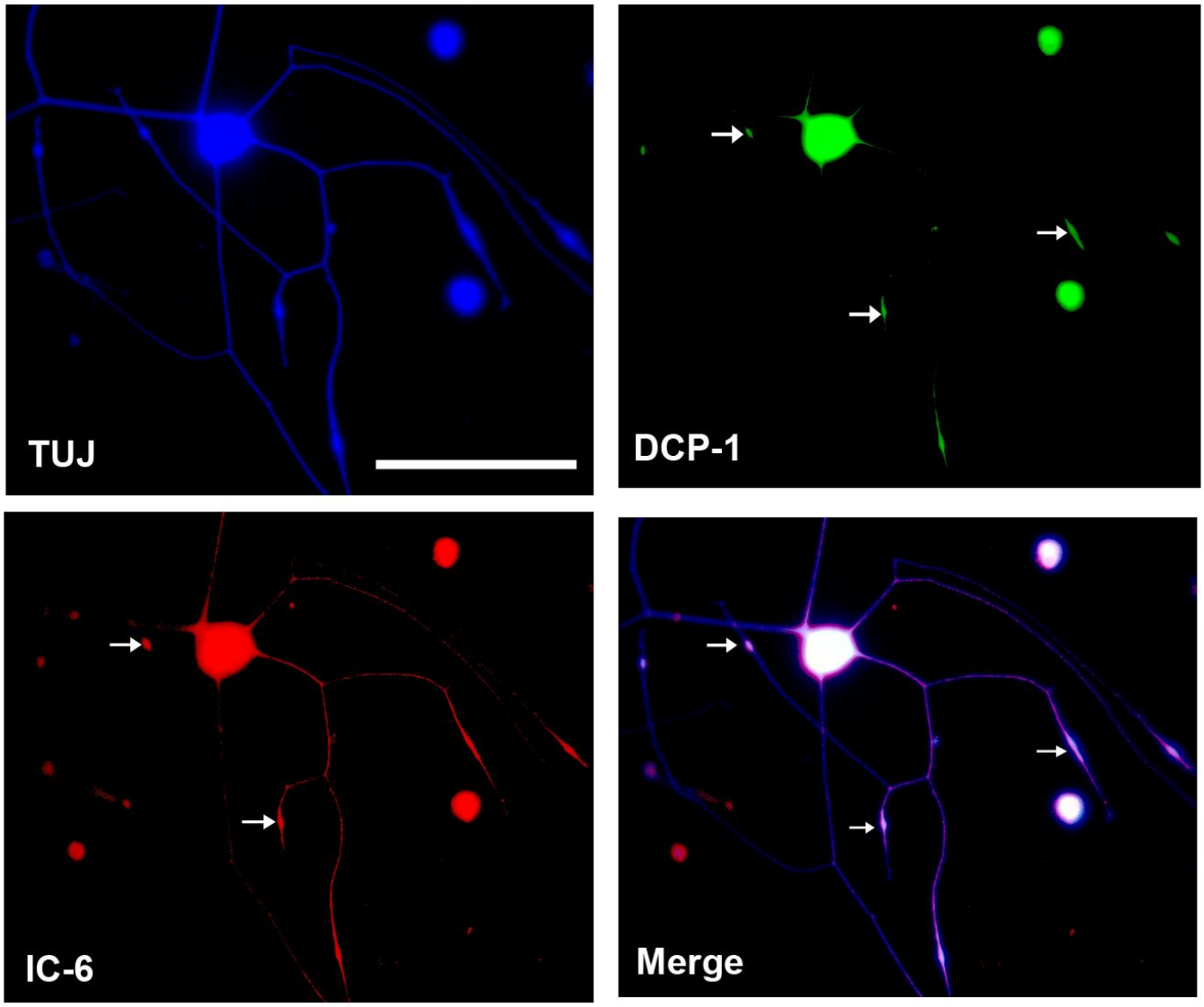

B

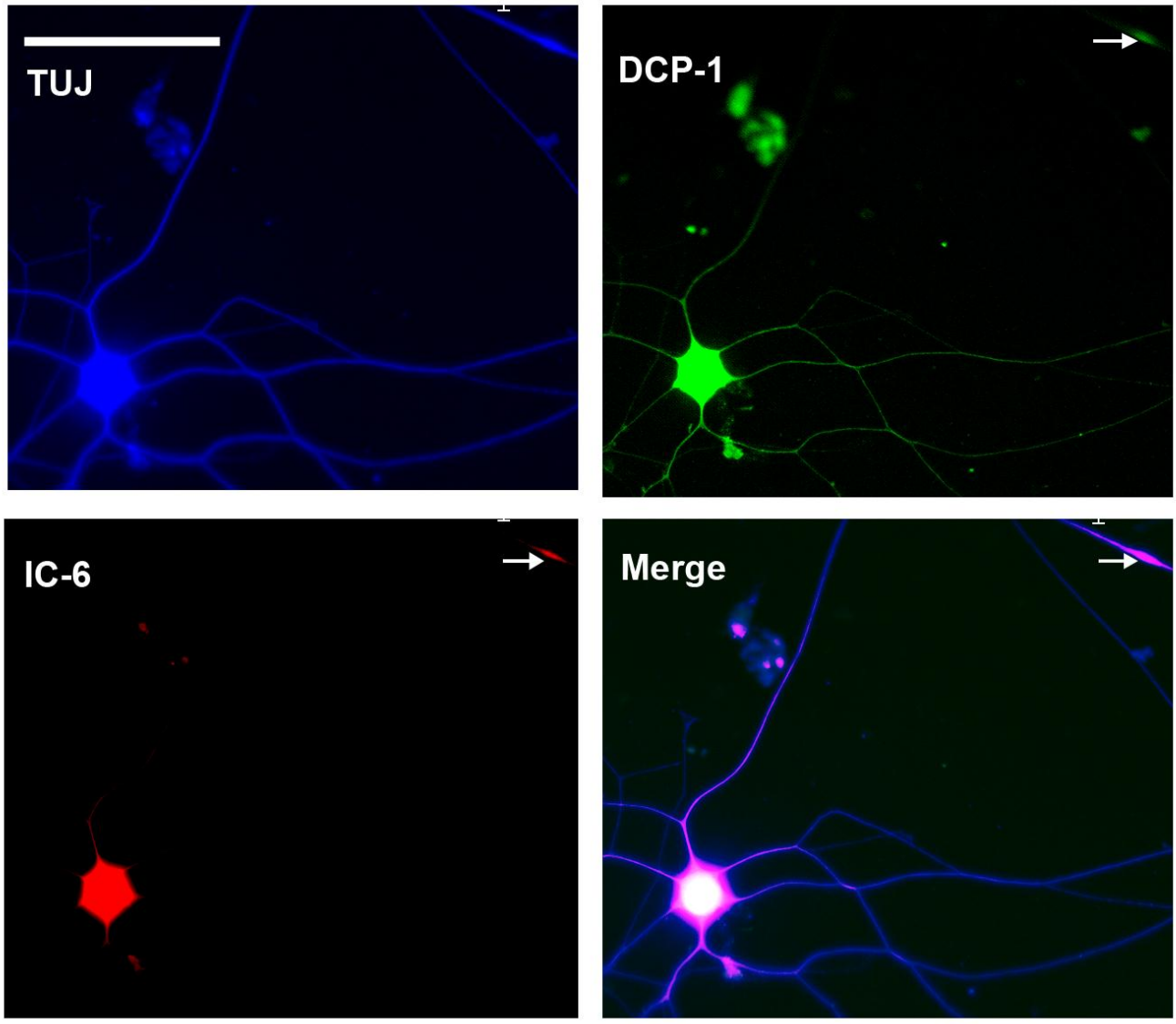

C

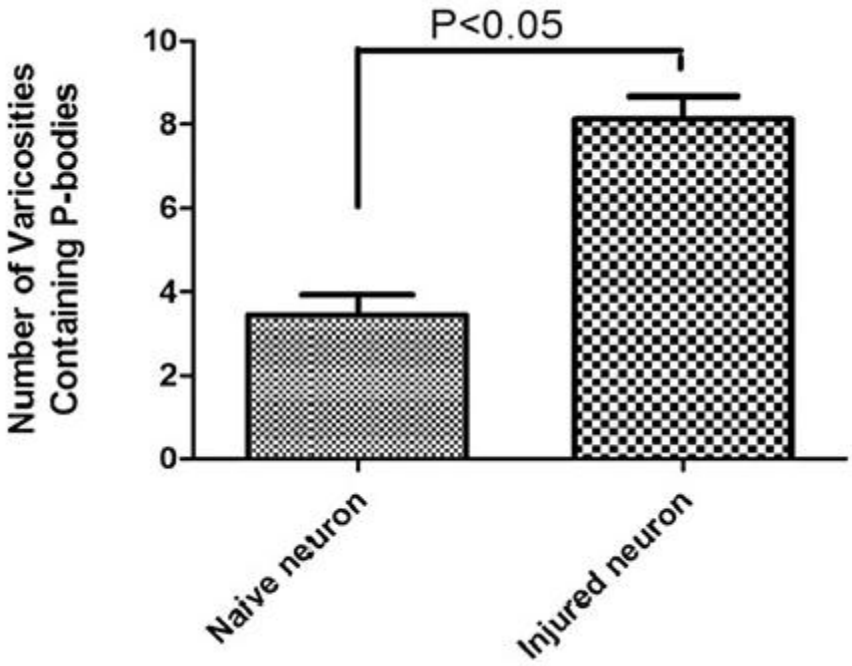
P<0.05
Number of Varicosities Containing P-bodies
10
8
6
4
2
0
Naive neuron
Injured neuron

Figure 3.5. Real-time qPCR for miRNAs.

Graphs indicated relative change in miRNA level. Total RNA was isolated from intact and crushed sciatic nerves (n=6). Based on miRNA array data, several miRNAs were selected for qPCR verification. Relative quantitation of miRNA level was calculated against the reference gene (S12), and a relative fold change was determined using the $2^{-\Delta\Delta CT}$ method (n=3, *$p<0.05$). The level of miR-142-5p and miR-21 showed significant increase in SN after nerve crush.

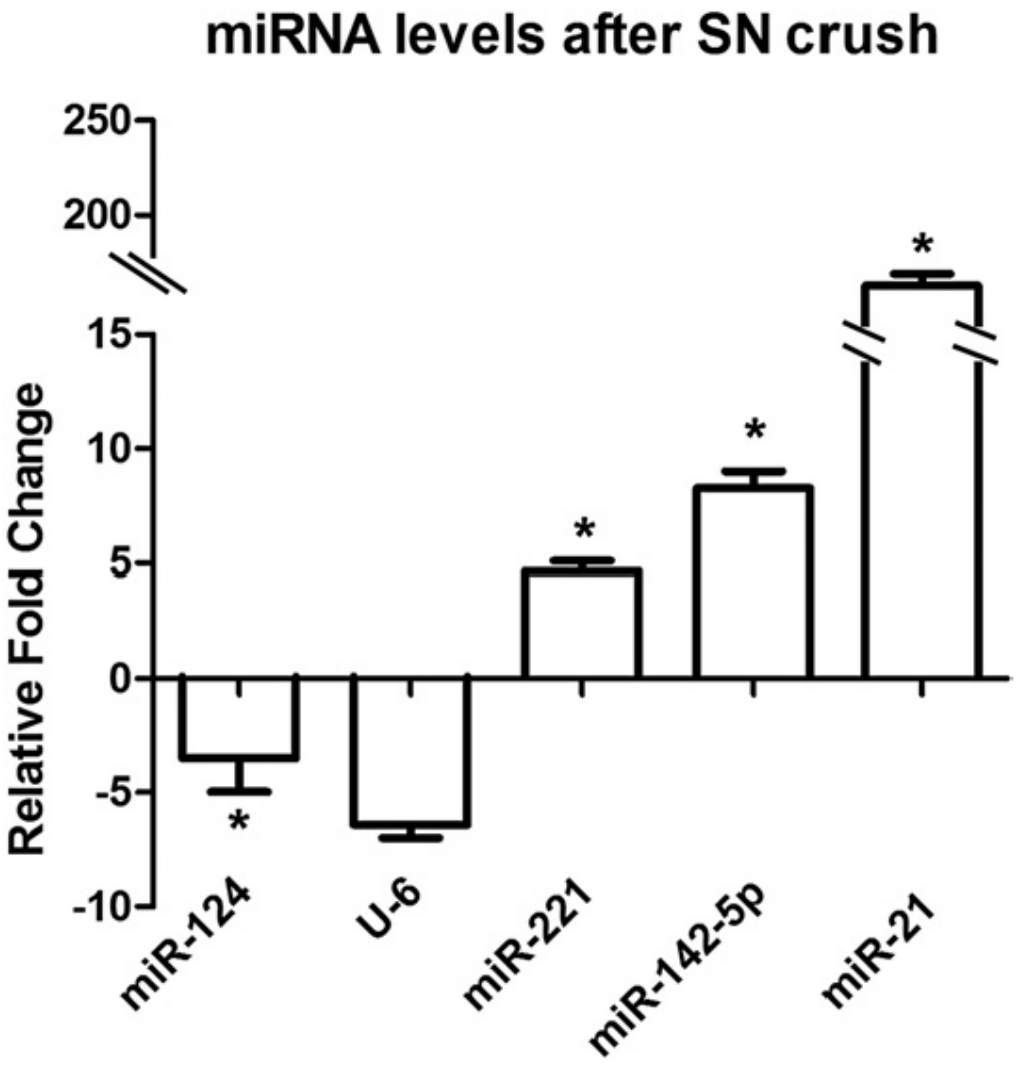
miRNA levels after SN crush
Relative Fold Change
250
200
15
10
5
0
-5
-10
*
*
*
*
miR-124
U-6
miR-221
miR-142-5p
miR-21

Figure 3.6. Colocalization of miRNAs and GWB in neurons and axons.

Fluorescent in-situ hybridization for miR-21 (A), miR-142-5p (B) revealed the distribution of miRNAs in axon. Immunofluorescence for neuronal β-tubulin served as a neuronal marker and immunostaining for GWB protein exhibited the localization of P-bodies. U6, a small nuclear RNA locates only in nucleus was used as one control (C). Scrambled probes were used as another negative control. Green fluorescence shows the distribution of miRNAs and U6. Red fluorescence indicates immunodetection of neuronal β-tubulin protein with TUJ1 antibodies (1:100). Blue signals indicate GWB protein. White arrows indicate fluorescent signals within the axons where miRNA and P-bodies components resided. Arrows with tail indicate neuronal cell bodies, small arrows show P-bodies, arrow heads indicates the non-neuronal cells (Scale bar = 75μm).

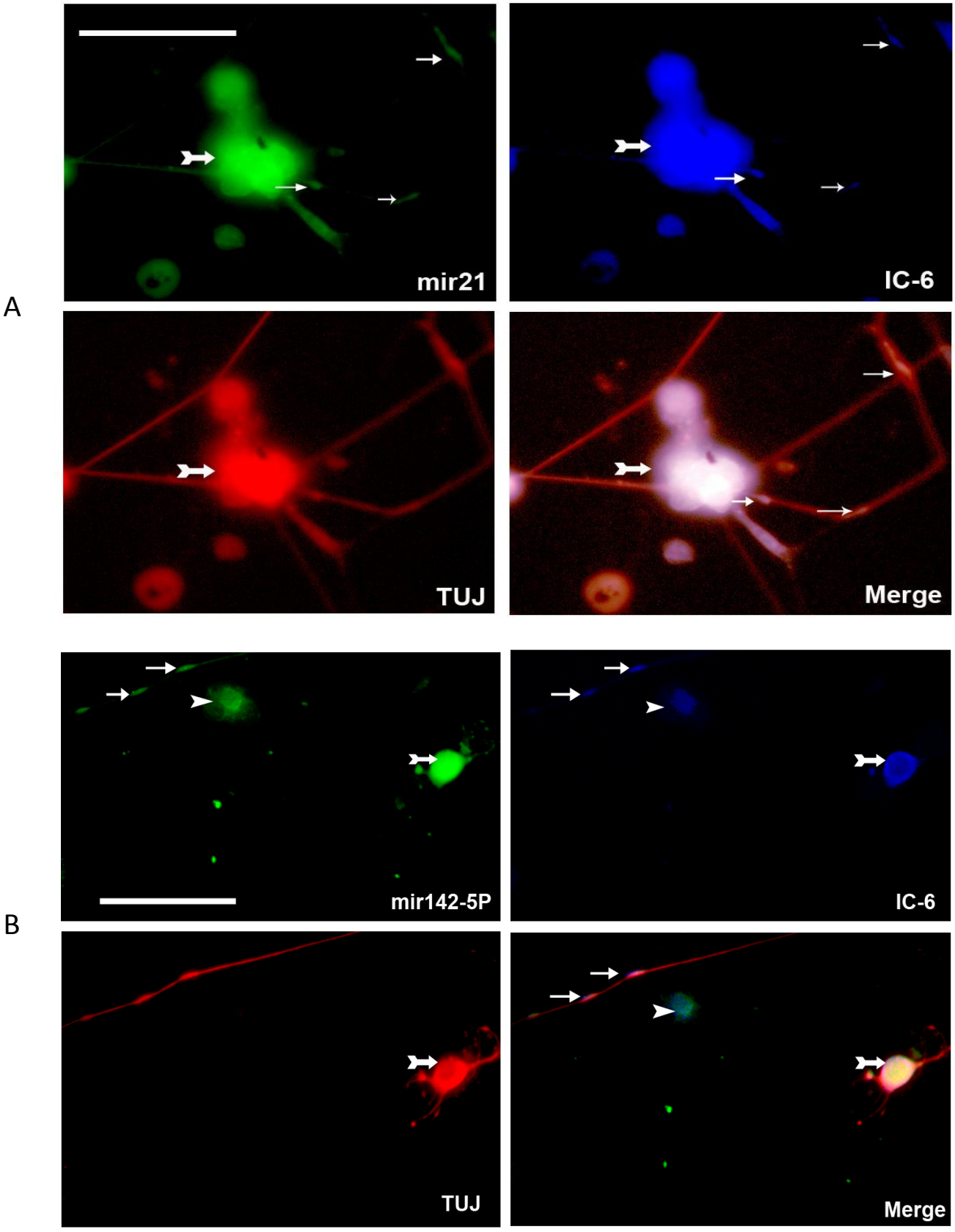
A
mir21
IC-6
TUJ
Merge
B
mir142-5P
IC-6
TUJ
Merge

C

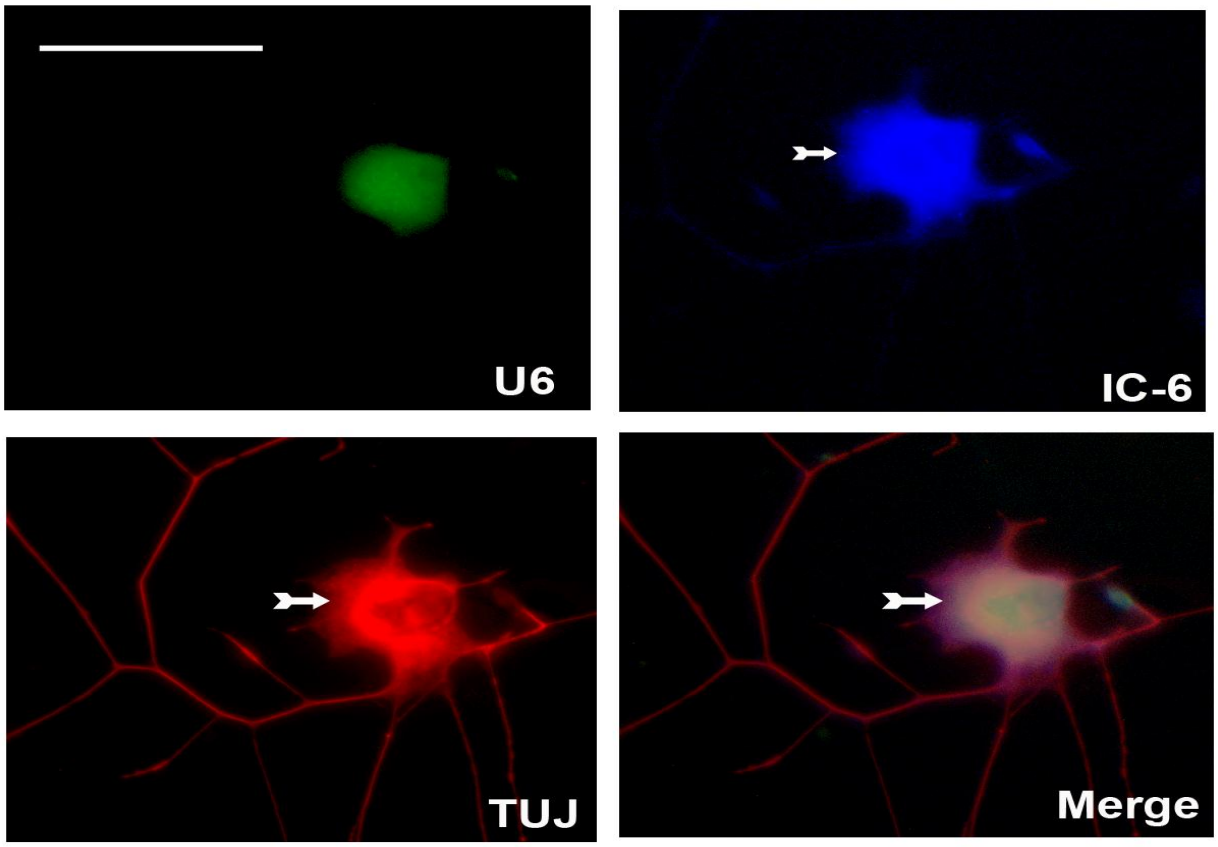

D

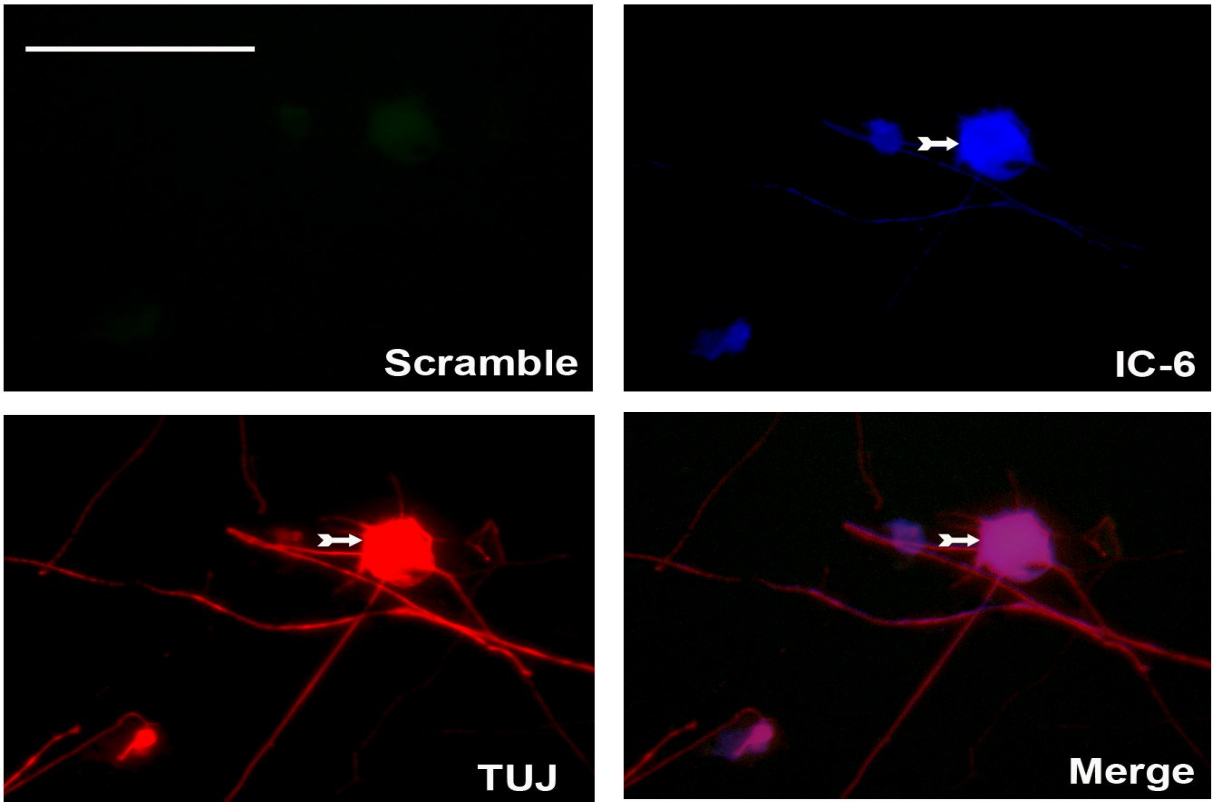

Discussion

Our study demonstrated that the expression of miRNA biosynthetic protein complexes was increased following sciatic nerve injury, as well as some miRNAs. Recent studies have shown that RNAi machinery exists and is functional in peripheral nerve axons (Buckingham et al., 2004, Hengst et al., 2006, Murashov et al., 2007). In addition, stable expression of a number of miRNAs that were enriched in the superior cervical ganglia (SCG) axons has recently been identified (Natera-Naranjo et al., 2010). In our previous studies, we demonstrated that miRNA biosynthetic enzymes are present in peripheral nerve axons *in vivo* and *in vitro* (Murashov et al., 2007). However, whether the miRNA biosynthetic pathway is involved in peripheral nerve regeneration has not been documented yet. In this report, we investigated the response of miRNAs biosynthetic pathway to peripheral nerve injury. Specifically, we found differential miRNA levels regulated by injury. In addition, we demonstrated that several components of RISC and P-bodies were differentially expressed in the sciatic nerve and DRG axons in response to crush injury, supporting a potential physiological role of miRNA pathway in regulation of peripheral nerve regeneration.

Components of RISC and P-bodies respond to injury of peripheral nerve

In our previous experiments, we detected expression of several RISC components in mouse sciatic nerve (Murashov et al., 2007). In the current report, we observed increased protein levels of Ago2, FMRP, and p100 in response to sciatic nerve crush. The observed injury-regulated expression of these RISC components may indicate that induction of RISC may be a part of the PNs regenerative response. Interestingly, Ago2 , the pivotal RISC protein, was recently detected in P-bodies, as well as in the stress granules (SGs), which suggested a potential

functional relationship between RISC, SGs, and P-bodies in physiological response to cellular stresses (Leung et al., 2006, Didiot et al., 2009). P-bodies are an important component of the miRNA machinery as the sites for either degrading or protecting and sequestering mRNA (Parker and Sheth, 2007, Balagopal and Parker, 2009). P-bodies are dynamic complexes whose assembly are dependent on, and proportional to, the cytoplasmic pool of translationally repressed messenger ribonucleoproteins (mRNPs) (Teixeira et al., 2005, Franks and Lykke-Andersen, 2008). Although the complete composition of P-bodies is not yet established, they are known to include the decapping enzymes DCP1/DCP2, the activator of decapping Dhh1/RCK/p54, Pat1, Scd6/RAP55, Edc3, the Lsm1-7 complex and the exonuclease, Xrn1 (Parker and Sheth, 2007, Balagopal and Parker, 2009). In agreement with previous reports that various cellular stresses initiate the formation of P-bodies (Balagopal and Parker, 2009), we detected the change in the expression level of P-bodies components after crush injury using immunoblotting analyses.

In particular, we made an interesting observation that sciatic nerve injury led to elevated levels of GWB IC-6 and Dcp1, but decreased the expression of Dcp2. The apparent discrepancy may be partially explained by recent report in which, *in vitro* depletion of the decapping enzyme Dcp2 caused increased P-bodies assembly (Franks and Lykke-Andersen, 2008). Although Dcp1 and Dcp2 are both core components of P-bodies, which catalyze removal of the 5' cap structure from mRNA, they are structurally and functionally different. DCP1 behaves as a decapping enzyme regulatory subunit, whereas DCP2 functions as a catalytic subunit of decapping enzyme (Sheth and Parker, 2003, She et al., 2008). Therefore, decreased level of Dcp2 may result in accumulation of undigested mRNAs and thus in additional P-bodies assembly. At the same time, another recent observation points out that mammalian cells possess multiple mRNA decapping

enzymes and Dcp2 protein may only modestly contribute to bulk mRNA decay in mouse and human tissues (Song et al., 2010).

We also observed an increase in the number and the size of P-bodies after conditional nerve lesion in the regenerating DRG axons. It is well known that conditioning sciatic nerve crush produces robust regenerative response with concomitant increase in mRNA and protein synthesis (Willis and Twiss, 2006). We presume that the increase in the pool of mRNA may initiate P-bodies assembly. Indeed, overexpression of a nontranslating mRNA in yeast was shown to potentiate P-bodies formation (Teixeira et al., 2005). Moreover, the size and number of P-bodies are proportional to the pool of untranslated mRNAs (Teixeira et al., 2005, Parker and Sheth, 2007). Therefore, when mRNAs are trapped in association with ribosomes, P-bodies decline; conversely, when mRNAs dissociate from ribosomes because of inhibition of translation initiation, P-bodies increase in size and numbers (Teixeira et al., 2005, Parker and Sheth, 2007, Balagopal and Parker, 2009). Consequently, nerve crush nerve crush may lead to a larger pool of untranslated mRNA and to increase in the number and size of functional P-bodies (Kedersha et al., 2005, Koritzinsky et al., 2006).

We made another intriguing observation that P-bodies were preferentially localized to the axon VR. The number of VR was markedly higher in the regenerating versus naïve DRG axons. Although the physiological role of varicosities (VR) is not clear their alleged function has been associated with presynaptic terminals, places of action potential waveform modulation, and organelle accumulation and sequestration (Bennett and Muschol, 2009). In addition, VR were described as the sites of mRNA concentration and protein synthesis (Lee and Hollenbeck, 2003). Interestingly, it was recently suggested that VR are the sites of clustering of excess growth resources along developing neuritis (Malkinson and Spira, 2010). Our data are complimentary to

these observations suggesting that P-body machinery localized to VR cab regulate the growth resources by managing mRNA pool.

Identification of miRNAs specifically expressed in injured sciatic nerve

We used microarrays and RT-PCR to profile miRNA expression changes in the sciatic nerve of mice after injury. The results revealed a group of miRNA expressed in an injury-regulated pattern. For analysis, we chose three most highly upregulated miRNAs, that is miR-21, miR-142-5p, and miR-221, as well as brain specific miR-124a, which was significantly downregulated after nerve crush.

Interestingly, miRNAs miR-21 and miR 142-5P were reported to be also up-regulated after brain injury (Lei et al., 2009). In addition, miR-221 was found to be relatively abundant in distal axons of SCG and had elevated expression level after spinal cord injury (Liu et al., 2009, Natera-Naranjo et al., 2010). It has been reported that the brain-enriched miRNA miR-124 is an important regulator of the temporal progression of adult neurogenesis in mice. Knockdown of endogenous miR-124 maintained subventricular zone stem cells as dividing precursors, whereas ectopic expression led to increased neuron formation. Furthermore, blocking miR-124 function during regeneration led to hyperplasias, followed by a delayed burst of neurogenesis (Cheng et al., 2009). Although the changes in the miRNA expression profile following injury and development have been reported, the mechanism that regulates miRNA expression has not been yet elucidated. In the current article, we revealed that expression of several miRNA biosynthetic enzymes were injury-regulated. This let us to propose that the change in levels of miRNA biosynthetic proteins may play a role in the injury-regulated expression of miRNAs.

Taken together, our data identify a role for the miRNA biosynthetic pathway in peripheral nerve response to injury. Further studies should provide important insight into the role of specific miRNAs in peripheral nerve regeneration. This finding may have significant clinical potential in the treatment of neurodegenerative diseases, specifically those involving peripheral nerves.

Although no previous study has directly associated P-bodies wit peripheral nerve health, identification of patients with autoimmunity to GWBs suggests such a role. Clinical studies indicate that these patients most often suffer from motor and sensory peripheral neuropathy (Bhanji et al., 2007). Although it is not known whether the resulting neuropathy is axonal or glial in its origin, it is logical to presume that autoimmune decrease of P-bodies in axon may negatively affect intra-axonal translation and become detrimental to axon physiology.

Conclusion

This work offers insights into the functional interplay between miRNAs and their biosynthetic enzymes in peripheral nerve injury. In conclusion, we show that injury to peripheral axons induces changes in the content and distribution of some biosynthetic proteins of the miRNA machinery in cultured DRG neurons and their axons. Together with previous findings, these observations suggest that, in addition to RISC, other factors such as P-bodies might underlie the changes in regenerating axons induced by injury. Those factors probably act in a synergistic way thus leading to the promoting regenerative axon growth.

CHAPTER IV: *Dicer*-microRNA Pathway is Critical for Peripheral Nerve Regeneration and Functional Recovery *in vivo* and Regenerative Axon Growth *in vitro*

Summary

Both central and peripheral axons contain pivotal microRNA (miRNA) proteins. While recent observation demonstrated that miRNA biosynthetic machinery responds to peripheral nerve lesion in an injury-regulated pattern, the physiological significance of this phenomenon remains to be elucidated. In the current paper we hypothesized that deletion of *Dicer* would disrupt production of *Dicer*-dependent miRNAs and would negatively impact regenerative axon growth. Taking advantage of tamoxifen-inducible *CAG-CreERt:Dicer*$^{fl/fl}$ knockout (*Dicer* KO), we investigated the results of *Dicer* deletion on sciatic nerve regeneration *in vivo* and regenerative axon growth *in vitro*. Here we show that the sciatic functional index, an indicator of functional recovery, was significantly lower in *Dicer* KO mice in comparison to wild-type animals. Restoration of mechanical sensitivity recorded in the von Frey test was also markedly impaired in *Dicer* mutants. Further, *Dicer* deletion impeded the recovery of nerve conduction velocity and amplitude of evoked compound action potentials *in vitro*. Histologically, both total number of regenerating nerve fibers and mean axonal area were notably smaller in the *Dicer* KO mice. In addition, *Dicer*-deficient neurons failed to regenerate axons in dissociated dorsal root ganglia (DRG) cultures. Taken together, our results demonstrate that knockout of *Dicer* clearly impedes regenerative axon growth as well as anatomical, physiological and functional recovery.

Our data suggest that the intact *Dicer*-dependent miRNA pathway is critical for the successful peripheral nerve regeneration after injury.

Introduction

MicroRNAs (miRNAs) are important molecular switches which play a major role in post-transcriptional gene regulation (Jackson et al., 2010). Pri-miRNAs are initially processed by biosynthetic enzymes, *Drosha* and *DGCR8/Pasha*, while in cytoplasm RNAse III enzyme *Dicer* cleaves pre-miRNAs into the mature miRNAs (Bernstein et al., 2001, Lee et al., 2003). *Dicer* plays a critical part in the miRNA biosynthetic pathway and the system wide ablation of *Dicer* in mice results in early embryonic lethality (Bernstein et al., 2003). Therefore, to investigate the role of miRNAs in the nervous system many groups have used *Cre*-mediated recombination systems to ablate *Dicer* in a tissue or developmentally specific manner (Cuellar et al., 2008). Studies show that during early development, the deletion of *Dicer* in the neural crest (NC) lineage leads to the cell loss in enteric, sensory, and sympathetic nervous systems (Zehir et al., 2010). During the late embryonic stage cortical-specific *Dicer* conditional knockout affects survival and differentiation of cortical neural progenitors resulting in the abnormal migration of neurons in the cortex as examined at E 18.5 (Kawase-Koga et al., 2009). Postnatally, conditional loss of *Dicer* in excitatory forebrain neurons disrupts cellular morphogenesis, resulting in an array of phenotypes including microcephaly, reduced dendritic branch elaboration, and increased cortical apoptosis (Davis et al., 2008). Loss of *Dicer* in dopaminoceptive neurons is associated with ataxia, reduced brain size, and decreased lifespan to 10-12 weeks (Cuellar et al., 2008). Similarly, conditional inactivation of *Dicer* in Purkinje cells leads to relatively rapid disappearance of Purkinje cell-expressed miRNAs, followed by a slow cerebellar degeneration and development of ataxia between 13 to 17 week of age (Schaefer et al., 2007).

Thus while these data strongly suggest an indispensable role of miRNAs during neural development and maturation in the CNS, little information is available on the role of miRNAs in the adult PNS. Although no reports have directly linked miRNA regulation with peripheral nerve physiology, recent observations show that loss of *Dicer* in Schwann cells may arrest Schwann cell differentiation (Bremer et al., 2010), alter myelin-related gene expression (Pereira et al., 2010), and cause a severe neurological phenotype resembling congenital hypomyelination (Yun et al., 2010). Interestingly, components of RNA-induced silencing complex (RISC) and mRNA-processing bodies (P-bodies), which are the local foci of mRNA degradation, have been detected in severed sciatic nerve fibers and regenerating dorsal root ganglia (DRG) axons *in vitro* (Hengst et al., 2006, Murashov et al., 2007, Wu et al., 2011a). In addition, a comprehensive list of miRNAs residing within the distal axonal domain of superior cervical ganglia has recently been reported (Natera-Naranjo et al., 2010). Thus, current observations suggest that miRNAs may play an important regulatory role in peripheral nerve health even after development.

In the current study we asked whether the genetic ablation of *Dicer* would affect peripheral nerve regeneration. Taking advantage of tamoxifen-inducible *CAG-CreERt:Dicer*$^{fl/fl}$ knockout mice (*Dicer* KO), we investigated the results of *Dicer* deletion on sciatic nerve regeneration *in vivo* and regenerative axon growth *in vitro*. Here we show that deletion of *Dicer* impaired nerve regeneration according to functional behavioral tests, electrophysiological and histological analyses. In addition, *Dicer*-deficient neurons failed to regenerate axons in dissociated dorsal root ganglia (DRG) cultures. To the best of our knowledge, this is the first demonstration that the intact *Dicer*-dependent miRNA pathway is necessary for the successful functional recovery after peripheral nerve injury in adult animal.

Results

Tamoxifen treatment induced *Dicer* gene knockout in sciatic nerve.

To confirm that tamoxifen treatment could activate *Cre* expression and result in *Dicer* KO, we used a *ROSA26 Cre* reporter gene. All animals carried *ROSA26* stop/flox locus annexed to a *lazZ* reporter, in which *lazZ* expression was conditional upon the removal of the floxed stop codon. When *Cre* recombinase was expressed, it excised the genomic region between the two loxP sites, allowing expression of *lazZ.* The breeding pairs of *CAG-CreERt:Dicer*$^{fl/fl}$ were heterozygous for *Cre* alleles. Correspondingly, their offspring genotype was either *CAG-CreERt:Dicer*$^{fl/fl}$, or *Dicer*$^{fl/fl}$. X-gal staining for sciatic nerves from those offspring showed that only the *CAG-CreERt:Dicer*$^{fl/fl}$ mice treated with tamoxifen exhibited blue tissue staining. For the other two control groups of mice neither the *CAG-CreERt:Dicer*$^{fl/fl}$ mice with vehicle treatment nor the *Dicer*$^{fl/fl}$ littermates with tamoxifen administration showed any staining in their tissues (Fig. 4.1A). These results confirmed that tamoxifen treatment successfully activated *Cre* recombinase in *CAG-CreERt:Dicer*$^{fl/fl}$ mice. *CAG-CreERt:Dicer*$^{fl/fl}$ mice receiving vehicle injection and *Dicer*$^{fl/fl}$ mice receiving tamoxifen treatment lacked *Cre* expression, and therefore, had no *lacZ* expression.

The ablation of *Dicer* expression after tamoxifen treatment in *CAG-CreERt:Dicer*$^{fl/fl}$ mice was assessed by Western blot analysis. Sciatic nerves were collected both at the day of nerve crush and 21 days after nerve injury. Western blot data provided the evidence that at both time points, there was a significant decrease in the *Dicer* expression at the protein level in *Dicer* KO group (Fig. 4.1B). On the day of nerve crush, *Dicer* expression in the sciatic nerve was down-regulated to 42 ± 2.09% of the vehicle treated group level. At 21 days after nerve crush, *Dicer*

expression in the knockout group was decreased to 32 ± 2.33% of the vehicle treated group level, possibly reflecting over time depletion of *Dicer* protein pool (Fig. 4.1C).

To confirm these data at the mRNA level, tissue samples were collected from 3 groups of mice at 2 different time points, and total RNA was isolated from sciatic nerves. Quantification of 3 independent RT-qPCR experiments revealed that, tamoxifen treatment reduced *Dicer* mRNA levels to 40 ± 6.11% and 27 ± 5.31% in sciatic nerve at day 0 and day 21 respectively (Fig. 4.1D), when compared to two controls. Since *Dicer* is a key enzyme in the microRNA biogenesis pathway, we used RT-qPCR to determine the effect of *Dicer* deletion on microRNA expression. The expression levels of the following 4 different miRNAs, miR-199a, miR-21, miR-142-5p and miR9, were significantly down regulated (Fig. 4.1E, F) following inducible *Dicer* deletion. At day 0, the expression levels of miR-199a, miR-21, miR-142-5p and miR-9 were reduced to 64 ± 3.51 %, 42.67 ± 7.27%, 35.33 ± 3.18%, and 38.33 ± 9.39% respectively in comparison with the control groups, and at day 21, the expression levels of miR-199a, miR-21, miR-142-5p and miR-9 were reduced to 56.67 ± 9.77, 38 ± 9.07%, 28.67 ± 4.10%, and 26 ± 3.78%, respectively. These results confirmed that *Cre* activation induced by tamoxifen treatment in *CAG-CreERt:Dicer*$^{fl/fl}$ mice led to the ablation of *Dicer* and marked loss of miRNAs expression in the nervous system.

Dicer deletion delayed functional recovery in walking corridor test

In order to determine the effect of miRNA depletion on the recovery of motor function, we performed a walking corridor behavioral test (N = 20 for each group). As shown in Fig 4.2A, during the baseline test, the SFI was normal (close to zero) for 3 groups of mice before sciatic nerve crush. Two days after nerve crush, the values of SFI were close to -100 (vehicle control

group: -91.51 ± 2.83; no-*Cre* control group: -102.4 ± 2.70; *Dicer* KO group: -96.80 ± 2.69) in all three groups of the mice. The SFI was recovering during the observation period of three weeks. At earlier time points, there were no significant differences between the *Dicer* KO group and two control groups (Day 4: vehicle control group: -84.45 ± 3.29; no-*Cre* control group: -78.27 ± 7.54; *Dicer* KO group: -88.75 ± 2.43. Day7: vehicle control group: -82.23 ± 2.43; no-*Cre* control group: -70.27 ± 2.70; *Dicer* KO group: -84.54 ± 2.20). However, although the trends for the development of SFI were similar for the 3 groups of mice, the SFI values of *Dicer* KO were slightly lagging behind. The SFI values for *Dicer* KO group at day 14 and day 21 after injury became significantly lower ($P<0.05$) than those of two control groups (Day 14: vehicle control group: -34.71 ± 3.78; no-*Cre* control group: -25.49 ± 6.93; *Dicer* KO group: -61.00 ± 5.38. Day21: vehicle control group: 24.56 ± 2.22; no-*Cre* control group: -14.07 ± 4.71; *Dicer* KO group: -43.53 ± 7.49.). It should be noted that, at day 21, the SFI value of the no-*Cre* control group resembled the pre-operation level, whereas the SFI value of the *Dicer* KO group was still significantly lower than pre-operation level. Thus, the data demonstrated that loss of *Dicer* resulted in a slower recovery of motor function.

***Dicer* deletion resulted in a delayed recovery from allodynia.**

In our experiments, we used the von Frey test to assess pre-injury mechanical sensitivity and the injury-induced changes in mechanical sensitivity following *Dicer* deletion (N = 15 for each group). Two pre-injury tests were used to determine the baseline value and the tests to evaluate the recovery of the sensory function were conducted 2, 4, 7, 14, and 21 days after injury. Following sciatic nerve injury, mice typically became hypersensitive and responded to filaments of lesser intensities, indicating the presence of mechanical allodynia (Vogelaar et al., 2004). In our experiments, the decrease in the threshold was observed at the first post-injury

behavioral test and progressed with time (Fig. 4.2B). During the second week after injury, mice in the two control groups showed signs of recovery from allodynia. From day 7 to day 14, the sensory threshold of the control animals increased from 32.09 ± 4.5% to 41.56 ± 4.73% of pre-operation levels, whereas the *Dicer* KO further decreased their thresholds to mechanical stimuli, from 38.01 ± 6.4% to 33.33 ± 6.07% of pre-operation level. On the last day of the observation periods (Day 21), there were significant differences in the sensory thresholds between control groups and *Dicer* KO group (vehicle control group: 50.34 ± 6.92; no-*Cre* control group: -51.03 ± 5.71; *Dicer* KO group: -26.57 ± 3.36, $P<0.05$, N = 15). Thus, the significantly lower mechanical withdrawal thresholds in *Dicer* KO at Day 21 indicated the delayed recovery from allodynia.

Electrophysiological evaluation of sciatic nerve regeneration

The electrophysiological assessments, performed at 14 days and 21 days after nerve crush, provided further evidence for the delayed physiological recovery of crushed sciatic nerve in *Dicer* KO animals. Nerve conduction velocity (NCV) decreased after crush and then was restored upon the regeneration of nerve fibers (Fig. 4.3 and 4.4). At both 14 (Fig. 4.3B) and 21 (Fig. 3.4B) days after injury, NCV was significantly slower in *Dicer* KO group compared with controls (Day 14: vehicle control group: 5.10 ± 0.43 m/s; no-*Cre* control group: 5.96 ± 0.89 m/s; *Dicer* KO group: 2.28 ± 0.38 m/s (Fig. 4.3 B_2). Day 21: vehicle control group: 15.14 ± 0.74 m/s; no-*Cre* control group: 13.1 ± 1.23 m/s; *Dicer* KO group: 6.40 ± 0.83 m/s. N = 5, $P<0.05$ (Fig. 4.4B)). The increase of NCV from day 14 to day 21 was also significantly smaller in *Dicer* KO group (vehicle control group: 100 ± 7.33%; no-*Cre* control group: 71.22 ± 12.27%; *Dicer* KO group: 46.94 ± 9.07% (Fig. 4.4C)). After nerve injury, the waveforms of the evoked action potentials recorded from distal sciatic nerve had dramatically changed. Instead of single identifiable CAPs, several waveform signals with lower amplitude were recorded (Fig. 4.3A_1,

4.3A_2). A quantification of these data, after rectification and integration of the appropriate time windows, revealed that during the period of recovery, both at 14 days (Fig. 4.3C_2) and 21 days (Fig. 4.4D), the response was considerably smaller in the *Dicer* KO group. At 14 days after nerve crush (Fig. 4.3C_2), the CAP in vehicle treated groups was 100 ± 20.24%; in no-*Cre* animals was 124.5 ± 26.73%, while the action potential in *Dicer* knock out animals was 49.96 ± 15.21%. At 21 days (Fig.4.4D), similar to day 14 data, *Dicer* KO (32.13±8.14%) displayed delayed recovery comparing to vehicle treated (100 ± 21.89%) or no-*Cre* group (100.8 ± 18.76%) at 21 days. The wave shapes recorded from control groups 21 days after nerve crush also showed greater restoration compared with the group of *Dicer* KO. 21 days after nerve injury, the initial response amplitude remained reduced and was followed by several small waves (Fig 4.4A upper graph). In the *Dicer* KO group, the response remained delayed and only small waveform signals were recorded from the distal end of the nerve, which exhibited wave shapes similar to 14 day's data (Fig. 4.4A lower graph).

The effect of *Dicer* KO on anatomical recovery of crushed sciatic nerve

Semi-thin cross sections of sciatic nerves were stained with osmium tetroxide and Richard's dye to help visualize myelinated nerve fibers. Myelinated nerve fiber mean areas as well as the number of myelinated nerve fibers were quantified with NIH ImageJ software. At day 14 after nerve crush, the sizes and number of the individual myelinated nerve fibers of regenerating nerves in *Dicer* KO group were smaller than those observed in control nerves (Fig. 4.5A-C). The compromised regeneration in *Dicer* mutants became apparent at 21 days (Fig. 4.5D-F) when the difference in size and numbers of axon fibers between the control and the knockout groups reached statistical significance (Fig. 4.5G and H) (number of regenerated nerve fibers: vehicle control group: 1349.50 ± 28.04; no-*Cre* control group: 1345.50 ± 36.37; *Dicer*

KO group: 1115.50 ± 52.73; myelinated axon area: vehicle control group: 4.13 ± 0.05; no-*Cre* control group: 4.05 ± 0.09; *Dicer* KO group: 3.26 ± 0.09. N = 6, P<0.05). Thus, the histological data confirmed that *Dicer* deletion impairs anatomical recovery of peripheral nerve following crush injury.

Direct effect of *Dicer* deletion on regenerating DRG neurons *in vitro*

To assess the direct effects of *Dicer* deletion on regenerative axon growth, *in vitro* studies were performed in dissociated DRG neuronal cultures. DRGs from tamoxifen or vehicle treatment *CAG-CreERt:Dicer*$^{fl/fl}$ mice and tamoxifen treated *Dicer*$^{fl/fl}$ mice were collected at day 5 after conditioning sciatic nerve lesion. After such injury the regenerative capacity of the neurons are improved and can be detected as an increased axonal outgrowth in comparison to uninjured contralateral neurons. The neuronal cells were dissociated and plated sparsely on coverslips coated with poly-d-lysine and laminin. Immunostaining with the neuronal marker TUJ was used to visualize the neuronal cell bodies and axons in the cultures. The measurement of axon length and the counting of branches demonstrated that, in the absence of *Dicer*, the regenerative axon growth was significantly impaired compared to control groups (Fig. 4.6).

Mean axon length of *Dicer* KO DRG neuron was approximately 200 μm after 24 hr culturing. In the two control groups, dissociated DRG neurons had more robust regenerative growth. The mean axon length was around 350 μm after 24 hr culturing. For statistical analysis, we normalized all of the data to the vehicle treated group. DRG neurons from the tamoxifen treated *Dicer*$^{fl/fl}$ mice had approximately the same axon length in comparison with vehicle treatment *CAG-CreERt:Dicer*$^{fl/fl}$ group (vehicle control group: 100 ± 6.75%, no-*Cre* control group: 83.20 ± 5.28% (Fig. 4.6D)). The axon length in the tamoxifen treated *CAG-*

CreERt:Dicer$^{fl/fl}$ group decreased to 39.83 ± 4.82% of the control level, due to *Dicer* KO. *Dicer* deletion also significantly inhibited axon branching. After 24hr of culturing, the number of branches in *Dicer* KO DRG neurons was 63% lower than that of the two control groups (Vehicle control group: 100 ± 6.6%; no-*Cre* control group: 105.10 ± 9.75%; *Dicer* KO group: 36.81 ± 5.26%. N = 30, P<0.05 (Fig. 4.6E)). Therefore, *in vitro* studies provided further evidence that the intact *Dicer*-dependent miRNA pathway is critical for regenerative axon growth in isolated neurons.

The same assessments were also performed on DRG neurons with inducible *Dicer* KO in neuronal cell cultures. To exclude the influence from the loss of *Dicer* in other types of cells, mice did not receive any treatments until euthanasia. All treatments were applied to neuronal cell cultures *in vitro*. As with the previous studies, we had 3 groups of cell culture in this study. DRGs form *Dicer*$^{fl/fl}$ mice cultured with DMSO was the vehicle treated group. DRGs collected form *Dicer*$^{fl/fl}$ mice with tamoxifen in culture media was considered the no-*Cre* control group. DRGs from *CAG-CreERt:Dicer*$^{fl/fl}$ mice with tamoxifen in the culture media was the *Dicer* knockout group. The differences in the regenerative growth between *Dicer* knockout group and control groups resulted from the loss of *Dicer* expression in neuronal cells.

From the quantified data shown in Figure 6 F and 6 G, DRG neurons with *Dicer* knockout *in vitro* exhibited similarly impaired regenerative axon growth as with *Dicer* knockout in whole animals. The axon length in *Dicer* KO group decreased to 61.79 ± 5.79% of the vehicle control group level, whereas the tamoxifen treated DRG neurons from *Dicer*$^{fl/fl}$ mice (the no-*Cre* group) had longer axon (not statistic significant), in comparison with vehicle treated group (vehicle control group: 100 ± 11.17%, no-*Cre* control group: 121.1 ± 5.28% (Fig. 4.6F)). Similarly, *Dicer* deletion *in vitro* also significantly inhibited axon branching. The number of

branches in *Dicer* knockout group was 66.75% of the control groups (Vehicle control group: 100 ± 12.35%; no-*Cre* control group: 95.68 ± 8.35%; *Dicer* KO group: 66.73 ± 6.46%. N = 30, $P<0.05$ (Fig. 4.6G)). Our results showed that loss of *Dicer* ally specific in neuronal cells inhibited neurite outgrowth, and the phenotype was more severe when *Dicer* knockout was induced at whole animal level. These data suggested that the delayed nerve regeneration can be explained by the loss of *Dicer* in neuronal cell, and loss of *Dicer* in other cell types in peripheral nerves enhanced the phenotype.

Figure 4.1. *Cre* activation induces loss of *Dicer* in *CAG-CreERt:Dicer*$^{fl/fl}$ mice.

Tamoxifen treatment of *CAG-CreERt:Dicer*$^{fl/fl}$ mice activated *Cre* recombinase, under the control of the estrogen promoter. (A) *Cre* activation was assessed by X-gal staining of sciatic nerves. *LacZ* expression was not observed in two control groups: vehicle treated *CAG-CreERt:Dicer*$^{fl/fl}$ mice (left) and tamoxifen treated *Dicer*$^{fl/fl}$ mice (middle)**.** X-gal staining was obvious in sciatic nerve of tamoxifen treated *CAG-CreERt:Dicer*$^{fl/fl}$ mice (right). (B) Western blot shows successful depletion of *Dicer* in sciatic nerve. Sciatic nerves were collected from 3 groups of mice (Tamoxifen treated *CAG-CreERt:Dicer*$^{fl/fl}$ mice, vehicle treated *CAG-CreERt:Dicer*$^{fl/fl}$ mice, and tamoxifen treated *Dicer*$^{fl/fl}$ mice) at both the day of sciatic nerve crush surgery and 21days after nerve crush. (C) Protein levels of *Dicer* were quantified by band densitometry and normalized to α-tubulin level. (D) Decrease in *Dicer* expression at mRNA level in pooled samples of sciatic nerves after tamoxifen treatment measured by Real-Time qPCR. (E), (F), Real-Time qPCR confirmed declined levels of selected miRNAs after *Cre* induced *Dicer* ablation at day 0 (E) and day 21(F) after nerve crush (**$p<0.01$).

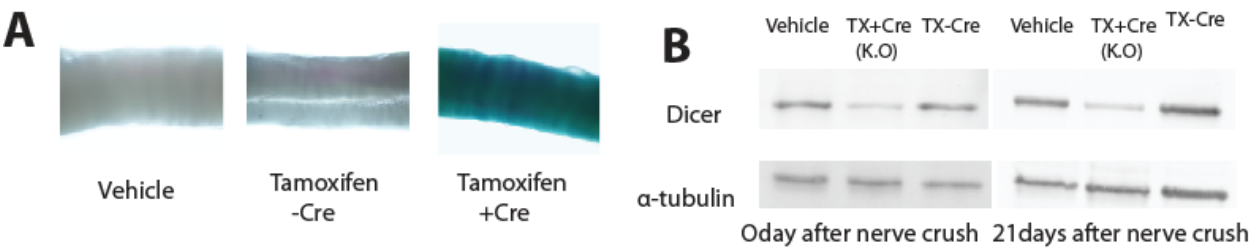
A
Vehicle
Tamoxifen -Cre
Tamoxifen +Cre
B
Vehicle
TX+Cre (K.O)
TX-Cre
Vehicle
TX+Cre (K.O)
TX-Cre
Dicer
α-tubulin
Oday after nerve crush
21days after nerve crush

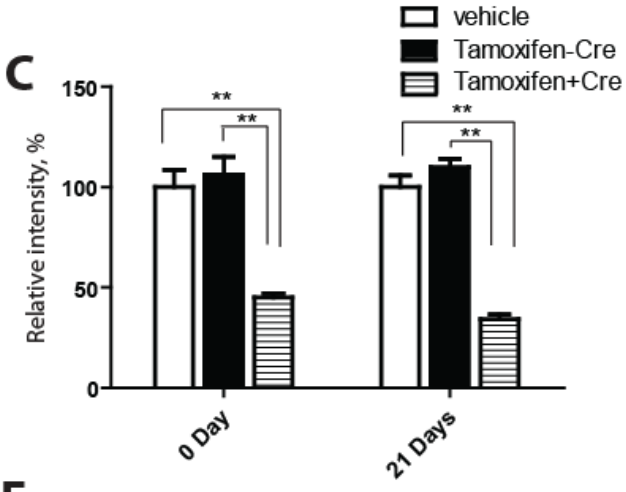
C
vehicle
Tamoxifen-Cre
Tamoxifen+Cre
Relative intensity, %
150
100
50
0
**
0 Day
21 Days

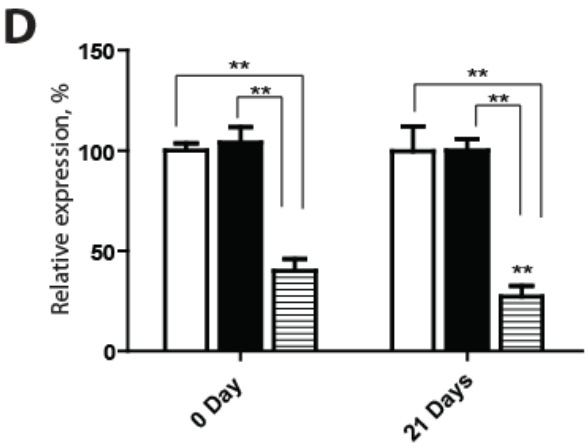
D
Relative expression, %
150
100
50
0
**
0 Day
21 Days

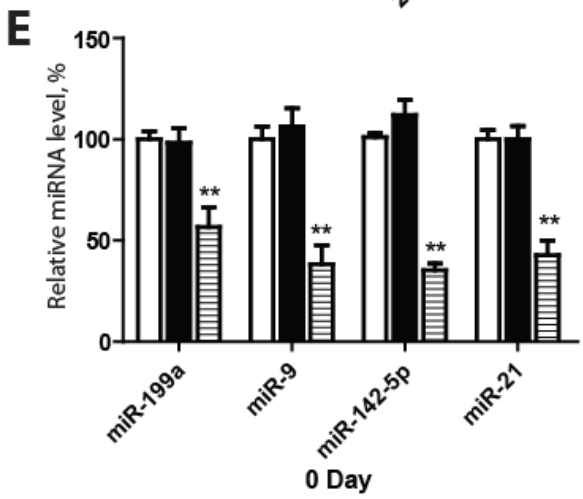
E
Relative miRNA level, %
150
100
50
0
**
miR-199a
miR-9
miR-142-5p
miR-21
0 Day

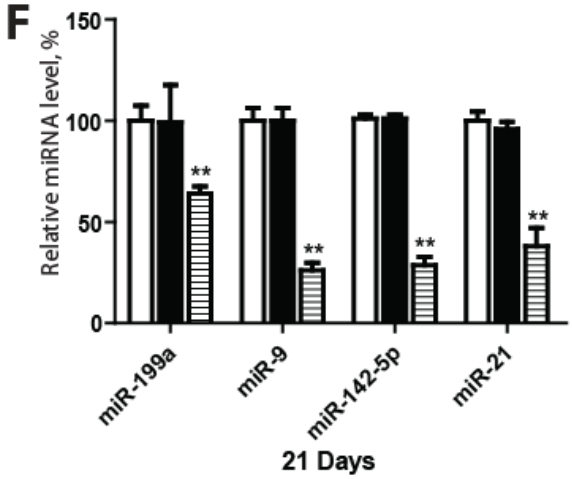
F
Relative miRNA level, %
150
100
50
0
**
miR-199a
miR-9
miR-142-5p
miR-21
21 Days

Figure 4.2. Behavioral tests reflect impaired restoration of sensory and motor function in *Dicer* KO.

(A) Sciatic functional index (SFI) ± the standard error of the mean (SEM) shows the recovery of motor function from sciatic nerve crush with/without *Dicer* deletion over the course of time. Tamoxifen treated *CAG-CreERt:Dicer*$^{fl/fl}$ mice (*Dicer* KO) demonstrated delayed recovery compared to vehicle treated animals and tamoxifen treated *Dicer*$^{fl/fl}$ mice. The difference between SFI reached statistical significance at day 14 and day 21 (N=20, * $p<0.05$). (B) von Frey test assessed mechanical sensitivity at 2, 4, 7, 14, and 21 days after nerve injury. All data were normalized to pre-injury baseline level. At 21 days post-injury, the threshold to mechanical stimuli was significantly lower in the *Dicer* KO group (N=15, * $p<0.05$). Tamoxifen treated *CAG-CreERt:Dicer*$^{fl/fl}$ mice are represented by dot lines, tamoxifen treated *Dicer*$^{fl/fl}$ mice are represented by dashed lines, and vehicle treated *CAG-CreERt:Dicer*$^{fl/fl}$ mice are represented by full lines.

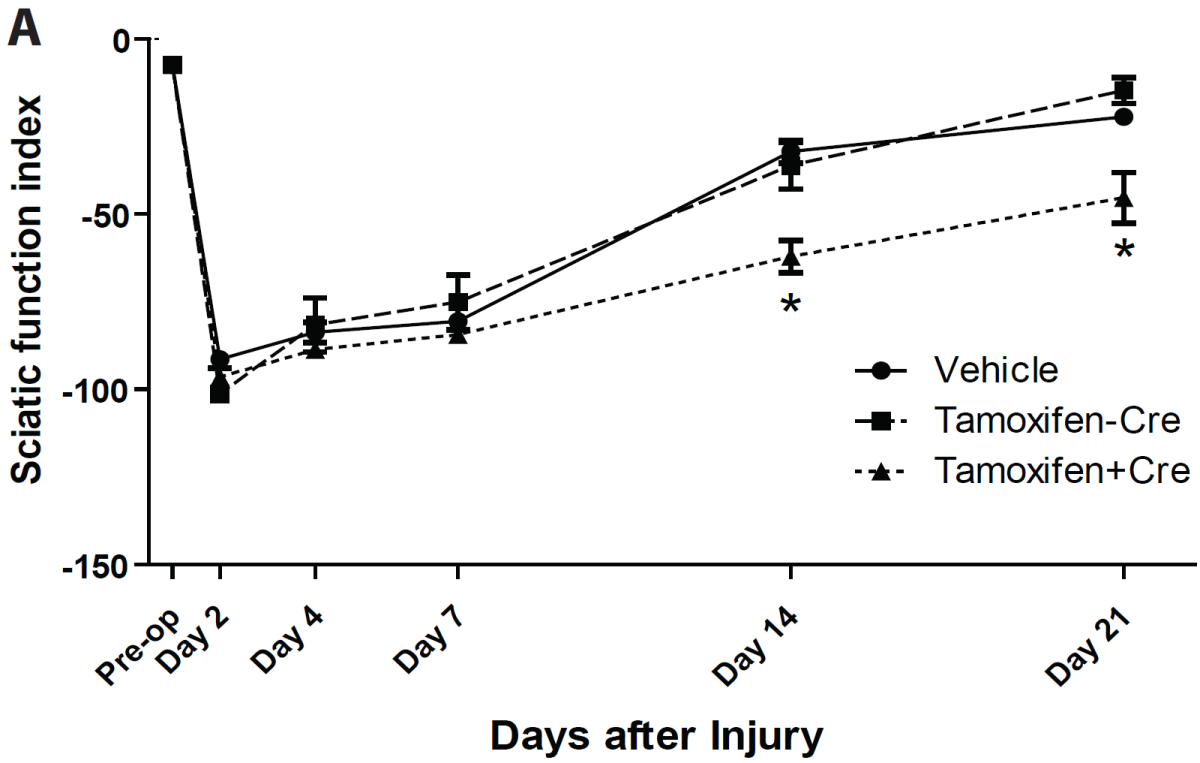
A
Sciatic function index
0
-50
-100
-150
Vehicle
Tamoxifen-Cre
Tamoxifen+Cre
*
*
Pre-op
Day 2
Day 4
Day 7
Day 14
Day 21
Days after Injury

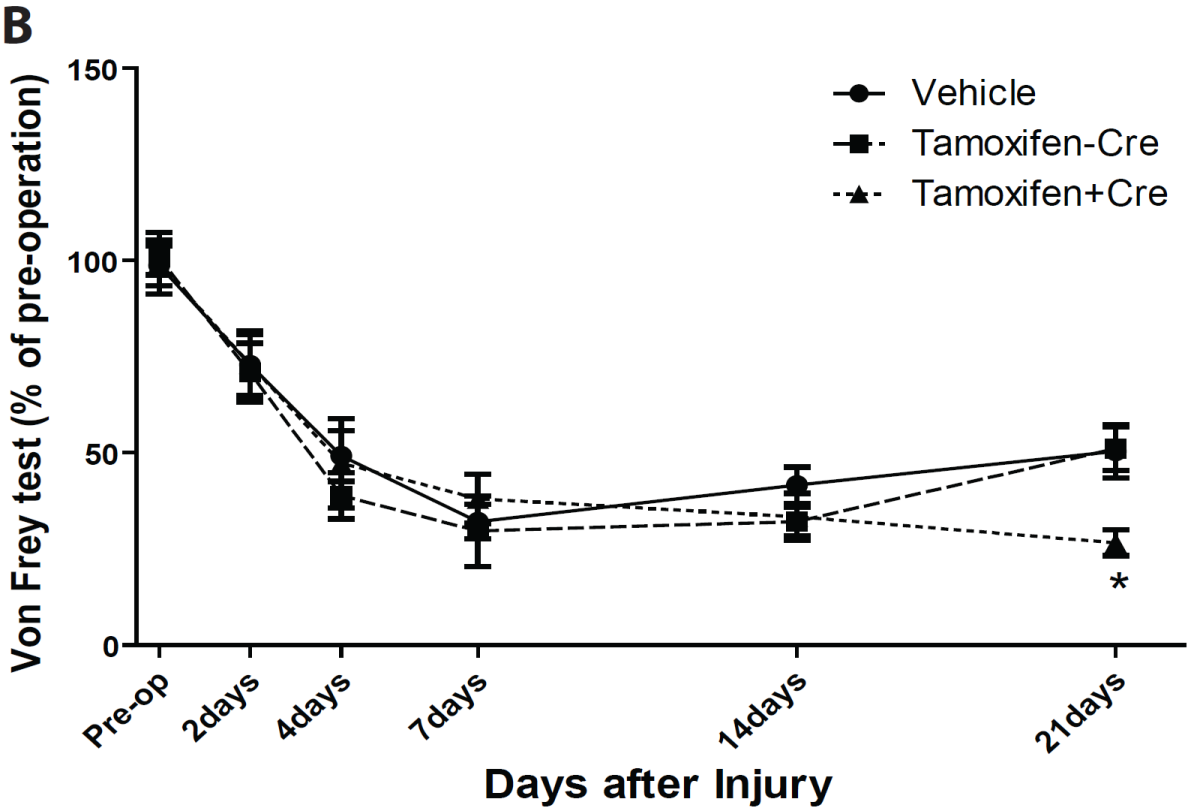
B
Von Frey test (% of pre-operation)
150
100
50
0
Vehicle
Tamoxifen-Cre
Tamoxifen+Cre
*
Pre-op
2days
4days
7days
14days
21days
Days after Injury

Figure 4.3. Electrophysiological evaluations of sciatic nerve functional recovery at 14 days after sciatic nerve crush.

(A) Typical examples of responses recorded from the distal side of the sciatic nerve after electrical stimulation. Stimulation of the proximal side of the sciatic nerves (500 μA, 100 μsec) induced a fast response with a single CAP in the intact nerve and a delayed and spread-out response in the regenerating nerve. (A_1) Compound action potentials (CAPs) recorded from the controlateral uninjured sciatic nerve. The signals recorded from vehicle treated mice and tamoxifen treated *Dicer*$^{fl/fl}$ mice (no *Dicer* deletion) were similar to that recorded from tamoxifen treated *CAG-CreERt:Dicer*$^{fl/fl}$ mice (*Dicer* KO). The duration from the stimulation artifact to onset of compound action potential was used for the calculation of nerve conduction velocity. No difference of NCV (B_1) or rectified and integrated compound action potential amplitude (C_1) was observed between the different groups in the controlateral uninjured nerves. (A_2) Delayed responses were recorded from the injured sciatic nerves 14 days after crush. Note the additional delay in the response of *Dicer* KO sciatic nerve of nearly 6 ms, indicating a reduced nerve conduction velocity, and suggesting a slower rate of functional recovery after injury in the *Dicer* KO animals.(B_2) Animals from all 3 groups gradually restored NCV on the crushed nerve with time. However, animals with *Dicer* KO (tamoxifen treated *CAG-CreERt:Dicer*$^{fl/fl}$) have a significantly lower NCV compared with control animals (tamoxifen treated *Dicer*$^{fl/fl}$ mice and vehicle treated mice). (C_2) *Dicer* KO animals also exhibited smaller rectified and integrated response amplitude (N=5, * $p<0.05$).

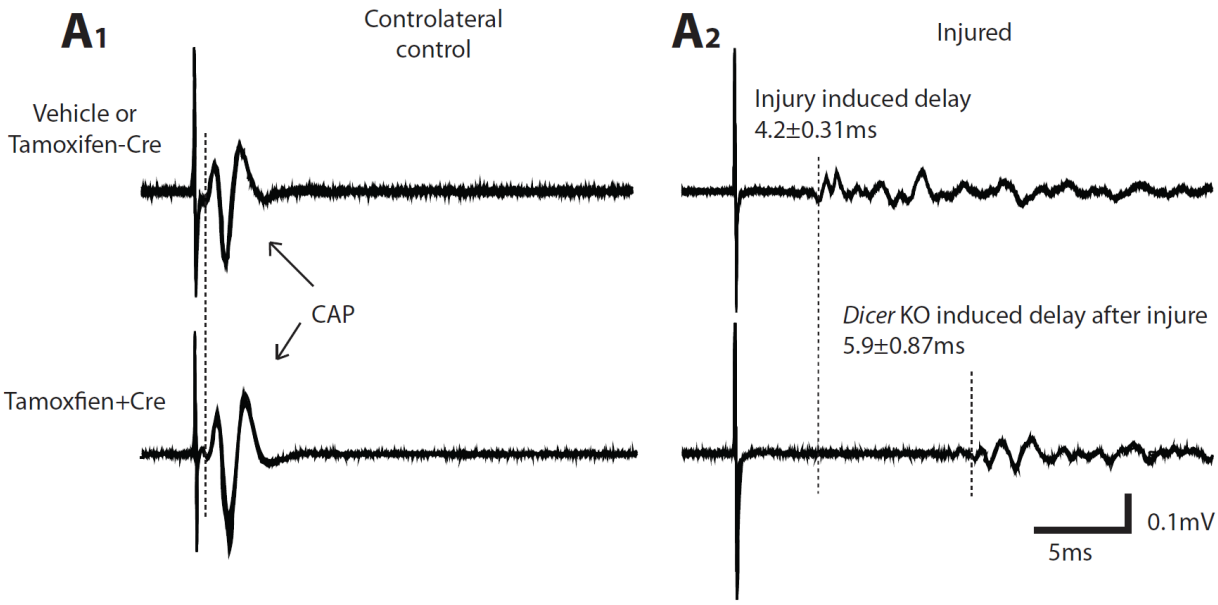
A1
Controlateral control
Vehicle or Tamoxifen-Cre
CAP
Tamoxfien+Cre
A2
Injured
Injury induced delay
4.2±0.31ms
Dicer KO induced delay after injure
5.9±0.87ms
0.1mV
5ms

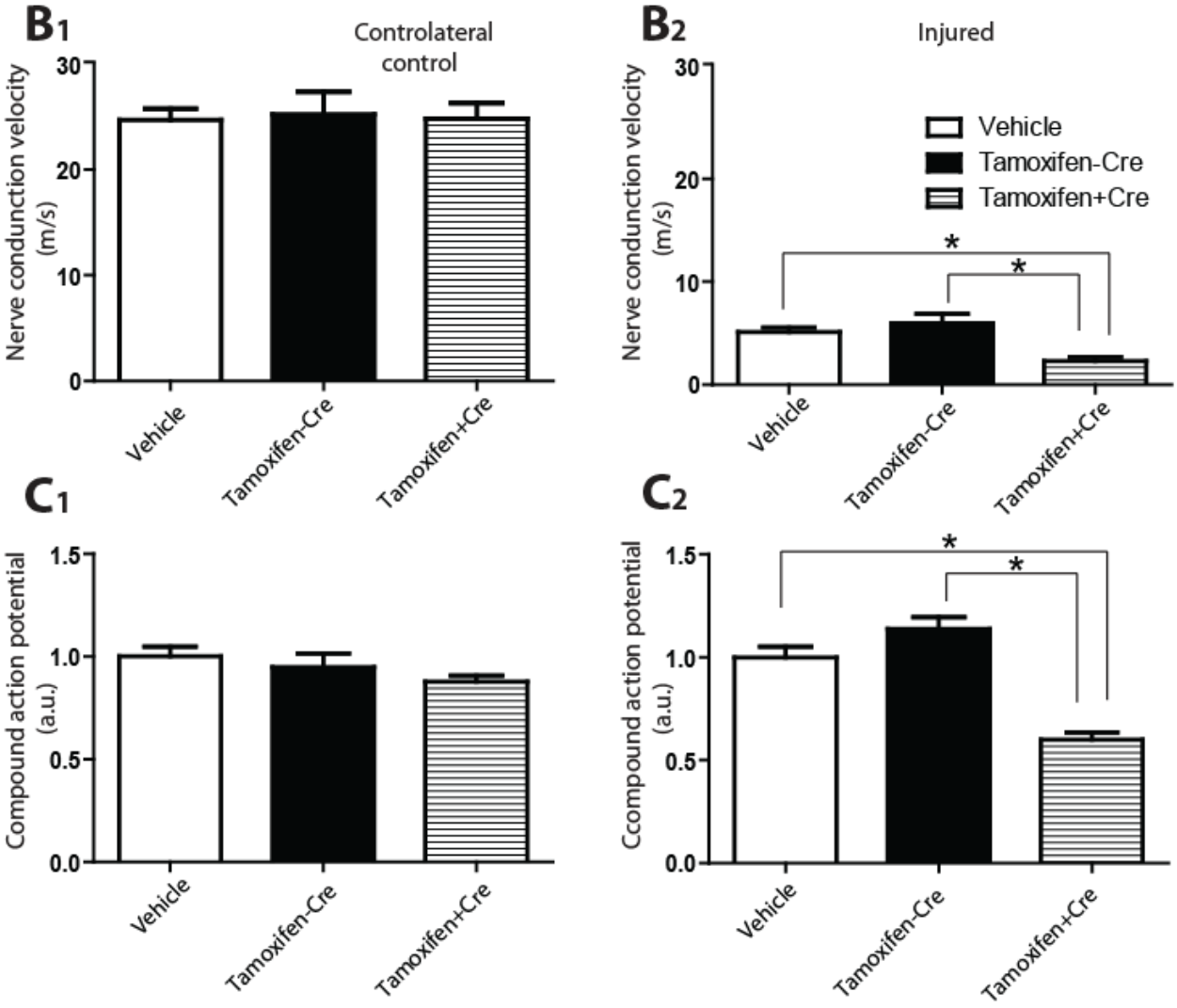
B1
Controlateral control
Nerve conduction velocity (m/s)
30
20
10
0
Vehicle
Tamoxifen-Cre
Tamoxifen+Cre
B2
Injured
Vehicle
Tamoxifen-Cre
Tamoxifen+Cre
*
*
C1
Compound action potential (a.u.)
1.5
1.0
0.5
0.0
C2
Ccompound action potential (a.u.)

Figure 4.4. Electrophysiological evaluations of sciatic nerve functional recovery at 21 days after sciatic nerve crush.

(A) Typical examples of delayed responses were recorded from the injured sciatic nerve 21 days after nerve crush with electrical stimulations at the proximal ends. Note the appearance of a quick response in signals from the control animals, while *Dicer* KO sciatic nerve still showed only a delayed response without any fast component. Waveform signals recorded at 14 days after nerve injury are repeated from Figure 3 A_2 for comparison purposes. (B) The NCV were compared between control groups (vehicle treated mice and tamoxifen treated $Dicer^{fl/fl}$) and *Dicer* KO groups (tamoxifen treated $CAG\text{-}CreERt{:}Dicer^{fl/fl}$). Animals with *Dicer* KO had a significantly lower NCV. (C) Difference in NCV between 14 and 21 days in three groups of mice. Although animals from all groups showed restored NCV with time, the increase in NCV was significantly smaller in *Dicer* KO animals from day 14 to day 21. (D) *Dicer* KO animals exhibited smaller rectified and integrated response amplitude 21 days after injury (N=5, * $p<0.05$).

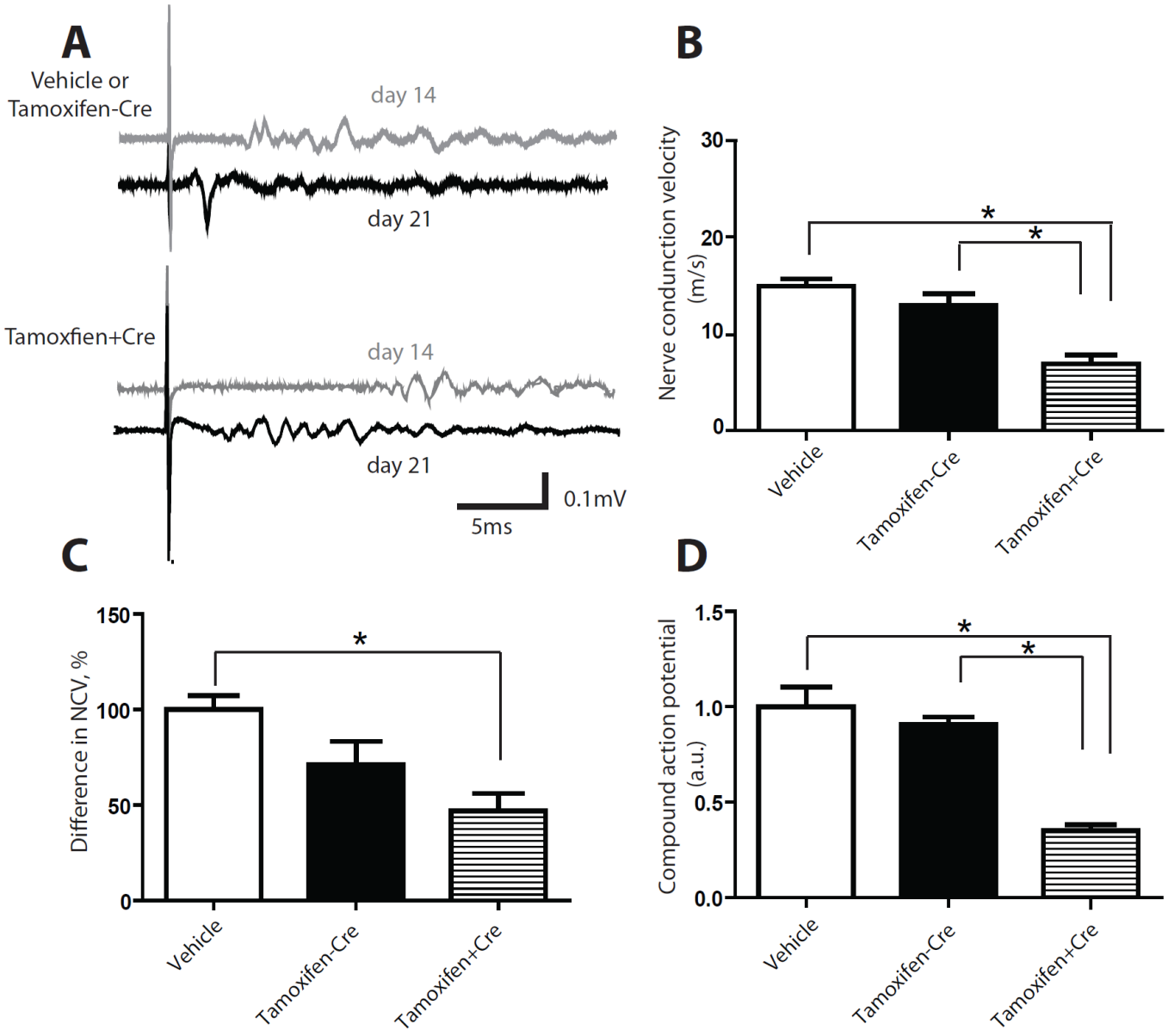
A
Vehicle or
Tamoxifen-Cre
day 14
day 21
Tamoxfien+Cre
day 14
day 21
0.1mV
5ms
B
Nerve conduction velocity (m/s)
30
20
10
0
*
*
Vehicle
Tamoxifen-Cre
Tamoxifen+Cre
C
Difference in NCV, %
150
100
50
0
*
Vehicle
Tamoxifen-Cre
Tamoxifen+Cre
D
Compound action potential (a.u.)
1.5
1.0
0.5
0.0
*
*
Vehicle
Tamoxifen-Cre
Tamoxifen+Cre

Figure 4.5. Light microphotographs of semi-thin sections of sciatic nerve give evidence of delayed regeneration of sciatic nerve fibers after *Dicer* deletion.

Transverse semi-thin sections of sciatic nerve distal to the injury sites were examined under light microscopy. Light micrographs of nerves from vehicle treated group (A, D) and tamoxifen treated *Dicer*$^{fl/fl}$ group (B, E) were compared with that of tamoxifen treated *CAG-CreERt:Dicer*$^{fl/fl}$ (*Dicer* knockout) group (C, F) at 14 days (upper panel) and 21 days (lower panel) post injury. Images obtained at higher magnification (D_1, E_1, F_1) clearly showed the regenerating axons with new myelin wrappings. Note smaller axons with thinner myelin in *Dicer* knockout group (F_1) compared to the two control groups (D_1, E_1), The statistical analysis showed that the number of myelinated axons (G) and myelinated mean axon area (H) at day 21 after crush were significantly lower in *Dicer* knockout mice (Scale bar = 10 μm, N = 6, * $p<0.05$).

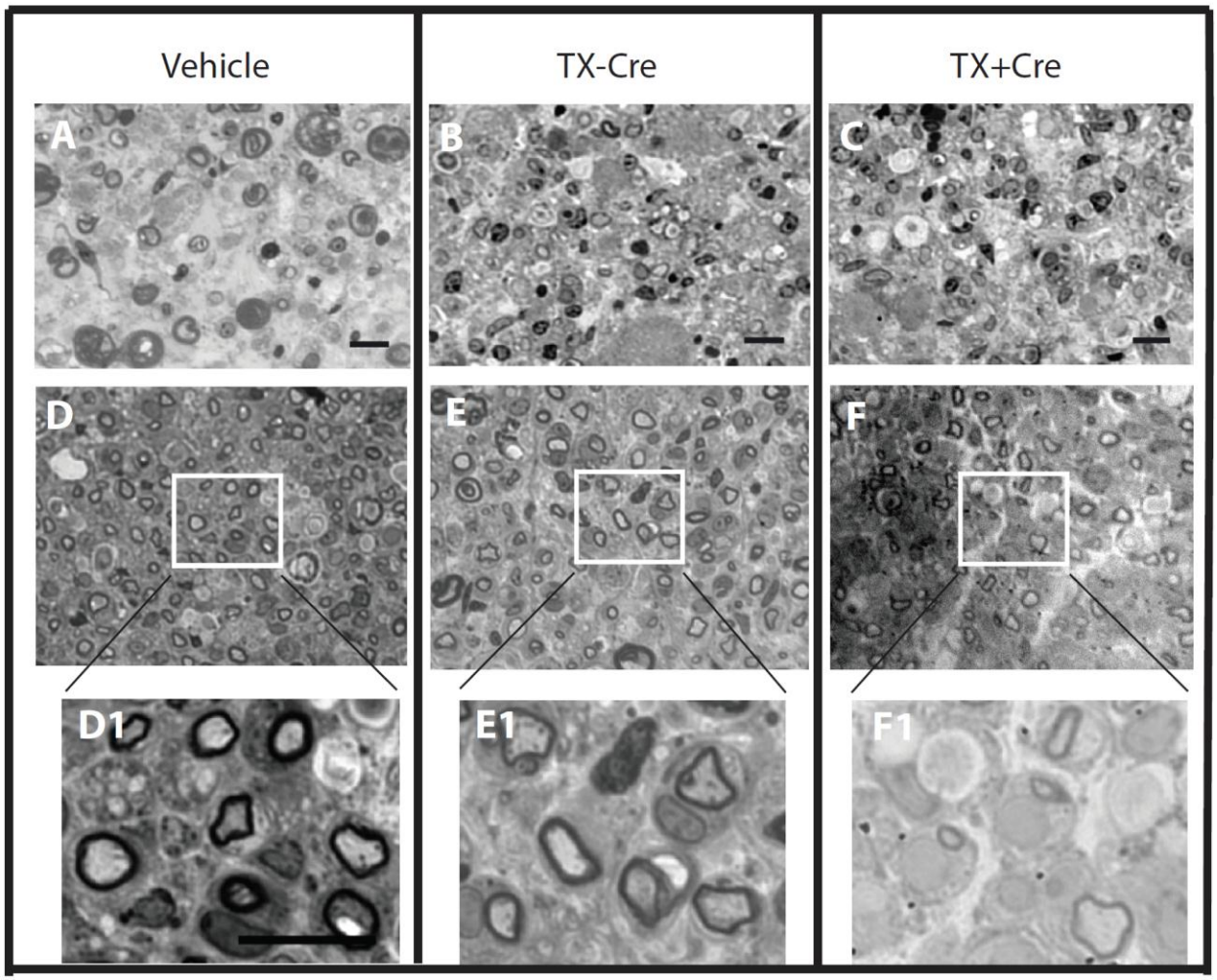
Vehicle
TX-Cre
TX+Cre
A
B
C
D
E
F
D1
E1
F1

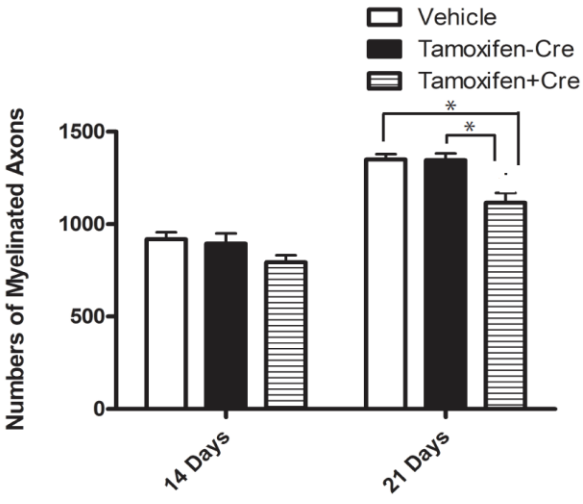
Vehicle
Tamoxifen-Cre
Tamoxifen+Cre
Numbers of Myelinated Axons
1500
1000
500
0
*
*
14 Days
21 Days

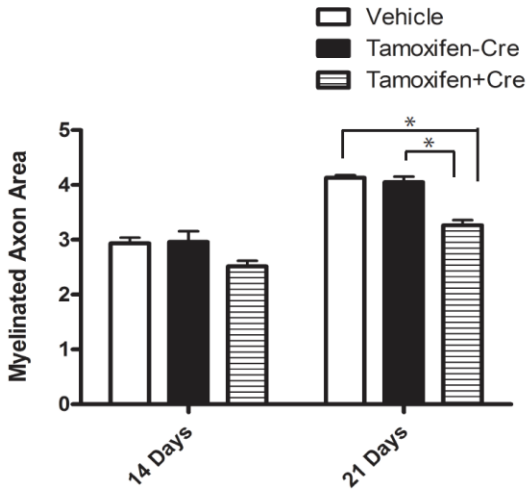
Vehicle
Tamoxifen-Cre
Tamoxifen+Cre
Myelinated Axon Area
5
4
3
2
1
0
*
*
14 Days
21 Days

Figure 4.6. *In vitro* study showed an arrested regenerative axon growth after *Dicer* deletion.

(A) DRG culture from vehicle treated CAG-CreERt:*Dicer*fl/fl. (B) DRG culture from *Dicer*fl/fl mice with tamoxifen treatment. (C) DRG culture from CAG-CreERt:*Dicer*fl/fl (knockout) mice with tamoxifen treatment. Fixed cells were incubated with antibodies against neuronal marker β-tubulin and signals were visualized with TX-Red conjugated secondary antibody. The statistical analyses were performed on the length (D) and the branch number (E) of the axons in dissociated DRG cultures. DRGs cultured from *Dicer* KO had significantly less axon branches and shorter axons compared with control groups. When DRGs were collected with animals with no treatment and tamoxifen was applied to cell cultures to induced neuronal cell specific *Dicer* knockout, similar inhibition in neurite growth was observed. Quantified data showed a significant decrease of the length (F) and the branch number (G) of the axons in dissociated DRG from CAG-CreERt:*Dicer*fl/fl mice with tamoxifen treatment (*Dicer* Knockout group) comparing to two control groups. (Scale bar=50 μm, N=30, * $p<0.05$).

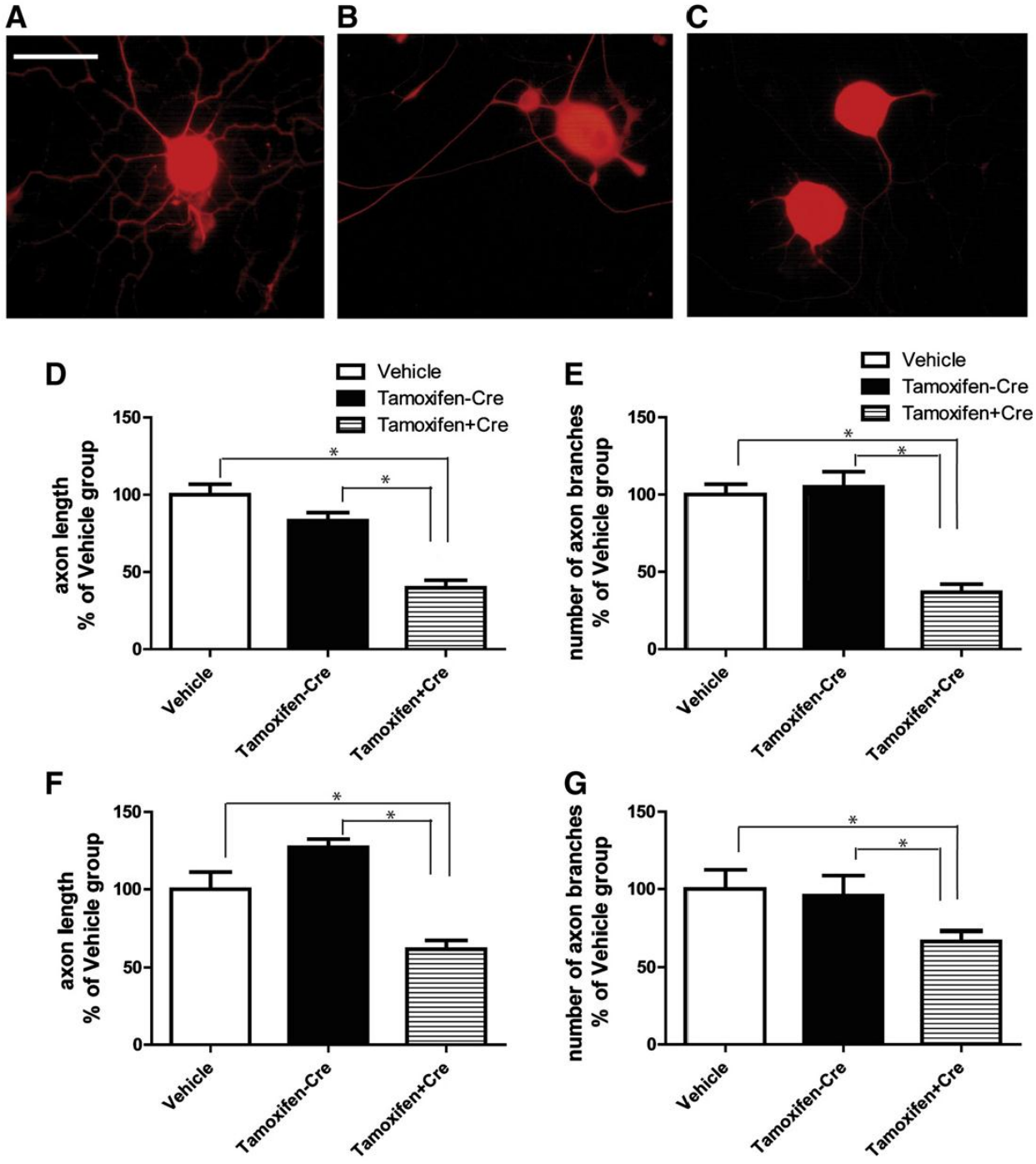
A
B
C
D
Vehicle
Tamoxifen-Cre
Tamoxifen+Cre
axon length
% of Vehicle group
150
100
50
0
*
*
Vehicle
Tamoxifen-Cre
Tamoxifen+Cre
E
Vehicle
Tamoxifen-Cre
Tamoxifen+Cre
number of axon branches
% of Vehicle group
150
100
50
0
*
*
Vehicle
Tamoxifen-Cre
Tamoxifen+Cre
F
axon length
% of Vehicle group
150
100
50
0
*
*
Vehicle
Tamoxifen-Cre
Tamoxifen+Cre
G
number of axon branches
% of Vehicle group
150
100
50
0
*
*
Vehicle
Tamoxifen-Cre
Tamoxifen+Cre

Discussion

Dicer ablation resulted in delayed functional recovery

Our experiments demonstrated a delayed functional recovery of *Dicer* KO in comparison to control groups in walking corridor and von Frey behavioral tests. Walking corridor SFI data are complementary to a recent study that showed progressive locomotor dysfunction and muscular atrophy after specific ablation of *Dicer* in post-mitotic postnatal motor neurons (Haramati et al., 2010). The authors also reported the perturbed expression of neurofilament subunits in their *Dicer* KO model and linked this observation to deregulation of miR-9 (Haramati et al., 2010). In another observation, loss of miR-206 accelerated progression of amyotrophic lateral sclerosis (ALS) and diminished survival (Williams et al., 2009). It was also suggested that the beneficial actions of miR-206 were mediated by muscle-derived factors that promote nerve-muscle interactions in response to injury of motor neurons (Williams et al., 2009). Therefore, our SFI data together with current observations suggest a significant role of miRNAs in motor neuron health and response to injury.

We have also observed delayed recovery of sensory function in *Dicer* KO using von Frey analysis. This observation is supported by previous findings which revealed that *Dicer* deletion led to severe defects in axon pathfinding of retinal ganglion cell (RGC) at the optic chiasm (Pinter and Hindges, 2010). This work has shown that miRNAs are essential regulatory elements for correct axon guidance decisions and the establishment of circuitry during neural development. Another recent report demonstrated that deletion of *Dicer* in Nav1.8^{+} sensory neurons attenuated or abolished inflammatory pain with corresponding decrease of nociceptor-specific pre-mRNA transcripts (Zhao et al., 2010). Furthermore, spinal nerve ligation changed

expression of the sensory organ-specific cluster of miRNAs in injured rat DRGs, which was linked to mechanical hypersensitivity (Aldrich et al., 2009). Thus, recent observations indicated a possible role for miRNAs in mechanism of pain. It has been recently proposed that miRNAs may participate in the regulatory mechanisms of genes associated with the pathophysiology of chronic pain as well as the nociceptive processing following acute noxious stimulation (Kusuda et al., 2011). Collectively, our von Frey data and previous reports propose a critical role of miRNAs in sensory neuron physiology and response to injury.

Dicer deletion impaired electrophysiological recovery.

CAP amplitude and NCV are routinely used as two indexes to evaluate progression of nerve regeneration (Shen et al., 2008, Sun et al., 2009). CAP and NCV may be affected by both damage to peripheral nerve and by muscle atrophy caused by denervation of target tissue (Navarro et al., 2007). To avoid muscle influence, this study was performed on isolated sciatic nerve preparation. Our electrophysiological data provided further evidence of the impaired nerve regeneration in the absence of *Dicer*. Measured NCV and CAP were significantly lower in *Dicer* KO animals at 14 and 21 day of regeneration. The delayed recovery of electrophysiological indexes may be explained by a failure in axon outgrowth and/or remyelination of the new fibers. After peripheral nerve injury, Schwann cells provide trophic and mechanical support for regenerating axons and subsequently form new myelin sheath (Navarro et al., 2007). Interestingly, Schwann cell-specific deletion of *Dicer* fully arrest Schwann cell differentiation, resulting in early postnatal lethality (Bremer et al., 2010). Specifically, most Schwann cells arrest at the promyelinating stage (Pereira et al., 2010). *In vivo*, this results in a neurological phenotype similar to congenital hypomyelination (Yun et al., 2010). Conversely, several miRNAs were identified as regulators of myelination (Bremer et al., 2010, Yun et al., 2010). For instance, miR-

138 was described as a potential repressor of key immature Schwann cell genes, thus facilitating myelination (Yun et al., 2010). Another miRNA, miR-219, was demonstrated to play a critical role in enabling the rapid transition from proliferating oligodendrocyte precursor cells to myelinating oligodendrocytes (Dugas et al., 2010). Therefore, current data suggest that during nerve regeneration, disrupted miRNA biogenesis could result in failed remyelination and consequently in loss of saltatory propagation. Ablation of *Dicer* might also hamper the ionic remodeling process. Indeed, recent observation has identified a group of miRNAs regulating voltage-gated sodium channel Scn11a, alpha 2/delta1 subunit of voltage-dependent Ca-channel, and purinergic receptor P2rx ligand-gated ion channel 4 in the spinal nerve ligation model of neuropathic pain (von Schack et al., 2011). Thus, the impaired function in ion channels might be another factor potentially contributing to the delayed recovery of peripheral nerve electrophysiological characteristics.

Delayed anatomical recovery in *Dicer* mutants

Our histological evaluation showed that *Dicer* KO reduced the total number of myelinated axons as well as diminished the mean axonal area in regenerating sciatic nerve. Previous studies demonstrated the critical role for miRNAs in the transition of Schwann cells from the pro-myelin stage to the myelinating stage (Bremer et al., 2010, Pereira et al., 2010, Yun et al., 2010). Ultrastructural and biochemical analysis of sciatic nerves from postnatal mice revealed a severe myelination defect in Schwann cell-specific *Dicer KO* animals (Bremer et al., 2010, Pereira et al., 2010, Yun et al., 2010). *Dicer*-deficient Schwann cells not only failed to myelinate, but were also unable to form normal Remak bundles of unmyelinated small-caliber axons (Bremer et al., 2010). Western blot analyses of Schwann cell-DRG co-cultures grown under myelinating conditions revealed that reduced levels of *Dicer* led to a decrease in the

expressions of myelin basic protein and protein zero, which were accompanied by significant reductions in synthesis of myelin (Verrier et al., 2010). Loss of *Dicer* specifically in Schwann cells can also result in signs of axonal degeneration, which suggest the involvement of miRNAs in the maintenance of axon integrity (Pereira et al., 2010). Taken together, our data and previous findings suggest that ablation of *Dicer* might lead to myelination defect, perturbation of axon integrity and consequently to the failure of axon to grow back.

Dicer **ablation impaired regenerative ability of PNS neuron** ***in vitro***

To answer the question whether the loss of *Dicer* could directly impact regenerative ability of PNS neuron, we performed a study in dissociated DRG cultures after conditioning sciatic nerve lesion. Interestingly, while conditioning lesion resulted in robust axon outgrowth in wild type neurons, *Dicer*-deficient neurons exhibited striking decrease in axon length and branching-arborization. The observed regenerative failure in DRG neurons after ablation of *Dicer* provided new evidence that miRNA pathway per se may play a critical role in intrinsic mechanism of axon growth. Several previous studies implicated miRNAs in translational control in dendrite outgrowth, as well as synaptic plasticity (Ashraf et al., 2006, Siegel et al., 2009). For example, miR-134, which is localized at synaptic sites, inhibits translation of *lim-domain-containing protein kinase1* (*Limk1*) mRNA. *Limk1* regulates actin filament dynamics and its ablation resulted in abnormalities in dendritic spine structure (Schratt et al., 2006). In addition, miR-134 constrains neuritogenesis by down-regulating the expression of its target Pumillio, an evolutionarily conserved dendritogenesis promoting factor (Fiore et al., 2009). MiR-138 controls the expression of acyl protein thioesterase 1 (APT1), an enzyme regulating the palmitoylation status of proteins that are known to function at the synapse (Siegel et al., 2009). Recent studies have also shown that in cultured cortical and hippocampal neurons, miR-132 functions

downstream from CREB to mediate dendritic growth and spine formation. Deletion of the miR-212/132 locus caused a dramatic decrease in dendrite length, arborization, and spine density (Magill et al., 2010). Thus, while previous reports demonstrated an important role of miRNAs in neurito- and dendritogenesis our current observation revealed a critical role of *Dicer*-dependent miRNA pathway in axonogenesis.

Potential role of *Dicer*-dependent miRNAs in nerve regeneration

Our data clearly showed that albeit *Dicer* KO animals did recover after sciatic nerve crush, the recovery was significantly slower than in wild type controls. The remaining regenerative ability of peripheral nerves in *Dicer* mutants could be explained by remaining miRNAs, which were still detectable in the tamoxifen-treated samples. According to the literature, the tamoxifen-inducible *Dicer* KO usually results in around 80% elimination of *Dicer* mRNA (Pereira et al., 2010, Albinsson et al., 2011). Since in our study activation of *Cre* did not completely eliminated *Dicer* expression in sciatic nerves either, it is conceivable that the remaining gene was still functional. In addition, the mature miRNAs appear to be rather stable (O'Rourke et al., 2007) and could continue to function for quite some time before being completely degraded (Kawase-Koga et al., 2009). Therefore some stable miRNAs could also contribute to the process of nerve regeneration even after *Dicer* deletion. Conversely, some miRNA species can still be processed by alternative *Dicer*-independent biogenesis pathway recently uncovered in vertebrates (Yang and Lai, 2010). In this pathway, the pre-miRNA is loaded into Ago2 and then cleaved by the Ago2 catalytic center to the mature form (Cheloufi et al., 2010). Thus, *Dicer*-independent miRNA biogenesis pathway might be another potential source of miRNAs production, and therefore provide some functional compensation after the ablation of *Dicer*.

Conclusion

In conclusion, we have provided the first evidence that the intact *Dicer*-mediated miRNAs pathway is required for effective and timely regeneration of peripheral nerve *in vivo* and regenerative axon growth *in vitro*. Axon loss has been largely neglected as a therapeutic target in a variety of neurological symptoms and disorders including multiple sclerosis, stroke, traumatic brain and spinal cord injury, peripheral neuropathies and chronic neurodegenerative diseases including Alzheimer's (Coleman and Perry, 2002). Understanding how axon-degeneration/regeneration process is initiated by these diverse insults could lead to new treatments. We anticipate that our study could pave the way for further explorations of miRNA-regulated regenerative mechanisms in the peripheral as well as central nervous systems and possibly herald novel miRNA based therapies of neurological disorders and injuries.

CHAPTER V: Injury-induced miR-431 Promotes Regenerative Axon Growth in DRG Neurons

Summary

miRNAs are small, non-coding RNAs that function as important post-transcriptional regulators in developmental and physiological processes. Our previous work showed that peripheral nerve axons *in vivo* and *in vitro* contain functional miRNA machinery that would respond to peripheral nerve injury. In addition, we demonstrated that the deletion of *Dicer*, a key enzyme responsible for generation of miRNAs, can delay regenerative axon growth *in vivo* and *in vitro*. These studies have indicated that miRNAs are likely to be important mediators of neuronal plasticity during peripheral nerve regeneration. In this study, we reveal a group of injury-regulated miRNAs in dorsal root ganglion (DRG) neurons after conditioning sciatic nerve lesion by miRNA array analyses. Among those miRNAs, miR-431 was highly induced in DRG neurons following sciatic nerve crush. In dissociated murine DRG neurons, the gain and loss of function analyses for miR-431 revealed that overexpression of miR-431 promoted neurite outgrowth. Potential gene targets for miR-431 were predicted by bioinformatics tools and validated experimentally. Wnt pathway-related transmembrane protein *Kremen1* was the target for miR-431. The reverse correlation between the expression of *Kremen1* and miR-431 was proven with RT-qPCR at mRNA level and Western blot at protein level. miR-431 induced association between *Kremen1* mRNA and RISC was shown by cross linked immunoprecipitation. These data show that miR-431 could be an important regulator of regenerative axon growth and a promising candidate for the future miRNA based therapies that enhance the endogenous neuroregenerative capacity.

Introduction

After axonal injury, changes occur in the region of the axotomized neuronal cell bodies as well as in the microenvironment immediately adjacent to the site of injury (Zigmond, 2011). Further, gene expression profiles in neurons, such as DRG (Kuo et al., 2011), superior cervical sympathetic ganglia (SCG) (Boeshore et al., 2004), and retinal ganglion cells (RGC) (McCurley and Callard, 2010) also are altered after axotomy. At the protein level, increases and decreases of gene expressions have also been documented, which translate into phenotypic changes that enable the regeneration of severed axons (Strickland et al., 2011).

Considerable attention has focused on the underlying mechanisms that contribute to neural regeneration. The studies on DRG neurons following sciatic nerve injury revealed several classes of genes responding to injury, such as neuropeptides, signal transduction molecules, cell cytoskeletal components, and inflammatory mediators (Strickland et al., 2011). However, the mechanisms that are responsible for the global regulation in gene expressions remain largely unclear.

One possible regulatory mechanism involved in nerve regeneration is controlled by miRNA pathway. miRNAs are short, non-coding RNAs that silence mRNA expression by imperfect binding to miRNA recognition elements in mRNA targets (Bartel, 2004, Filipowicz et al., 2008). Their ability to simultaneously regulate the expression of several genes suggests that miRNAs are potential regulators for complex transcriptional networks (Yu et al., 2011a, Yu et al., 2011c). In the nervous system, miRNAs have been linked to neurodevelopment (Smith et al., 2010), neurogenesis (Shi et al., 2010), and neurological disorders (Hebert and De Strooper, 2007,

Kim et al., 2007). More recently, research established that a group of miRNAs reside within the distal axonal domain of superior cervical ganglia neuron (Natera-Naranjo et al., 2010). Further, changes in the expression of miRNA machinery in response to peripheral nerve lesion have also been reported (Wu et al., 2011a). Lastly, altered miRNA levels in DRG after sciatic nerve injury also suggested the contribution of miRNAs pathway in nerve regeneration (Yu et al., 2011a, Zhang et al., 2011).

Recent studies in our lab showed the importance of miRNAs in peripheral nerve regeneration using an inducible *Dicer* knockout model. Blocking *Dicer* dependent miRNA biogenesis markedly delayed the regenerative axon growth *in vivo* and *in vitro*, giving an indication of the functions of miRNAs in then PNS (Wu et al., 2012). In the current study, we investigated the role of individual miRNAs, which followed an injury-regulated expression pattern during peripheral axonal regeneration by *in vitro* functional analysis. Herein, we reported that miR-431, an injury-induced miRNA, promoted regenerative axon growth in DRG neurons. In addition, its potential target gene *Kremen1* was validated experimentally. *Kremen1* functions as a negative regulator of the Wnt signaling pathway. Our observations suggest that upregulation of miR-431 after nerve injury inhibits the expression of *Kremen1*, leading to the activation of Wnt pathway. Collectively, our observations provide additional evidence for a role for miRNA pathway in regulating axonal regeneration following peripheral nerve injury.

Results

miRNAs are differentially expressed in DRG upon sciatic nerve injury

We analyzed miRNA expressions in DRGs from CD1 mice using microarrays at 4 days after sciatic nerve crush. DRGs were collected from both the pre-conditioned side, as well as the contralateral uninjured side. RNA from the contralateral uninjured side served as a control group. At 4 days post-injury, pre-conditioned DRG neurons showed robust regenerative axon growth in previous studies (Forman et al., 1980). RNA from the pre-conditional DRG was considered the actively regenerating group. By comparing the miRNA expression profiles from preconditioned DRG and control DRG, miRNAs that were upregulated and downregulated during the process of regeneration were determined. Several miRNAs demonstrated differential expression based on regenerative growth condition. Using 1.5-fold cut-off, statistical analyses revealed that 19 miRNA were differentially expressed in the pre-conditioned DRG compared to the non-conditioned contralateral DRG. Of those 19, 11 miRNAs had higher expression level in pre-conditioned group and the other 8 miRNAs had lower expression level in DRG during regeneration (Fig. 5.1A). miR-431, miR-714, miR-744, miR-877, miR-130b, miR-21, miR-323-3p, miR-325, miR-409-3p, miR-154*, and miR-681were significantly increased 4 days post sciatic nerve crush in pre-conditioned DRGs, while miR-190, miR-1, miR-33, miR-32, miR-153, miR-335-5p, miR-193, and miR-488 showed significantly decreased expression.

We validated the microarray data for miR-744, miR-431, and miR-21 using real time PCR. We also included miR-124 and miR-29a in our real time PCR experiments as negative controls. These two miRNAs play various roles in neurodevelopment and maintenance of neuronal cell homeostasis; however they did not show changes in their expression in our array

data. In agreement with the microarray data, miR-744, miR-431, and miR-21 were significantly upregulated when the neuronal cells were regenerating. There was a 2 fold upregulation of miR-744, 2.4 fold upregulation of miR-431, and 2.5 fold upregulation of miR-21, respectively (Fig. 5.1B). Further, RT-qPCR experiments showed that miR-29a and miR-124 did not change in their expression.

Optimization of transfection and silencing efficiencies

We first optimized transfection of miRNA mimics and inhibitors into primary neuronal cell cultures with a FAM-conjugated scrambled miRNAs. Transfection efficiency of RNA molecules was above 90% as determined under immunofluorescence microscope (Fig. 5.2A and B). Since DRG neurons are considered 'hard-to-transfect' cells, the efficiency of transfected miRNA mimics/inhibitors to alter their target gene expression in DRG neuronal cells was also determined. As part of this process, we utilized miR-1, a well-established positive control, in our samples. miR-1 effectively downregulated the expression of twinfilin-1, also known as PTK9, at the mRNA level once cell transfection occurred. Based on the expression level of PTK9, we analyzed the efficiency of miRNA mimics and miRNA inhibitors in our neuronal cell cultures. The mRNA levels of the miR-1 target gene PTK9 were quantified by RT-qPCR analysis in five groups of cell cultures. Our data show that the negative control of miRNA mimics did not change the mRNA level of PTK9, whereas miR-1 mimic caused the destabilization of its target mRNA, leading to the significant decrease of the PTK9 mRNA level (Fig. 5.2B). By applying the miR-1 inhibitor, it salvaged the expression of PTK9 mRNA and prevented the miR-1 induced degradation of PTK9 mRNA. Conversely, the negative control of miRNA inhibitors has a scrambled nucleotide sequences. This prevented its binding to miR-1 and therefore, the mRNA

level of PTK9 in the last group was comparable to its level in miR-1 mimic treated group (Fig 5.2C).

miR-431 promotes neurite regenerative outgrowth

To investigate the role of miR-431 in regenerative axon growth, we manipulated the level of miR-431 in dissociated DRG neurons. We observed a positive correlation between miR-431 expression and neurite outgrowth in dissociated DRG neuronal cell culture (Fig. 5.3A). Increased mir-431 level was achieved by applying miR-431 mimic into DRG neuronal cell cultures at a final concentration of 100 nM. Overexpression of miR-431 significantly increased axon length. Additionally, blocking miR-431 activity by miR-431 inhibitor significantly inhibited neurite extension (no treatment control group: 100 ± 5%; miR-431 mimic group: 130 ± 6%; mimic negative group: 91 ± 4%; miR-431 inhibitor group: 75% ± 7%; inhibitor negative control: 90 ± 8%) (Fig. 5.3A and B). Further, manipulating miRNA-431 levels also affected axon branching, and led to a decrease in the number of branches per neuron due to transfection of miR-431 inhibitor (no treatment control group: 100 ± 9%; miR-431 mimic group: 110 ± 10%; mimic negative group: 82 ± 7%; miR-431 inhibitor group: 64% ± 6%; inhibitor negative control: 86±10%) (Fig. 5.3A and C).

We next studied GAP-43 expression in DRG neurons with miR-431 mimic and inhibitor treatments, as a strong correlation between neurite outgrowth and expression of Gap-43 has been reported in previous studies (Benowitz and Routtenberg, 1997). GAP-43 mRNA level was detected with RT-qPCR. Fig 5.3E clearly demonstrates a significant increase in GAP-43 mRNA in the cultures treated with 100 nM of miR-431 mimics, as compared to the group treated with the scrambled miRNA mimic control. This correlated with previous morphological data that

axon length was significantly higher after overexpression of miR-431. Furthermore, antibodies against GAP-43 were utilized to detect the expression of GAP-43 protein in DRG neuron. Immunofluorescent image showed that GAP-43 localized in both neuronal cell bodies and axons, and transient transfection of miR-431 mimics increased the signal intensity from the antibodies against GAP-43 (Fig 5.3A and D). Sequestration of miR-431 by the use of miR-431 inhibitors had the opposite effect. However, the decrease of the GAP-43 expression was not statistically significant.

Kremen1 **is a potential target of miR-431**

Bioinformatic prediction revealed a large number of potential miR-431 targets. We used two databases (http://www.targetscan.org and http://www.microrna.org) to generate a list of mRNAs with potential binding site for miR-431 in their 3' UTR. The potential candidates were further selected based on evaluation of the gene expression profile of DRGs four days post sciatic nerve injury. We detected an increased expression of miR-431 in preconditioned DRG, suggesting that in the same RNA samples, the targets mRNAs of miR-431 should show decreased expression levels. Only 24 genes met both criteria, having conservative binding site for miR-431 in their 3' UTR and down-regulated expression level in DRG after sciatic nerve injury.

To investigate which genes may be regulated by miR-431, we applied miR-431 mimics to neuronal cells induced from PC12 cells and to DRG neurons. As shown in table 3, the mRNA expression of the 24 potential target genes were evaluated by RT-qPCR. CLIP experiments were performed to confirm the association of target genes with RISC. Employing the Western blotting analysis for proteins from DRG cultures with different treatments confirmed the correlation

between gene expressions and miRNA expression. Our experimental validation suggested *Kremen1* as the target gene for miR-431.

Kremen1 has one binding site for miR-431 at its 3' UTR, at the position 2530-2536 bp. It corresponds perfectly to nucleotides 2-7 of the mature miRNA in mouse, rat, and human. In addition, the seed target site is close the poly-A tail, which increases its accessibility. To show that miR-431 regulates endogenous *Kremen1* in DRG neurons, we transfected cells with miR-431 mimics, miR-431 inhibitors, mimic negative control, or inhibitor negative control. In protein analysis, miR-431 reduced *Kremen1* protein levels within DRG neurons, whereas when endogenous miR-431 was inhibited, the expression level of the *Kremen1* protein was significantly higher than in negative control groups. Quantification of three independent experiments revealed that miR-431 reduced *Kremen1* protein levels by 50% when compared with the mimic negative control group. On the other hand, inhibition of endogenous miR-431 resulted in a significant increase of *Kremen1* expression by 45% (Fig 5.4B and C).

Since miRNA-mediated gene regulation can destabilize target mRNA and reduce the level of the target mRNA, we used RT-qPCR to determine the effect of miR-431 on *Kremen1*. Similar to what we observed on the protein level, when miR-431 level was up-regulated by transient transfection of miR-431 mimics, the mRNA level of *Kremen1* went down 30% and when endogenous miR-431 was inhibited by miR-431 inhibitors, the mRNA level of *Kremen1* was significantly elevated (Fig 5.4A). These results demonstrated that miR-431 level is inversely correlated to *Kremen1* expression at both protein and mRNA level in DRG neurons.

To establish whether there is a direct interaction between *Kremen1* mRNA and miR-431 in the RNA-induced silencing complex (RISC), immunoprecipitation of the Ago2 protein, the

central component of the RISC was carried out. PCR was performed to quantify the level of *Kremen1* mRNA presented in the total RNA and IP fractions from DRG cultures treated with miRNA mimic negative control and miR-431 mimic. miR-431 mimic increased the level of miR-431 in DRG neuronal cell cultures (Fig. 5.4 D). In the total RNA samples from DRG cultures, overexpression of miR-431 reduced the amount of stable *Kremen1* mRNA when compared to the miRNA mimic negative control group (Fig 5.4E). In the Ago2 immunoprecipitated RNA samples, overexpression of miR-431 obviously increased the level of Ago2 associated *Kremen1* mRNA (Fig 5.4E). Nonspecific mouse serum conjugated beads were used as a negative control, since they could not precipitate Ago2 and Ago2 associated RNAs. In this IP negative control group, no detectable *Kremen1* mRNA was observed, confirming the specificity of the precipitation (Fig 5.4E). These data showed that in the miRNA mimic negative control groups, the amount of endogenous *Kremen1* RNA associated with Ago2 was very low. When the abundance of miR-431 was elevated, the interaction between miR-431 and *Kremen1* mRNA in RISC was enhanced. Therefore, the amount of *Kremen1* in association with Ago2 increased after miR-431 mimics were transfected into DRG neurons.

Together, these data suggest that miR-431 actively modulates *Kremen1* protein and RNA expression within DRG neurons through association to *Kremen1* mRNA in RISC.

Kremen1 **expression in DRG** ***in vivo***

After establishing a relationship between miR-431 and *Kremen1*, we next investigated the expression patterns of *Kremen1* during nerve regeneration. From gene expression array data, *Kremen1* expression in DRG decreased at 4 days after sciatic nerve injury, suggesting its expression was downregulated as peripheral nerve regenerated. To further confirm the functional

relationship between miR-431 and *Kremen1*, we collected DRGs 4 days after sciatic nerve injury, as we did prior for microarray analysis. We analyzed RNA and protein from control and injured mouse DRGs. RT-qPCR revealed that *Kremen1* RNA expression decreased 4 folds at 4 days after nerve crush when regenerative axon growth was taking place (Fig. 5.5A). Similarly, we found that *Kremen1* protein was reduced in DRG 4 days post injury. The Western blot data showed a significant 80% decrease in *Kremen1* expression after sciatic nerve injury when compared to control (Fig.5.5B).

The expression of *Kremen1* in DRG neuron was further examined *in vitro*. Immunostaining with antibodies against *Kremen1* revealed the localization of *Kremen1* in dissociated DRG neurons. In both preconditioned and control groups, the immunoreactivity of *Kremen1* was detected mainly in neuronal cell bodies, but there was less *Kremen1* immunostaining in the preconditioned group (Fig. 5.5C). The data further supported a functional relationship between miR-431 and *Kremen1* in regenerating DRG neurons and implicated the role of *Kremen1* in peripheral nerve regeneration.

Functional analysis for *Kremen1*

Given the effects of miR-431 on *Kremen1* expression and the role of miR-431 in neurite outgrowth, the effect of downregulating *Kremen1* expression on regenerative axon growth was investigated. Two groups of DRG neurons were culture *in vitro*. One group was transfected with siRNA specifically targeting *Kremen1* mRNA, which inhibit *Kremen1* expression in DRG neurons. A negative scrambled siRNA was transfected to the other group of DRG cultures to control for any nonspecific effects of transfection. The differences in the regenerative growth

between *Kremen1* siRNA group and control scrambled siRNA groups were specifically resulted from the knock down of *Kremen1* expression in neuronal cells.

From the quantified data shown in Fig. 5.6B and C, knockdown of *Kremen1* significantly changed axon length, but not the number of axon branches in dissociated DRG culture. The axon length in the *Kremen1* knockdown group increased 30% in comparison to the scrambled siRNA control group. This effect on axon outgrowth is similar to miR-431 overexpression on axon outgrowth, which suggests miR-431 mediated increase of axon growth is through *Kremen1* repression.

Figure 5.1. Sciatic nerve injury induced changes in miRNA expression profile in DRG

(A) Total RNA for the microarray expression analysis was isolated from DRG 4 days after sciatic nerve crush. Agilent arrays were done in duplicates and repeated twice. Normalization and analyses were performed with GeneSpring software. miRNAs with a statistically significant upregulation or downregulation over 1.5 fold were listed in the table. (B) Three miRNAs that were significantly upregulated were selected for further validation. Real-time qPCR for miRNA validated the relative changes in miRNA level. miRNA expression was normalized to reference gene s12. The graph indicates a significant increase of miR-744, miR-431 and miR-21 in DRG after sciatic nerve crush, whereas the expression level of miR-124 and miR 29a didn't change. (* $P<0.05$, ** $P<0.01$, $N=3$).

A

miRNA	Fold change	
mmu-miR-431	2.611244	up
mmu-miR-714	2.1570964	up
mmu-miR-744	2.1376243	up
mmu-miR-877	2.081734	up
mmu-miR-130b	1.7698824	up
mmu-miR-21	1.7598088	up
mmu-miR-323-3p	1.6689959	up
mmu-miR-325	1.5642644	up
mmu-miR-409-3p	1.5461996	up
mmu-miR-154*	1.517914	up
mmu-miR-681	1.5049202	up
mmu-miR-190	2.063784	down
mmu-miR-1	1.7755992	down
mmu-miR-33	1.6966436	down
mmu-miR-32	1.6579413	down
mmu-miR-153	1.6068152	down
mmu-miR-335-5p	1.595247	down
mmu-miR-193	1.5837495	down
mmu-miR-488	1.5546329	down

B

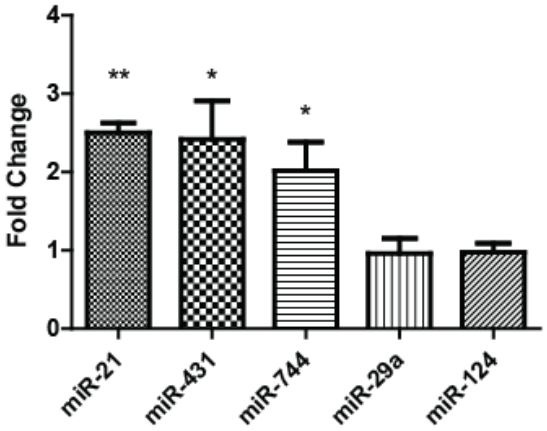

Figure 5.2. Transfection efficiency and silencing efficiency in functional analysis assay

RNA transfection efficiency was above 90% as determined using a fluorochrome-conjugated scrambled miRNA. (A) After culturing dissociated DRG neurons for 24h, neuronal somas and axons were visualized under a bright field. (B) FAM-conjugated scrambled miRNAs were observed within the neuronal cell body, indicating successful transfection of miRNAs into cells. Scale bar = 50 μm. (C) miR-1 mimics and inhibitors were used to test silencing efficiency of miRNA mimics and inhibitors by RT-qPCR in our studies. miR-1 was chosen as a positive control, since upon delivery into cells, it effectively down regulates the expression of twinfilin-1, also known as PTK9, at the mRNA level. Dissociated DRG culture without any treatment served as the control group. Pre-miR™ hsa-miR-1 miRNA precursors, short as miR-1 mimics, were transfected into dissociated DRGs and successfully suppressed the expression of PTK9 as shown in column 2. Pre-miR negative controls are random sequences of miRNA mimic molecules that have been validated not to produce identifiable effects on known miRNA function. Transfection of miRNA mimic negative controls did not cause significant change in PTK mRNA levels when comparing column 1 with column 3. Use of the Anti-miR miRNA-1 inhibitors significantly down regulated the inhibitory activity of miRNA-1, based on the expression of PTK9 in column 4. Anti-miR™ miRNA Inhibitor Negative Controls, short as miRNA inhibitor negative control, did not produce any effect on the function of miR-1 mimics, and there is significant change in PTK9 mRNA levels when comparing column 5 with column 3. (N=3, *$P<0.05$, **$P<0.01$)

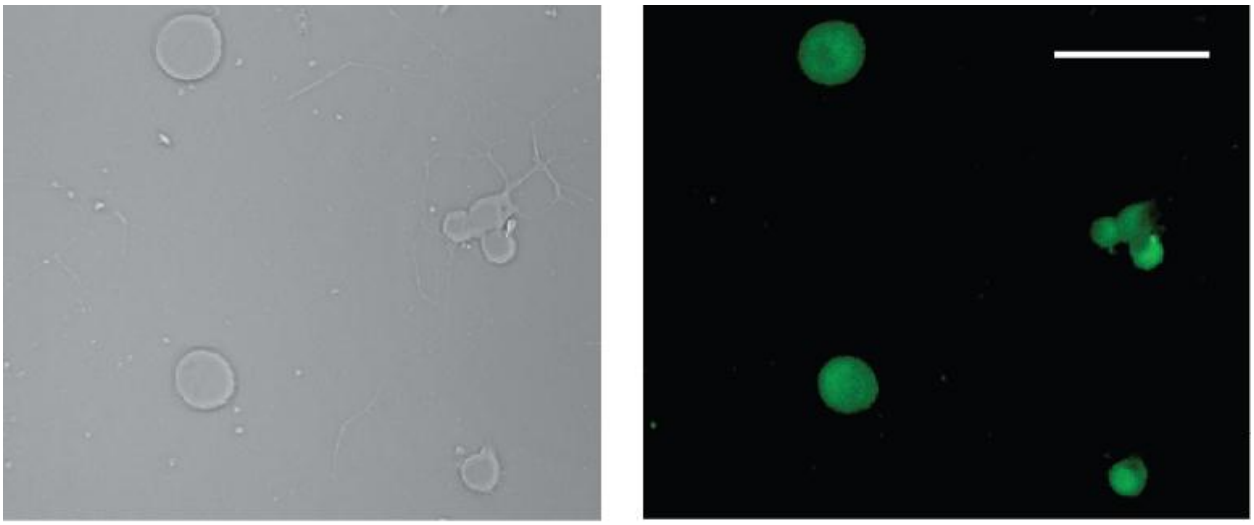

A B

C

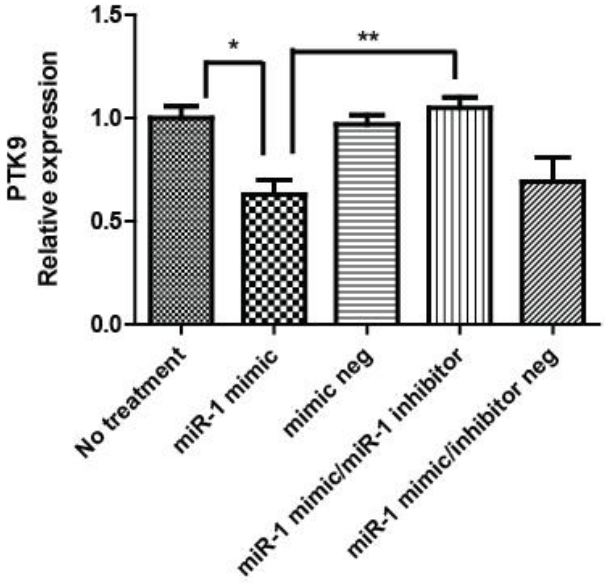
PTK9
Relative expression
1.5
1.0
0.5
0.0
*
**
No treatment
miR-1 mimic
mimic neg
miR-1 mimic/miR-1 inhibitor
miR-1 mimic/inhibitor neg

Figure 5.3. miR-431 increases neurite outgrowth in DRG neurons.

(A) Cell cultures were incubated with antibodies against neuronal β-tubulin and signals were visualized with TX-conjugated secondary antibody (Scare bar = 50 um). The expression of GAP-43 was detected using an anti-GAP-43 antibody. GAP-43 is expressed in both cell bodies and axons, but more highly in cell bodies. The effect of miR-431 on axon length (B) and on axon branching (C) was also quantified. Overexpression of miR-431 significantly increased axon extension, whereas suppression of miR-431 significantly blocked axon branching. The fluorescence signal intensity against GAP-43 was quantified in (D). (E) RNA from DRG cultures treated respectively with miR-431 mimics, mimic negative control, miR-431 inhibitor, or inhibitor negative control were collected. GAP-43 expression on mRNA level was quantified by RT-qPCR. GAP-43 expression correlated well between mRNA level and protein level. Over expression of miR-431 enhanced the expression of GAP-43, the regeneration marker for neurons. (* $P< 0.05$, ** $P<0.01$, $N=50$)

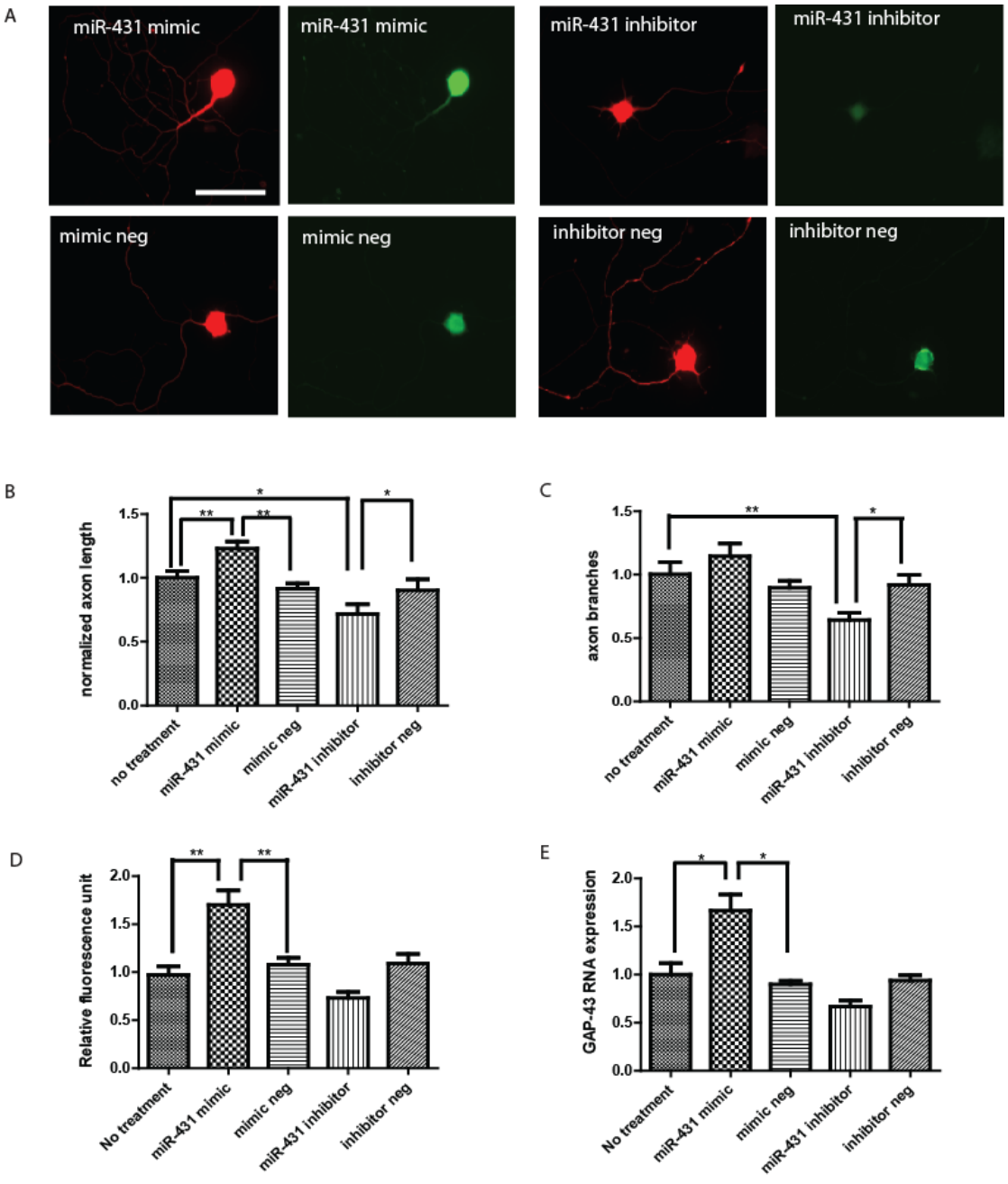
A
miR-431 mimic
miR-431 mimic
miR-431 inhibitor
miR-431 inhibitor
mimic neg
mimic neg
inhibitor neg
inhibitor neg
B
normalized axon length
1.5
1.0
0.5
0.0
**
**
*
*
no treatment
miR-431 mimic
mimic neg
miR-431 inhibitor
inhibitor neg
C
axon branches
1.5
1.0
0.5
0.0
**
*
no treatment
miR-431 mimic
mimic neg
miR-431 inhibitor
inhibitor neg
D
Relative fluorescence unit
2.0
1.5
1.0
0.5
0.0
**
**
No treatment
miR-431 mimic
mimic neg
miR-431 inhibitor
inhibitor neg
E
GAP-43 RNA expression
2.0
1.5
1.0
0.5
0.0
*
*
No treatment
miR-431 mimic
mimic neg
miR-431 inhibitor
inhibitor neg

Figure 3

Table 5.1. Relative expression of miR-431 potential target genes

24 genes meet the criteria of having conservative binding site for miR-431 in their 3’ UTR and down-regulated expression level in DRG after sciatic nerve injury. Changes in the expressions of these 24 genes in response to elevated miR-431 level were examined in neuron cells derived from PC12 cells. In the table, the values represent the relative expression levels of each gene after the application of miR-431 mimics. Colum 1 shows that 8 out of 24 potential target genes showed down regulated expression in PC12 cells after applying miR-431 mimics. Colum 2 shows the relative expression levels of those 8 genes in DRG neurons with the overexpression of miR-431.

	relative expression in PC12	relative expression in DRG	CLIP
Luc712	0.688073394		
Ncam1	1.1		
Vezt	1.25		
Eif2s2	0.44	0.83	
Zeb2	0.97		
Kremen1	0.38	0.67	+
netrin	0.67		
Ccnt1	-		
Prlr	-		
4931498A02Rik	0.3	0.53	
BC065397	0.58	1.19	
Nudcd3	0.91		
Fgf12	0.67		
Hip1	1.07		
Slc30a10	1.16		
Msi2	0.41	1.11	
Tcf712	2.04		
Cwf1912	5.8		
Wnk3	0.94		
Dlst	1.85		
Braf	0.32	0.51	-
Zkscan1	0.29	0.45	-
Tnrc6b	0.58	0.95	
Son	4		

Figure 5.4. miR-431 regulates *Kremen1* expression

(A) miR-431 negatively regulated *Kremen1* expression at mRNA level. Treatment of miR-431 mimics in DRG neuronal cultures significantly inhibited *Kremen1* expression as compared with that of control groups. On the contrary, suppression of miR-431 activity significantly enhanced the expression of *Kremen1* mRNA. (B) Western blot analysis of *Kremen1* expression exhibited similar negative correlation of miR-431 and *Kremen1* expression. Cells transfected with miR-431 mimics had decreased protein level of *Kremen1*, whiles cells transfected with miR-431 inhibitors had an increased expression of *Kremen1*. α-tubulin was used as the loading control and was used to normalize densitometry values. The quantification of *Kremen1* protein levels is shown in (C). (D). RT-qPCR confirmed the increase of miR-431 level in DRG neuron after the transfection of miR-431 mimic. (E) Although overexpression of miR-431 decreased *Kremen1* mRNA in total cell lysates (input), it enhanced the binding between *Kremen1* mRNA and Ago2 complex. In the Ago immunoprecipitated fractions, there was an increased amount of *Kremen1* mRNA. The lack of signal in the nonspecific serum IP sample confirmed the specificity of the IP.

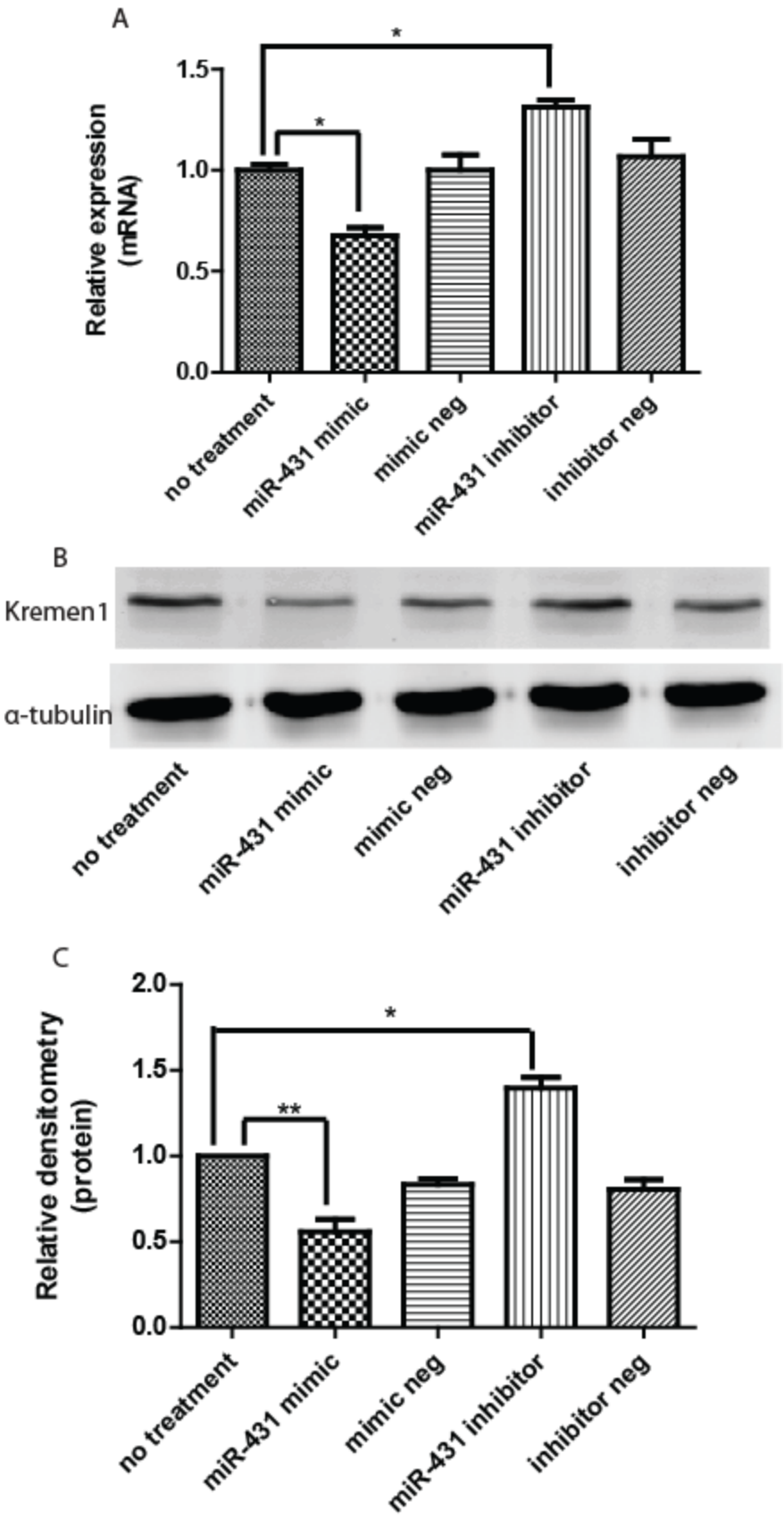
A
Relative expression (mRNA)
1.5
1.0
0.5
0.0
*
*
no treatment
miR-431 mimic
mimic neg
miR-431 inhibitor
inhibitor neg
B
Kremen1
α-tubulin
no treatment
miR-431 mimic
mimic neg
miR-431 inhibitor
inhibitor neg
C
Relative densitometry (protein)
2.0
1.5
1.0
0.5
0.0
*
**
no treatment
miR-431 mimic
mimic neg
miR-431 inhibitor
inhibitor neg

D

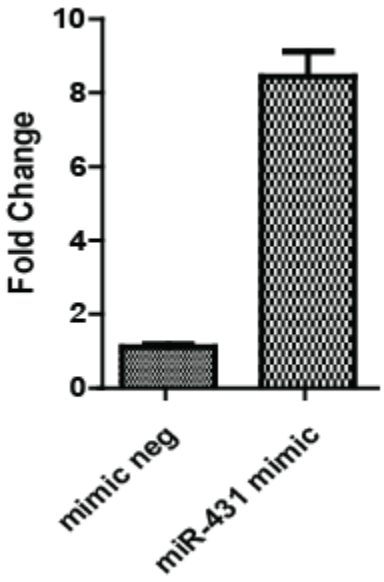
10
8
6
4
2
0
Fold Change
mimic neg
miR-431 mimic

E

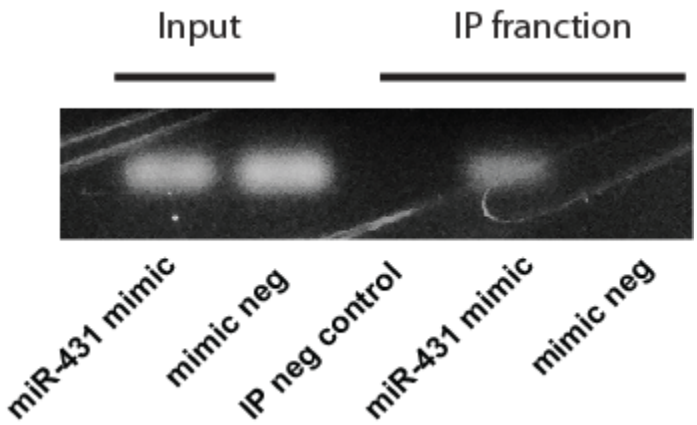
Input
IP franction
miR-431 mimic
mimic neg
IP neg control
miR-431 mimic
mimic neg

Figure 5.5. Nerve crush injury reduces *Kremen1* expression

(A) Total RNA was isolated from control or crush-injured mouse DRG, and relative expression of *Kremen1* was determined using RT-qPCR. GAPDH and S12 were used to normalize for RNA loading. (B) Western blot analysis of total DRG lysates at 4 days post crush injury. α-tublulin was shown as a loading control. As shown in the quantified densitometry data, there was a significant decrease of *Kremen1* expression during nerve regeneration. (C) Immunofluorescent staining in dissociated DRG neurons demonstrated the expression of *Kremen1* within neurons. *Kremen1* as a transmembrane receptor was shown to be located in cell bodies, but not axons. TUJ staining was used to visualize neuronal cells. Preconditioning of sciatic nerve obviously promotes regenerative axon growth in DRG neurons, and this phenomenon is accompanied by a decrease in *Kremen1* expression.

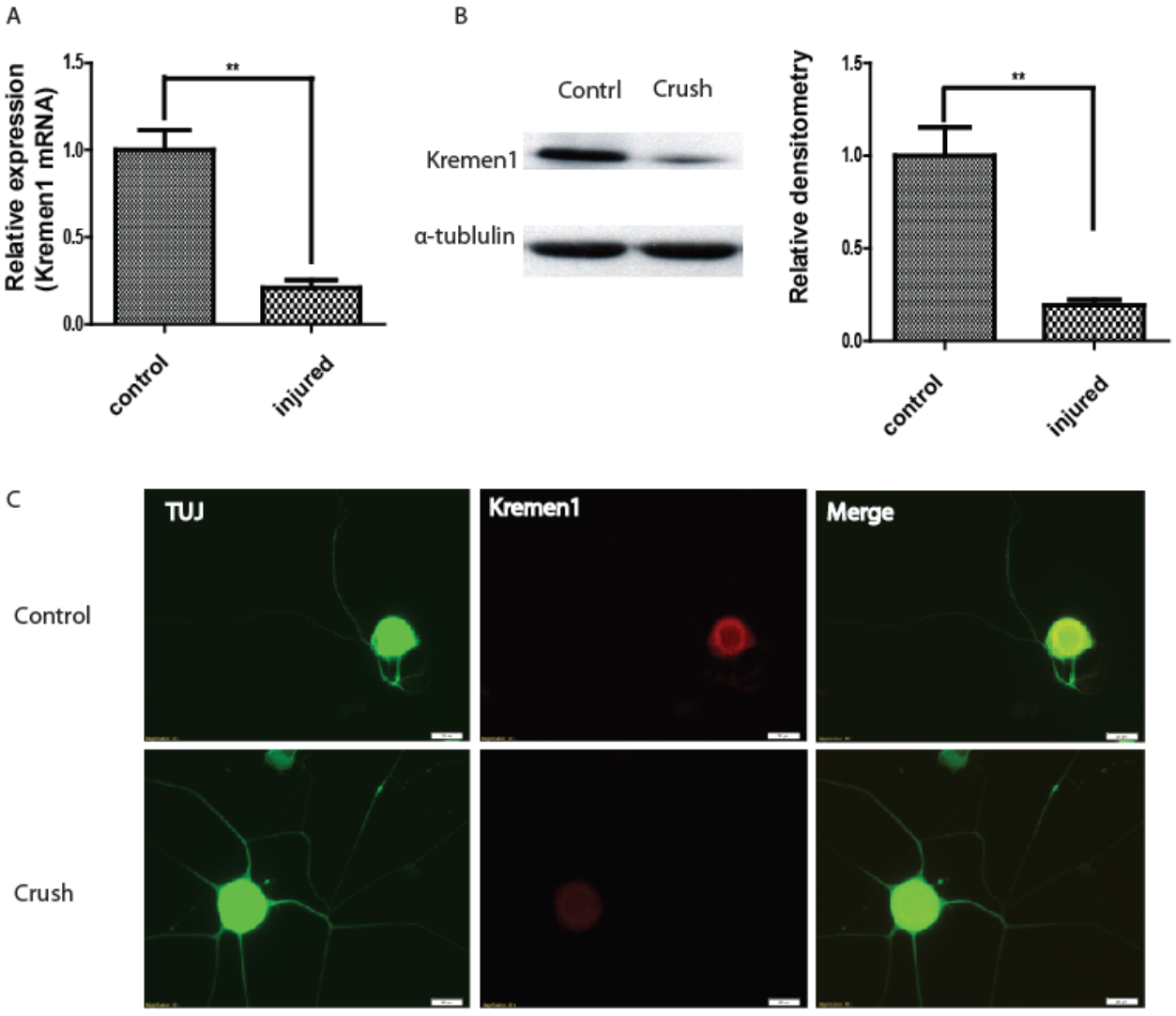
A
Relative expression (Kremen1 mRNA)
1.5
1.0
0.5
0.0
**
control
injured
B
Contrl
Crush
Kremen1
α-tublulin
Relative densitometry
1.5
1.0
0.5
0.0
**
control
injured
C
TUJ
Kremen1
Merge
Control
Crush

Figure 5

Figure 5.6. Knockdown of *Kremen1* increases neurite outgrowth.

Neurite outgrowth in *Kremen1* siRNA and scrambled siRNA treated DRG neurons was detected by TUJ immunostaining (A) Representative images show that *Kremen1* siRNA significantly decreased *Kremen1* expression level, which was accompanied by an increase of axon outgrowth. Scale bar = 20 um. As the quantification performed in miR-431 functional analysis, we measured the length of the longest axon for each neuron (B) and counted the number of branches for each neuron (C). Inhibition of *Kremen1* significantly increased the length of axon, however its effect on neurite branching was not significant. (*$p<0.05$)

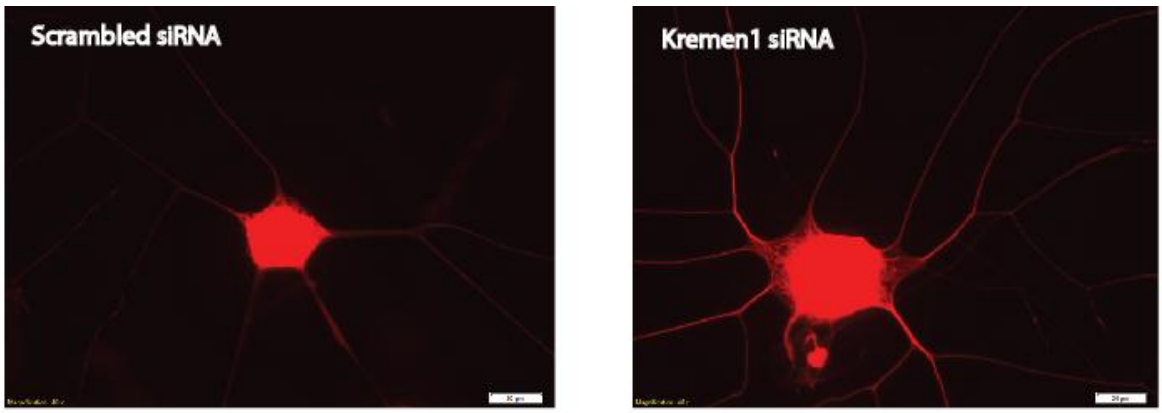
Scrambled siRNA
Kremen1 siRNA

A

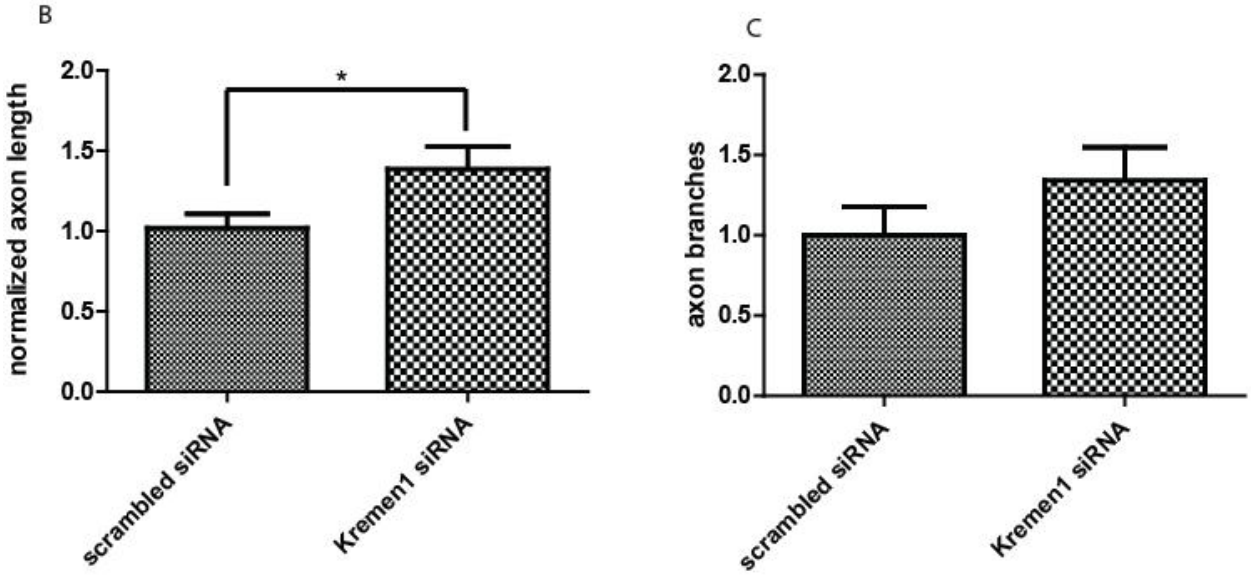
B
normalized axon length
2.0
1.5
1.0
0.5
0.0
*
scrambled siRNA
Kremen1 siRNA
C
axon branches
2.0
1.5
1.0
0.5
0.0
scrambled siRNA
Kremen1 siRNA

Discussion

Neurons of the peripheral nervous system have the intrinsic capacity to regenerate following injury. Previous studies on the molecular mechanisms that contribute to peripheral nerve regeneration have demonstrated that an alteration of gene expression in neurons, initiated by nerve injury, promotes neuronal cell survival and axonal regeneration (Hoffman, 2010). Further, the regulation of gene expression can take place at both transcriptional and post-transcriptional levels. While the regulation of transcriptional change through injury induced activation of transcription factors, such as c-Jun and ATF-3, has been widely studied, the understanding of post-transcriptional regulation of gene expression following nerve injury is just emerging (Broude et al., 1997, Tsujino et al., 2000, Hyatt Sachs et al., 2007, Dahlin et al., 2009).

In the present study, an *in vitro* model system was used to gain insight regarding the role of miRNAs in regenerative axon growth. Microarray analysis demonstrated that there are changes in the expression of a set of miRNAs following sciatic nerve injury in adult mouse DRG. One of the injury induced miRNA, miR-431, enhanced neurite outgrowth in dissociated mouse DRG neurons in our *in vitro* functional analysis. Using biochemical and molecular approaches, we have identified *Kremen1* as a target gene regulated by miR-431 in DRG cultures. In DRG neurons 4 days post sciatic nerve injury, *Kremen1* had decreased expression levels. Considering *Kremen1* functions as a gatekeeper for the Wnt pathway, this raised the possibility that overexpression of miR-431 after nerve injury inhibits *Kremen1* expression, leading to the activation of the Wnt pathway, which subsequently promotes regenerative axon growth.

Altered miRNA expression following sciatic nerve injury in mouse DRG

Our studies profiled the miRNA expression in DRG tissues 4 days post sciatic nerve injury in mice. In our data, 19 miRNAs exhibited significant changes in expression levels after sciatic nerve injury in DRG, with 11 miRNA significantly upregulated and 8 miRNA significantly downregulated. Similar studies profiling miRNA expression after nerve injuries have been carried out before, however, most of the studies focused on injuries in central nervous system. Alteration in temporal expression of miRNA following a contusive spinal cord injury in adult rats has been recently shown (Liu et al., 2009). In the injured spinal cord 4 h, 1 day and 7 days after acute SCI, 60 miRNAs showed significant changes in their expression level. Among those 60 miRNAs, 30 were up-regulated, 16 were down-regulated, and 14 showed early up-regulation at 4 hour followed by down-regulation at 1 and 7 days post-SCI (Liu et al., 2009). Microarray based analysis of miRNA in the rat cerebral cortex after traumatic brain injury revealed that a set of miRNAs were differentially express at 6 hours, 24 hours, 48 hours and 72 hours after injury. At all time points post injury, miR-21was consistently highly expressed in the cerebral cortex (Lei et al., 2009). Changes in miRNA expression in hippocampus after traumatic brain injury has also been studied by microarray analysis. Three and 24 hours after controlled cortical impact injury, 35 miRNA exhibited increased expression levels and 50 miRNA exhibited decreased expression level (Redell et al., 2009).

In the last year, miRNA expression following sciatic nerve injury in proximal stumps of injured sciatic nerve and in DRG has been profiled by microarray approaches and deep sequencing in several studies (Strickland et al., 2011, Yu et al., 2011b). In DRG tissues, 19 miRNAs showed significant changes at four early time points after sciatic nerve transaction. Notably, miR-188 was significantly upregulated at most time points. In contrast, miR-500 was

downregulated at most time points, but their functions remain largely unclear (Zhou et al., 2011). At 1, 4, 7, and 14 days after resection of the sciatic nerve in rats, 32 significantly upregulated and 18 downregulated miRNAs were identified in the DRG at four time points following sciatic nerve injury (Yu et al., 2011a). A more recent study showed that 20 miRNA transcripts displayed a significant change in expression levels at 7 day post-axotomy in rat DRG following sciatic nerve transection, with 8 miRNAs that were regulated more than 1.5 fold (Strickland et al., 2011). By comparing Strickland's data with ours, one interesting observation occurred. miR-21 and miR-431 have shown upregulation in DRG after sciatic nerve injury in both Strickland studies and our studies, suggesting these two miRNAs are constantly upregulated across species during nerve regeneration.

While these studies suggest the involvement of miRNA regulation after nerve injury, to understand the underlying mechanism and physiological relevance of the changes, additional studies are required to investigate the function and targets of these miRNAs.

Mir-21 is one of the most intensively studied miRNAs. It is one of the most highly upregulated miRNAs in cancers and cardiovascular disease, suggesting it has a fundamental role in cell growth and anti-apoptosis (Sayed et al., 2008, Feng et al., 2011). In Strickland's studies, miR-21 was not only persistently upregulated after sciatic nerve injury, but also promoted the intrinsic growth capacity of the injured neuron. According to Strickland, the observed promotion of axon regeneration by mir-21 was possibly mediated through the knocking down of SPRY2 (Strickland et al., 2011).

Our studies focused on miR-431. miR-431 has been identified in embryonic and postnatal mouse brains, it was evenly expressed between E13 and P10, especially strong in the Pons, but

accumulated at a much lower level in the adult brain (Wheeler et al., 2006). The Pons is particularly rich in synapses. Ninety percent of the descending axons passing through the midbrain synapse on neurons in the Pons, however the role of this miRNA in the nervous system has not yet been established. The only functional analysis of miR-431 investigated its role in cell viability in HuIFN-β sensitive cell line RSa and HuIFN- β resistant cell line, F-IFr cell lines. In RSa cells, miR-431 downregulates the expression of IGFIR and IRS2 at protein level, which subsequently modulates the activity of MAPK pathways (Tanaka et al., 2012).

Of all other miRNAs that were upregulated in our array data, only miR-323-3p and miR-681 were proved to be functional in neuronal cells. miR-323-3p is related to the pathology of Alzheimer's disease (AD). AD may result from amyloid precursor protein (APP) expression misregulation. miR-323-3p can regulate APP expression *in vitro* and under physiological conditions in cells (Delay et al., 2011). miR-323-3p can also target the 3' UTR of human FMR1, whose gene product FMRP is involved RNAi machinery, and a downregulation of FMRP leads to the expression of fragile X syndrome (Siomi et al., 2004, Yi et al., 2010). Another miRNA, miR-681, is predominantly localized in the hippocampus. Its expression level is up-regulated in long-lived mutant mice. These long-lived mutant mice exhibit heightened cognitive robustness and altered IGF1 signaling in the brain. miR-681 significantly reduced IGF1R expression, which is the key IGF1 signaling gene (Liang et al., 2011).

Other miRNAs showed enhanced expression during nerve regeneration, but have no clearly identified functions within the nervous system. Functional analysis of miR-744 revealed that miR-744 targets the predominant, short, isoform of transforming growth factor beta-1 (TRG-β1) 3' UTR in epithelial cell line. TGF- β1 is a cytokine that plays various roles in healing and inflammation of wounds (Martin et al., 2011). miR-130b was validated to be elevated in plasma

from severe pre-eclamptic pregnancies (Wu et al., 2011b). Loss of miR-130b expression contributes to the generation of drug resistance in ovarian cancer (Yang et al., 2012). miR-409-3p was significantly downregualted in gastric cancer cell lines. In addition, tissue and function analysis showed that overexpression of miR-409-3p in cancer cells dramatically suppressed cell proliferation and induced cell apoptosis through inhibiting transcriptional regulator PHF 10 (Li et al., 2012). In contrast rmiR-154* was upregulated in acute myeloid leukemia, which functions as a potential oncogenic miRNA (Dixon-McIver et al., 2008).

The role of miR-431 in regenerative axon growth

To define the role of miR-431 in regenerative axon growth, the effect of modulating miR-431 level in neuronal cell was investigated in dissociated DRG neuron cultures. Expression of miR-431 mimics substantially increased the intracellular miR-431 activities and promoted regenerative neurite outgrowth. Morphological evidences correlated with the measurement of the expression of nerve regeneration marker GAP-43. Overexpression of miR-431 correlated with longer axons, more branches, and high GAP-43 expression. In contract, inhibition of miR-431 activity by transfection of miR-431 inhibitors impaired the regenerative axon growth, as shorter axons and fewer branches were observed in DRG cultures.

Since miRNAs execute their functions through inhibiting the expression of their target genes, we employed both bioinformatics and experimental approaches to identify the target gene by which miR-431 promotes axon growth. Our data identified *Kremen1* as a target that mediates the effects of miR-431 on neuronal cells. We showed that miR-431 expression inversely correlates with *Kremen1*. The binding between miR-431 and *Kremen1* mRNA was validated by co-immunoprecipitating Ago2 associated RNA. Upregulation of intracellular miR-431 level

enhanced the association of *Kremen1* mRNA with Ago2 containing complex. Consistent with our *in vitro* study, increase of miR-431 after sciatic nerve crush accompanied the decrease of *Kremen1* expression at both protein and mRNA *in vivo*.

Kremen1 was originally discovered as a transmembrane protein containing the kringle domain. Later reports confirmed that both *Kremen1* and its relative Kremen2 were high-affinity receptors for Dickkopf1 (Dkk1), the inhibitor of Wnt/β-catenin signaling (Mao et al., 2002). The canonical Wnt/ β-catenin signaling is mediated by two receptor families, Frizzle protein and Lipoprotein-receptor-related protein 5 and 6 (LRP5/6). *Kremen1* functionally cooperates with Dkk1 to form a ternary complex composed of *Kremen1*, Dkk1, and Lrp5/6, and induces rapid endocytosis and removal of the Wnt receptor LRP5/6 from the cell membrane, which inhibits the transduction of Wnt/ β-catenin signaling (Fig 5.7).

Wnt/β-catenin signaling plays a vital role in diverse developmental and physiological processes, including cell-fate determination, tissue patterning and stem cell regulation (Diep et al., 2004). *Kremen1* is quite significant in these processes as a mechanism to regulate Wnt/β-catenin signaling. The transcription factor β-catenin can induce proliferation of undifferentiated precursor cells rather than differentiation (Brembeck et al., 2006). Other studies have shown that *Kremen1* expression gradually and continuously increases with developmental progression and cell differentiation (Nakamura and Matsumoto, 2008). Since Wnt/ β-catenin signaling maintains stem cells and precursor cells in a pluripotent state and maintains their self-renew, increased expression of *Kremen1* is likely to initiate cells into the path of differentiation through turning off Wnt/ β-catenin signaling (Scholzke and Schwaninger, 2007).

Wnt/ β-catenin signaling pathway also contributes to adult neurogenesis. Blocking Wnt signaling suppresses neurogenesis from adult hippocampal progenitor cells *in vitro* and abolishes neurogenesis almost completely *in vivo* (Lie et al., 2005). With ectopic expression of Dkk1, canonical Wnt/ β-catenin signaling is reduced in both the hippocampus and cortex. As a result, the cell cycle of neurogenic progenitor cells extended and proliferation of cells reduced, therefore, reducing the hippocampal field in size (Solberg et al., 2008). Recent studies have shown that the inhibition of Wnt/ β-catenin depletes the pool of multipotent progenitors from the adult hippocampal progenitor cells population (Wexler et al., 2009).

Studies have also established a role for Wnt signaling in regulating synaptic plasticity and axonal growth (Hall et al., 2000, Wang et al., 2006, Budnik and Salinas, 2011). Wnt signaling regulates axon terminal remodeling (Budnik and Salinas, 2011), formation of growth cones and lamellipodia (Hall et al., 2000), microtubules organization (Purro et al., 2008), and synaptic assembly (Ahmad-Annuar et al., 2006). Loss and gain of function studies in animal models demonstrated that loss of Wnt7a results in a strong deficit in the accumulation of synaptic markers at the cell synapses (Ahmad-Annuar et al., 2006). In contrast, in cultured mouse cerebellar granule cells, Wnt7a increased neurite spreading and branching as well as the expression of synaptic markers (Lucas and Salinas, 1997). Likewise, targeted disruption of Wnt receptor genes in mice produced severe defects in axon growth and guidance, resulting in loss of thalamocortical, nigrostriatal tracts and the anterior commissure (Wang et al., 2002a, Wang et al., 2006).

Wnt not only modulates the synapse formation but also promotes the remodeling of mature terminals elicited by changes in electrical activity and environmental experience (Budnik and Salinas, 2011). Chemically or electrically induced neuronal activity stimulates the

expression of Wnt proteins (Wayman et al., 2006). NMDA receptor activation in hippocampal neurons promotes dendritic arborization through increase expression of Wnt2 (Wayman et al., 2006). High frequency stimulation in hippocampal neurons can induce long-term potentiation, activate the Wnt signaling pathway, and promote synapse formation (Sahores et al., 2010), whereas blocking of Wnt signaling impairs long-term potentiation in brain slice (Chen et al., 2006). Moreover, spinal cord injury induced a time-dependent increase in Wnt expression, phosphorylation of Wnt receptors, and activity of β-catenin protein. The activation of the Wnt pathway after spinal cord injury suggests the involvement of Wnt pathway in nerve regeneration (Fernandez-Martos et al., 2011).

These abundant evidences from studies in animal models, cell and organ culture firmly established an important role of Wnt signaling in neurite outgrowth and axonal guidance. The function of Wnt signaling could potentially link our observation of increased miR-431 and decreased *Kremen1* expression to the enhanced axonal outgrowth. Furthermore, siRNA mediated downregulation of *Kremen1* had a similar positive effect on neurite outgrowth as upregulation of miR-431, though the effect was less profound. Since each miRNA has multiple targets, the effects of miR-431 on regenerative axon growth are likely to be mediated through *Kremen1* as wells as other unidentified targets. It will be interesting to determine these unidentified targets of miR-431 in DRG neurons in the future and identify the function of miR-431 targets in the DRG.

Taken together, our studies identified miR-431 as an endogenous, injury-regulated inhibitor of *Kremen1* which promotes regenerative axon growth. Increased miR-431 level enhanced axon elongation and branching possibly through activation of Wnt pathway. This study further confirmed that miRNAs play a critical role for peripheral nerve regeneration. Injury induced miRNAs may be beneficial for DRG neurons during the process of regeneration. Further

studies are necessary to fully define the role of miR-431 in axonal regeneration. These findings may not only contribute to our understanding of fundamental biological process, but also could have important implication for improving the therapeutic strategies for nerve injury.

Figure 5.7 *Kremen1* functions as gatekeeper for Wnt pathway

Kremen1 is a transmembrane high-affinity receptor for Dickkopf1 (Dkk1), the inhibitor of Wnt/β-catenin signaling. Under normal physiological condition, *Kremen1* functionally cooperate with Dkk1 to form a ternary complex composed of *Kremen1*, Dkk1, and Lrp5/6, and induces rapid endocytosis and removal of the Wnt receptor LRP5/6 from the cell membrane, which inhibits the transduction of Wnt/ β-catenin signaling (left picture). When *Kremen1*'s expression is suppressed, Wnt binds to its two receptor families, Frizzle protein and Lipoprotein-receptor-related protein 5 and 6 (LRP5/6), which prevent the phosphorylation and degradation of β-catenin. Increased β-catenin level leads to activation of Wnt target genes' expression (right picture).

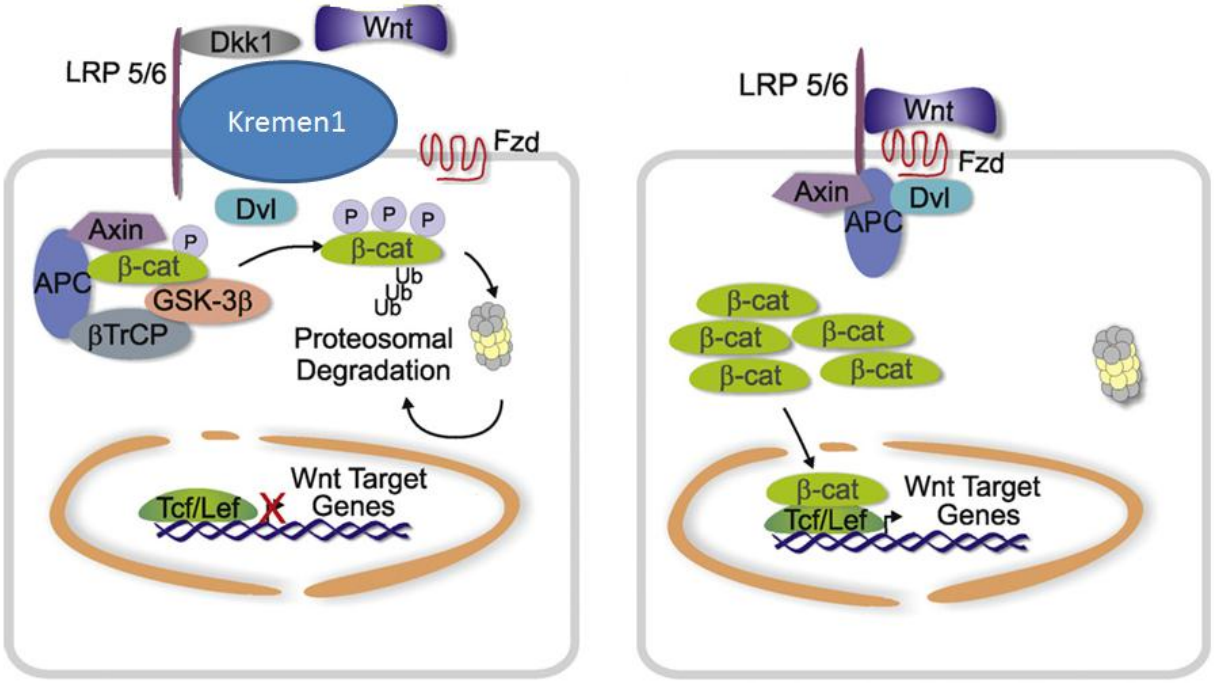
Dkk1
Wnt
LRP 5/6
Kremen1
Fzd
Dvl
Axin
P
β-cat
APC
GSK-3β
βTrCP
P P P
β-cat
Ub
Ub
Ub
Proteosomal
Degradation
Tcf/Lef
Wnt Target
Genes
LRP 5/6
Wnt
Fzd
Axin
Dvl
APC
β-cat
β-cat
β-cat
β-cat
β-cat
β-cat
Tcf/Lef
Wnt Target
Genes

CHAPTER VI: General Discussion

The mechanism of post-translational regulation of gene expression by small RNAs was first identified in *C. elegans* in 1998 (Fire et al., 1998). As one of the major discoveries in the history of molecular and cell biology, it has become a major focus of research in the last decade. Currently, over two dozen distinct families of noncoding RNAs have been discovered and the number continues to increase. Within the RNA family, miRNAs remain the most prominent family member of small RNA (Burian, 2007). miRNAs are encoded within the genome, however their sequences are not translated into protein, but bind to matching endogenous messenger RNAs and silence their expressions (Filipowicz et al., 2008). The understanding of miRNA pathway in neuroscience is growing at a rapid pace through intensive investigation of a variety of neurological events. Temporally and spatially specific miRNA expression has been identified in neurodevelopment and in neurological disease (Martino et al., 2009, Smith et al., 2010, Martins et al., 2011).

Although the miRNA machinery has been shown to be present in axonal compartments and are functional upon application of siRNA to peripheral nerve fibers (Hengst et al., 2006, Murashov et al., 2007), it is unclear if it can actively regulate local mRNA translation after peripheral nerve injury. To answer this intriguing question, the current study investigated the role of miRNA pathway in peripheral nerve regeneration following sciatic nerve crush. Sciatic nerve crush is a well-established model for regeneration studies, comprising a mixed population of motor and sensory axons, and studies on sciatic nerve regeneration have helped to identify many axonal signaling pathways that trigger axon regeneration (Yamazaki et al., 2009). Here, we used

the sciatic nerve crush model to elucidate the significance of miRNA pathway in regenerative axon growth.

Initially, we inquired about the involvement of the miRNA biosynthetic machinery in the regulation of intra-axonal local protein synthesis after injury. Previous studies in our lab have shown the existence of protein components of RISC in sciatic nerves. Transfection of siRNA against neuronal β-tubulin into axons initiated the formation of RISC and the suppressions of target genes (Murashov et al., 2007). In the current study, we hypothesized that there is an injury-regulated expression of biosynthetic enzymes, including components of RISC and P-bodies. The expressions of the corresponding enzymes were tested by immunoblotting and immunofluorescence analyses. We detected changes in the expression of miRNA machinery components in protein lysates from injured sciatic nerves. Their expression in the subcellular axon region was observed by immunofluorescence staining in dissociated DRG culture. An increase in the number and the size of P-bodies, the site for either degrading or sequestering mRNA, was observed in the regenerating axons. While the importance of local protein synthesis for nerve regeneration has been shown by an increase in local translation of proteins after peripheral nerve axotomy and the observation that inhibiting this synthesis greatly reduces the reproduction of growth cones (Verma et al., 2005), the underlying mechanism responsible for the regulation of the local protein synthesis is largely unknown. Our data suggests that miRNA could be one of the potential mechanisms that regulate axonal protein synthesis after peripheral nerve injury. This hypothesis is supported by the recent discovery of 130 miRNAs located at the distal axon area (Natera-Naranjo et al., 2010).

In addition, a group of miRNAs that are specifically expressed in an injury-regulated pattern in the regenerating sciatic nerves were identified by miRNA microarrays and confirmed

by qPCR. The most upregulated miRNA, miR-21 has shown the ability to promote axon growth in adult DRG neurons through targeting SPRY2 (Strickland et al., 2011). Overexpression of miR-21 also protects against ischemic neuronal death, probably mediated by its downregulation of FASLG, an important cell death-inducing ligand (Buller et al., 2010). The upregulated miR-29b exhibited neuronal protective effects (Kole et al., 2011). It was shown that miR-29b functions as a novel inhibitor of neuronal apoptosis by targeting multiple proapoptotic BH3-3 only gene family (Kole et al., 2011). Some of the upregulated miRNAs have injury-induced expression patterns in CNS as well, such as miR-211 and miR-142-5P. Their expression levels were increased after brain injury or spinal injury, respectively (Lei et al., 2009, Liu et al., 2009). The downregulated miRNA, miR-145, has been shown to inhibit neurite outgrowth *in vitro* with robo2 and srGAP2 validated as its potential target genes (Zhang et al., 2011). Surprisingly, some miRNAs showed a decrease in their expression level in our sciatic nerve microarray analysis correlating with a positive effect on axon outgrowth, such as miR-124a and miR-133. miR-124a decreased its level in sciatic nerves after crush, however it was required for hippocampal axogensis through Lhx2 suppression, which also prevents apoptosis in the developing retina (Sanuki et al., 2011). In zebrafish, miR-133 has been shown to promote tissue regeneration by targeting an inhibitor of axonal growth, the small GTPase RhoA (Yu et al., 2011c). Since the sciatic nerve is a heterogeneous tissue, the changes in miRNA expression profile may result from responses of Schwann cells as well as neuronal cells to nerve injury. This may partially explain why some of our array data did not correlate very well with the functions of the miRNA in neuronal cells. Thus, in the later studies, we performed microarray analyses in RNA samples isolated from DRG following sciatic nerve crush, whose cell population is primarily neuronal

cells. Only miR-21 was upregulated in both array data, which further confirmed the spatial specificity in miRNA expression.

While the first part of the study demonstrates the response of miRNA biogenesis to injury, the physiological significance of it was elucidated in the second part of the study. We used the approach of ablating the miRNA processing enzymes *Dicer*, causing a deduction of all miRNA production. In early studies, miRNA formation was interrupted at its proximal step by ablation of the components of *Drosha*, the enzymes responsible for processing primary miRNA into precursor miRNA intranuclearly (Rao et al., 2009). Recent studies observed an alternative origin of miRNA, which clustered at the outer edge of short introns. They are being processed into precursor miRNA by splicing, rather than depending on *Drosha* cleavage. The discovery of the non-classical splicing-dependent miRNA biogenesis pathway suggest *Dicer* knockout could be a better approach to block miRNA biogenesis, because both classical miRNA pathway and the non-classical miRNA pathway need the nuclease *Dicer* to process precursor miRNA into mature miRNA (Sibley et al., 2012). In the second part of the study, we hypothesize that the deletion of *Dicer* would disrupt production of *Dicer*-dependent small RNAs and would negatively impact peripheral nerve regeneration. Taking advantage of tamoxifen-inducible *CAG-CreERt:Dicer*$^{fl/fl}$ knockout mice (*Dicer* knockout), we examined the effect of blocking *Dicer*-dependent miRNA pathway on peripheral nerve regeneration *in vivo* and regenerative axon growth *in vitro*. Peripheral nerve regeneration after sciatic nerve injury was studied *in vivo* using functional behavioral tests and electrophysiology analyses. Restoration of motor and sensory function was markedly impaired by *Dicer* deletion. Further, *Dicer* deletion impeded the recovery of nerve conduction velocity and amplitude of evoked compound action potentials. Corresponding to our functional data, we found that at the histological level the total number of

regenerating nerve fibers and mean axonal area of myelinated fibers in *Dicer* knockout mice was notably smaller in comparison with control mice. In addition, the regenerative axonal growth was impeded by *Dicer* knockout in dissociated neuronal cultures from DRG neurons.

Our data provide an insight on the significance of *Dicer*-dependent miRNA pathway in regulation of regenerative axon growth, however it revealed little about the mechanisms of how miRNA contributes to regenerative axon growth. To better address this issue, we performed functional analyses for miRNAs that are upregulated during nerve regeneration. Since blocking miRNA would impede regenerative axon growth, we speculated that one or more of the miRNAs whose expression are induced by injury are necessary for normal nerve regeneration. Our miRNA array data revealed a group of miRNAs differentially expressed during peripheral nerve regeneration. We focused our studies on the miRNAs whose expression level were significantly higher after nerve injury. The significance of each miRNA was tested experimentally by evaluating the length of axons and number of branches per neuron, and miR-431 exhibited its effect by promoting neurite growth in adult DRG neurons. Since miRNAs function through inhibiting gene expression, it was also necessary to find out the target genes for the miR-431. In DRG neurons, we observed miR-431 induced knockdown of *Kremen1*, a gatekeeper for the Wnt pathway (Wang et al., 2008b). We further confirmed the binding between miR-431 and *Kremen1* in RISC with immunoprecipitation assays. Furthermore, with an increased expression of miR-431 in DRG after sciatic nerve crush, we detected a decreased expression of *Kremen1* in DRG tissue *in vivo*. Silencing *Kremen1* expression with an siRNA induced axon outgrowth, similar to overexpression of miR-431. Based on these observations, we postulated that the functional significance of injury-induced miR-431 is mediated through modulating *Kremen1* protein level.

Overall, our data provide an insight into the role of miRNA pathway in the regulation of regenerative axon growth and shed light on the mechanism of miR-431 induced neurite outgrowth. It appears clear that miRNAs are important players in the complex regulatory network that modulate axonal regeneration. Further work will be required to elucidate how miRNA pathway contributes to peripheral nerve regeneration and how to use it as a tool to treat nerve injuries.

Future Studies

Future studies must be conducted to further characterize the mechanism for miRNA-enhanced neurite out growth. Our data suggest that miR-431 promotes regenerative axon growth by suppressing the inhibition of Wnt pathway. To confirm this hypothesis, the activation of Wnt signaling must be investigated. We know that in the absence of Wnt stimulation, the Axin-based complex facilitates the phosphorylation of β-catenin, which targets them for rapid proteosomal degradation. Alternatively, activation of Wnt pathway dissociates the β-catenin degradation complex, resulting in the accumulation of β-catenin, which leads to its association with DNA-binding proteins in nucleus and turning on the expression of Wnt target genes (Endo and Rubin, 2007). To test if *Kremen1* specifically inhibits Wnt pathway in DRG and downregulation of *Kremen1* by miR-431 increases Wnt/β-catenin signaling, it will be necessary to test β-catenin's protein level and phosphorylation level in DRG neurons with overexpression of miR-431.

Also, it is unlikely that *Kremen1* is the only target of miR-431 in DRG neurons, since each miRNA has multiple target genes. Identification of further miR-431 target genes will help us to reveal other unidentified pathways by which miR-431 promotes axonal regeneration. In addition, until recently, limited information has been available regarding mechanisms

modulating miRNA expression. miRNA genes are usually transcribed by RNA polymerase II, and a novel RNA polymerase III regulated transcription of miRNAs has been determined too (Borchert et al., 2006). Transcription factors are also involved in the regulation of miRNA expression. Some miRNA are repressed by the RE1 induced silencing factor (REST) in non-neuronal cells. When REST-mediated repression of miRNA transcription was relieved, a neuronal phenotype was promoted (Conaco et al., 2006). Thus, understanding the regulatory mechanisms of miRNA expression will help us to further define the role of miR-431 in regenerative axon growth. The mechanisms through which neurons regulate expression of miR-431 after nerve injury are currently unknown. miR-431 is located in chromosome 12 in the mouse and chromosome 14 in humans (Altuvia et al., 2005). Its antisense locates in the exon of RTL1 gene, which is an imprinted gene with preferential expression from the paternal allele, and is related to multiple organ developments (Davis et al., 2005). miR-431, miR-433 and miR-127 are clustered across species. The distance between miR-433 and miR-127 across species was always between 986 and 1007 bp, and the position of transcription factor binding motifs in miR-433/127 locus from mouse, rat, dog, and human was strikingly similar, suggesting a conserved gene structure and transcriptional regulation of this locus (Song and Wang, 2009).

More importantly, all the functional analyses for miRNAs in our studies were performed in DRG neuronal cell cultures *in vitro*. Functional analysis for miR-431 *in vivo* would be the next step in our studies. Lentiviruses, adenoviruses, and adeno-associated viruses can be utilized for delivering small RNAs to the nervous system. Adenoviruses expressing shRNAs targeting transgenic eGFP has been successfully delivered to the mouse brain (Xia et al., 2002). siRNA has been delivered into brain, spinal cord and muscle with lentiviruses as well (Raoul et al.,

2005, Peng and Masliah, 2010). With these techniques, we should be able to analyze the role of miR-431 in peripheral nerve regeneration *in vivo*.

In the past decade, since the post-transcriptional regulation of gene expression was discovered, there has been rapid progress in deciphering the mechanisms underlying miRNA pathway. However, we are only at the initial stage of understanding the role of miRNA pathway in nerve injury and regeneration. As a mediator of gene silencing, miRNA has shown therapeutic efficacy in animal models of neurological conditions. Studies deciphering the functions mediated by miRNAs will have great significance in understanding basic cellular mechanism as well as inspiring miRNA based therapeutics.

REFERENCES

Abu-Elneel K, Liu T, Gazzaniga FS, Nishimura Y, Wall DP, Geschwind DH, Lao K, Kosik KS (2008) Heterogeneous dysregulation of microRNAs across the autism spectrum. Neurogenetics 9:153-161.

Ahlborn P, Schachner M, Irintchev A (2007) One hour electrical stimulation accelerates functional recovery after femoral nerve repair. Exp Neurol 208:137-144.

Ahmad-Annuar A, Ciani L, Simeonidis I, Herreros J, Fredj NB, Rosso SB, Hall A, Brickley S, Salinas PC (2006) Signaling across the synapse: a role for Wnt and Dishevelled in presynaptic assembly and neurotransmitter release. J Cell Biol 174:127-139.

Albinsson S, Skoura A, Yu J, DiLorenzo A, Fernandez-Hernando C, Offermanns S, Miano JM, Sessa WC (2011) Smooth muscle miRNAs are critical for post-natal regulation of blood pressure and vascular function. PLoS One 6:e18869.

Aldrich BT, Frakes EP, Kasuya J, Hammond DL, Kitamoto T (2009) Changes in expression of sensory organ-specific microRNAs in rat dorsal root ganglia in association with mechanical hypersensitivity induced by spinal nerve ligation. Neuroscience 164:711-723.

Altuvia Y, Landgraf P, Lithwick G, Elefant N, Pfeffer S, Aravin A, Brownstein MJ, Tuschl T, Margalit H (2005) Clustering and conservation patterns of human microRNAs. Nucleic Acids Res 33:2697-2706.

Andersson T, Rahman S, Sansom SN, Alsio JM, Kaneda M, Smith J, O'Carroll D, Tarakhovsky A, Livesey FJ (2010) Reversible block of mouse neural stem cell differentiation in the absence of dicer and microRNAs. PLoS One 5:e13453.

Artico M, Cervoni L, Nucci F, Giuffre R (1996) Birthday of peripheral nervous system surgery: the contribution of Gabriele Ferrara (1543-1627). Neurosurgery 39:380-382; discussion 382-383.

Ashraf SI, McLoon AL, Sclarsic SM, Kunes S (2006) Synaptic protein synthesis associated with memory is regulated by the RISC pathway in Drosophila. Cell 124:191-205.

Bagga S, Bracht J, Hunter S, Massirer K, Holtz J, Eachus R, Pasquinelli AE (2005) Regulation by let-7 and lin-4 miRNAs results in target mRNA degradation. Cell 122:553-563.

Balagopal V, Parker R (2009) Polysomes, P bodies and stress granules: states and fates of eukaryotic mRNAs. Curr Opin Cell Biol 21:403-408.

Bannerman P, James MA (2009) Molecular mechanisms to improve nerve regeneration following damage to the immature peripheral nervous system. J Bone Joint Surg Am 91 Suppl 4:87-89.

Bartel DP (2004) MicroRNAs: genomics, biogenesis, mechanism, and function. Cell 116:281-297.

Battle DJ, Kasim M, Wang J, Dreyfuss G (2007) SMN-independent subunits of the SMN complex. Identification of a small nuclear ribonucleoprotein assembly intermediate. J Biol Chem 282:27953-27959.

Behm-Ansmant I, Rehwinkel J, Izaurralde E (2006) MicroRNAs silence gene expression by repressing protein expression and/or by promoting mRNA decay. Cold Spring Harb Symp Quant Biol 71:523-530.

Bennett CB, Muschol M (2009) Large neurohypophysial varicosities amplify action potentials: results from numerical simulations. Endocrinology 150:2829-2836.

Benowitz LI, Routtenberg A (1997) GAP-43: an intrinsic determinant of neuronal development and plasticity. Trends Neurosci 20:84-91.

Benowitz LI, Yin Y (2007) Combinatorial treatments for promoting axon regeneration in the CNS: strategies for overcoming inhibitory signals and activating neurons' intrinsic growth state. Dev Neurobiol 67:1148-1165.

Bernstein E, Caudy AA, Hammond SM, Hannon GJ (2001) Role for a bidentate ribonuclease in the initiation step of RNA interference. Nature 409:363-366.

Bernstein E, Kim SY, Carmell MA, Murchison EP, Alcorn H, Li MZ, Mills AA, Elledge SJ, Anderson KV, Hannon GJ (2003) Dicer is essential for mouse development. Nat Genet 35:215-217.

Beveridge NJ, Gardiner E, Carroll AP, Tooney PA, Cairns MJ (2010) Schizophrenia is associated with an increase in cortical microRNA biogenesis. Mol Psychiatry 15:1176-1189.

Bhanji RA, Eystathioy T, Chan EK, Bloch DB, Fritzler MJ (2007) Clinical and serological features of patients with autoantibodies to GW/P bodies. Clin Immunol 125:247-256.

Bi Y, Liu G, Yang R (2009) MicroRNAs: novel regulators during the immune response. J Cell Physiol 218:467-472.

Bloomston M, Frankel WL, Petrocca F, Volinia S, Alder H, Hagan JP, Liu CG, Bhatt D, Taccioli C, Croce CM (2007) MicroRNA expression patterns to differentiate pancreatic adenocarcinoma from normal pancreas and chronic pancreatitis. Jama 297:1901-1908.

Boeshore KL, Schreiber RC, Vaccariello SA, Sachs HH, Salazar R, Lee J, Ratan RR, Leahy P, Zigmond RE (2004) Novel changes in gene expression following axotomy of a sympathetic ganglion: a microarray analysis. J Neurobiol 59:216-235.

Boissonneault V, Plante I, Rivest S, Provost P (2009) MicroRNA-298 and microRNA-328 regulate expression of mouse beta-amyloid precursor protein-converting enzyme 1. J Biol Chem 284:1971-1981.

Bomze HM, Bulsara KR, Iskandar BJ, Caroni P, Skene JH (2001) Spinal axon regeneration evoked by replacing two growth cone proteins in adult neurons. Nat Neurosci 4:38-43.

Bonetti LV, Korb A, Da Silva SA, Ilha J, Marcuzzo S, Achaval M, Faccioni-Heuser MC (2011) Balance and coordination training after sciatic nerve injury. Muscle Nerve 44:55-62.

Borchert GM, Lanier W, Davidson BL (2006) RNA polymerase III transcribes human microRNAs. Nat Struct Mol Biol 13:1097-1101.

Brembeck FH, Rosario M, Birchmeier W (2006) Balancing cell adhesion and Wnt signaling, the key role of beta-catenin. Curr Opin Genet Dev 16:51-59.

Bremer J, O'Connor T, Tiberi C, Rehrauer H, Weis J, Aguzzi A (2010) Ablation of Dicer from murine Schwann cells increases their proliferation while blocking myelination. PLoS One 5:e12450.

Broude E, McAtee M, Kelley MS, Bregman BS (1997) c-Jun expression in adult rat dorsal root ganglion neurons: differential response after central or peripheral axotomy. Exp Neurol 148:367-377.

Buckingham SD, Esmaeili B, Wood M, Sattelle DB (2004) RNA interference: from model organisms towards therapy for neural and neuromuscular disorders. Hum Mol Genet 13 Spec No 2:R275-288.

Budnik V, Salinas PC (2011) Wnt signaling during synaptic development and plasticity. Curr Opin Neurobiol 21:151-159.

Buller B, Liu X, Wang X, Zhang RL, Zhang L, Hozeska-Solgot A, Chopp M, Zhang ZG (2010) MicroRNA-21 protects neurons from ischemic death. Febs J 277:4299-4307.

Burian RM (2007) On microRNA and the need for exploratory experimentation in post-genomic molecular biology. Hist Philos Life Sci 29:285-311.

Cai D, Qiu J, Cao Z, McAtee M, Bregman BS, Filbin MT (2001) Neuronal cyclic AMP controls the developmental loss in ability of axons to regenerate. J Neurosci 21:4731-4739.

Cao X, Pfaff SL, Gage FH (2007) A functional study of miR-124 in the developing neural tube. Genes Dev 21:531-536.

Caroni P, Aigner L, Schneider C (1997) Intrinsic neuronal determinants locally regulate extrasynaptic and synaptic growth at the adult neuromuscular junction. J Cell Biol 136:679-692.

Carthew RW, Sontheimer EJ (2009) Origins and Mechanisms of miRNAs and siRNAs. Cell 136:642-655.

Caudy AA, Ketting RF, Hammond SM, Denli AM, Bathoorn AM, Tops BB, Silva JM, Myers MM, Hannon GJ, Plasterk RH (2003) A micrococcal nuclease homologue in RNAi effector complexes. Nature 425:411-414.

Cheloufi S, Dos Santos CO, Chong MM, Hannon GJ (2010) A dicer-independent miRNA biogenesis pathway that requires Ago catalysis. Nature 465:584-589.

Chen J, Park CS, Tang SJ (2006) Activity-dependent synaptic Wnt release regulates hippocampal long term potentiation. J Biol Chem 281:11910-11916.

Chendrimada TP, Gregory RI, Kumaraswamy E, Norman J, Cooch N, Nishikura K, Shiekhattar R (2005) TRBP recruits the Dicer complex to Ago2 for microRNA processing and gene silencing. Nature 436:740-744.

Cheng LC, Pastrana E, Tavazoie M, Doetsch F (2009) miR-124 regulates adult neurogenesis in the subventricular zone stem cell niche. Nat Neurosci 12:399-408.

Choi BH, Zhu SJ, Kim BY, Huh JY, Lee SH, Jung JH (2005) Transplantation of cultured bone marrow stromal cells to improve peripheral nerve regeneration. Int J Oral Maxillofac Surg 34:537-542.

Chu CY, Rana TM (2006) Translation repression in human cells by microRNA-induced gene silencing requires RCK/p54. PLoS Biol 4:e210.

Coleman MP, Perry VH (2002) Axon pathology in neurological disease: a neglected therapeutic target. Trends Neurosci 25:532-537.

Conaco C, Otto S, Han JJ, Mandel G (2006) Reciprocal actions of REST and a microRNA promote neuronal identity. Proc Natl Acad Sci U S A 103:2422-2427.

Crosby ME, Devlin CM, Glazer PM, Calin GA, Ivan M (2009) Emerging roles of microRNAs in the molecular responses to hypoxia. Curr Pharm Des 15:3861-3866.

Cuellar TL, Davis TH, Nelson PT, Loeb GB, Harfe BD, Ullian E, McManus MT (2008) Dicer loss in striatal neurons produces behavioral and neuroanatomical phenotypes in the absence of neurodegeneration. Proc Natl Acad Sci U S A 105:5614-5619.

Dahlin L, Johansson F, Lindwall C, Kanje M (2009) Chapter 28: Future perspective in peripheral nerve reconstruction. Int Rev Neurobiol 87:507-530.

Darnell JC, Fraser CE, Mostovetsky O, Stefani G, Jones TA, Eddy SR, Darnell RB (2005) Kissing complex RNAs mediate interaction between the Fragile-X mental retardation protein KH2 domain and brain polyribosomes. Genes Dev 19:903-918.

Davare MA, Fortin DA, Saneyoshi T, Nygaard S, Kaech S, Banker G, Soderling TR, Wayman GA (2009) Transient receptor potential canonical 5 channels activate Ca2+/calmodulin kinase Igamma to promote axon formation in hippocampal neurons. The Journal of neuroscience : the official journal of the Society for Neuroscience 29:9794-9808.

Davis E, Caiment F, Tordoir X, Cavaille J, Ferguson-Smith A, Cockett N, Georges M, Charlier C (2005) RNAi-mediated allelic trans-interaction at the imprinted Rtl1/Peg11 locus. Curr Biol 15:743-749.

Davis TH, Cuellar TL, Koch SM, Barker AJ, Harfe BD, McManus MT, Ullian EM (2008) Conditional loss of Dicer disrupts cellular and tissue morphogenesis in the cortex and hippocampus. J Neurosci 28:4322-4330.

De Pietri Tonelli D, Pulvers JN, Haffner C, Murchison EP, Hannon GJ, Huttner WB (2008) miRNAs are essential for survival and differentiation of newborn neurons but not for expansion of neural progenitors during early neurogenesis in the mouse embryonic neocortex. Development 135:3911-3921.

Delay C, Calon F, Mathews P, Hebert SS (2011) Alzheimer-specific variants in the 3'UTR of Amyloid precursor protein affect microRNA function. Mol Neurodegener 6:70.

Deumens R, Bozkurt A, Meek MF, Marcus MA, Joosten EA, Weis J, Brook GA (2010) Repairing injured peripheral nerves: Bridging the gap. Prog Neurobiol 92:245-276.

Didiot MC, Subramanian M, Flatter E, Mandel JL, Moine H (2009) Cells lacking the fragile X mental retardation protein (FMRP) have normal RISC activity but exhibit altered stress granule assembly. Mol Biol Cell 20:428-437.

Diep DB, Hoen N, Backman M, Machon O, Krauss S (2004) Characterisation of the Wnt antagonists and their response to conditionally activated Wnt signalling in the developing mouse forebrain. Brain Res Dev Brain Res 153:261-270.

Ding L, Han M (2007) GW182 family proteins are crucial for microRNA-mediated gene silencing. Trends Cell Biol 17:411-416.

Dixon-McIver A, East P, Mein CA, Cazier JB, Molloy G, Chaplin T, Andrew Lister T, Young BD, Debernardi S (2008) Distinctive patterns of microRNA expression associated with karyotype in acute myeloid leukaemia. PLoS One 3:e2141.

Doench JG, Sharp PA (2004) Specificity of microRNA target selection in translational repression. Genes Dev 18:504-511.

Dostie J, Mourelatos Z, Yang M, Sharma A, Dreyfuss G (2003) Numerous microRNPs in neuronal cells containing novel microRNAs. Rna 9:180-186.

Dugas JC, Cuellar TL, Scholze A, Ason B, Ibrahim A, Emery B, Zamanian JL, Foo LC, McManus MT, Barres BA (2010) Dicer1 and miR-219 Are required for normal oligodendrocyte differentiation and myelination. Neuron 65:597-611.

Dziennis S, Alkayed NJ (2008) Role of signal transducer and activator of transcription 3 in neuronal survival and regeneration. Rev Neurosci 19:341-361.

Elbashir SM, Harborth J, Lendeckel W, Yalcin A, Weber K, Tuschl T (2001) Duplexes of 21-nucleotide RNAs mediate RNA interference in cultured mammalian cells. Nature 411:494-498.

Endo Y, Rubin JS (2007) Wnt signaling and neurite outgrowth: insights and questions. Cancer Sci 98:1311-1317.

English AW, Wilhelm JC, Sabatier MJ (2011) Enhancing recovery from peripheral nerve injury using treadmill training. Ann Anat 193:354-361.

Eulalio A, Behm-Ansmant I, Izaurralde E (2007a) P bodies: at the crossroads of post-transcriptional pathways. Nat Rev Mol Cell Biol 8:9-22.

Eulalio A, Behm-Ansmant I, Schweizer D, Izaurralde E (2007b) P-body formation is a consequence, not the cause, of RNA-mediated gene silencing. Mol Cell Biol 27:3970-3981.

Eulalio A, Helms S, Fritzsch C, Fauser M, Izaurralde E (2009a) A C-terminal silencing domain in GW182 is essential for miRNA function. Rna 15:1067-1077.

Eulalio A, Tritschler F, Izaurralde E (2009b) The GW182 protein family in animal cells: new insights into domains required for miRNA-mediated gene silencing. Rna 15:1433-1442.

Faghihi MA, Zhang M, Huang J, Modarresi F, Van der Brug MP, Nalls MA, Cookson MR, St-Laurent G, 3rd, Wahlestedt C (2010) Evidence for natural antisense transcript-mediated inhibition of microRNA function. Genome Biol 11:R56.

Fasanaro P, Greco S, Ivan M, Capogrossi MC, Martelli F (2009) microRNA: Emerging therapeutic targets in acute ischemic diseases. Pharmacol Ther.

Feng YH, Wu CL, Tsao CJ, Chang JG, Lu PJ, Yeh KT, Uen YH, Lee JC, Shiau AL (2011) Deregulated expression of sprouty2 and microRNA-21 in human colon cancer: Correlation with the clinical stage of the disease. Cancer Biol Ther 11:111-121.

Fernandez-Martos CM, Gonzalez-Fernandez C, Gonzalez P, Maqueda A, Arenas E, Rodriguez FJ (2011) Differential expression of Wnts after spinal cord contusion injury in adult rats. PLoS One 6:e27000.

Ferrara G (1596) Nova Selva di Cirugia Divisa in Due Parti. Venice: Bartolomeo Carampello.

Fichtlscherer S, Zeiher AM, Dimmeler S (2011) Circulating microRNAs: biomarkers or mediators of cardiovascular diseases? Arterioscler Thromb Vasc Biol 31:2383-2390.

Filipowicz W, Bhattacharyya SN, Sonenberg N (2008) Mechanisms of post-transcriptional regulation by microRNAs: are the answers in sight? Nat Rev Genet 9:102-114.

Fiore R, Khudayberdiev S, Christensen M, Siegel G, Flavell SW, Kim TK, Greenberg ME, Schratt G (2009) Mef2-mediated transcription of the miR379-410 cluster regulates activity-dependent dendritogenesis by fine-tuning Pumilio2 protein levels. EMBO J 28:697-710.

Fire A, Xu S, Montgomery MK, Kostas SA, Driver SE, Mello CC (1998) Potent and specific genetic interference by double-stranded RNA in Caenorhabditis elegans. Nature 391:806-811.

Forman DS, McQuarrie IG, Labore FW, Wood DK, Stone LS, Braddock CH, Fuchs DA (1980) Time course of the conditioning lesion effect on axonal regeneration. Brain Res 182:180-185.

Franks TM, Lykke-Andersen J (2008) The control of mRNA decapping and P-body formation. Mol Cell 32:605-615.

Garbay B, Heape AM, Sargueil F, Cassagne C (2000) Myelin synthesis in the peripheral nervous system. Prog Neurobiol 61:267-304.

Geuna S, Raimondo S, Ronchi G, Di Scipio F, Tos P, Czaja K, Fornaro M (2009) Chapter 3: Histology of the peripheral nerve and changes occurring during nerve regeneration. Int Rev Neurobiol 87:27-46.

Glass JD (2004) Wallerian degeneration as a window to peripheral neuropathy. J Neurol Sci 220:123-124.

Gordon T, Chan KM, Sulaiman OA, Udina E, Amirjani N, Brushart TM (2009a) Accelerating axon growth to overcome limitations in functional recovery after peripheral nerve injury. Neurosurgery 65:A132-144.

Gordon T, Udina E, Verge VM, de Chaves EI (2009b) Brief electrical stimulation accelerates axon regeneration in the peripheral nervous system and promotes sensory axon regeneration in the central nervous system. Motor Control 13:412-441.

Grimson A, Farh KK, Johnston WK, Garrett-Engele P, Lim LP, Bartel DP (2007) MicroRNA targeting specificity in mammals: determinants beyond seed pairing. Mol Cell 27:91-105.

Hall AC, Lucas FR, Salinas PC (2000) Axonal remodeling and synaptic differentiation in the cerebellum is regulated by WNT-7a signaling. Cell 100:525-535.

Hammond SM, Boettcher S, Caudy AA, Kobayashi R, Hannon GJ (2001) Argonaute2, a link between genetic and biochemical analyses of RNAi. Science 293:1146-1150.

Hanz S, Fainzilber M (2006) Retrograde signaling in injured nerve--the axon reaction revisited. J Neurochem 99:13-19.

Hanz S, Perlson E, Willis D, Zheng JQ, Massarwa R, Huerta JJ, Koltzenburg M, Kohler M, van-Minnen J, Twiss JL, Fainzilber M (2003) Axoplasmic importins enable retrograde injury signaling in lesioned nerve. Neuron 40:1095-1104.

Haramati S, Chapnik E, Sztainberg Y, Eilam R, Zwang R, Gershoni N, McGlinn E, Heiser PW, Wills AM, Wirguin I, Rubin LL, Misawa H, Tabin CJ, Brown R, Jr., Chen A, Hornstein E (2010) miRNA malfunction causes spinal motor neuron disease. Proc Natl Acad Sci U S A 107:13111-13116.

Hebert SS, De Strooper B (2007) Molecular biology. miRNAs in neurodegeneration. Science 317:1179-1180.

Hebert SS, Horre K, Nicolai L, Papadopoulou AS, Mandemakers W, Silahtaroglu AN, Kauppinen S, Delacourte A, De Strooper B (2008) Loss of microRNA cluster miR-29a/b-1 in sporadic Alzheimer's disease correlates with increased BACE1/beta-secretase expression. Proc Natl Acad Sci U S A 105:6415-6420.

Hengst U, Cox LJ, Macosko EZ, Jaffrey SR (2006) Functional and selective RNA interference in developing axons and growth cones. The Journal of neuroscience : the official journal of the Society for Neuroscience 26:5727-5732.

Hoffman PN (2010) A conditioning lesion induces changes in gene expression and axonal transport that enhance regeneration by increasing the intrinsic growth state of axons. Exp Neurol 223:11-18.

Hou ST, Jiang SX, Smith RA (2008) Permissive and repulsive cues and signalling pathways of axonal outgrowth and regeneration. Int Rev Cell Mol Biol 267:125-181.

Huang T, Liu Y, Huang M, Zhao X, Cheng L (2010) Wnt1-cre-mediated conditional loss of Dicer results in malformation of the midbrain and cerebellum and failure of neural crest and dopaminergic differentiation in mice. J Mol Cell Biol 2:152-163.

Huang ZP, Neppl RL, Jr., Wang DZ (2011) Application of microRNA in cardiac and skeletal muscle disease gene therapy. Methods Mol Biol 709:197-210.

Hutchison ER, Okun E, Mattson MP (2009) The therapeutic potential of microRNAs in nervous system damage, degeneration, and repair. Neuromolecular Med 11:153-161.

Hyatt Sachs H, Schreiber RC, Shoemaker SE, Sabe A, Reed E, Zigmond RE (2007) Activating transcription factor 3 induction in sympathetic neurons after axotomy: response to decreased neurotrophin availability. Neuroscience 150:887-897.

Ikeda K, Satoh M, Pauley KM, Fritzler MJ, Reeves WH, Chan EK (2006) Detection of the argonaute protein Ago2 and microRNAs in the RNA induced silencing complex (RISC) using a monoclonal antibody. J Immunol Methods 317:38-44.

Ishizuka A, Siomi MC, Siomi H (2002) A Drosophila fragile X protein interacts with components of RNAi and ribosomal proteins. Genes Dev 16:2497-2508.

Islamov RR, Chintalgattu V, Pak ES, Katwa LC, Murashov AK (2004) Induction of VEGF and its Flt-1 receptor after sciatic nerve crush injury. Neuroreport 15:2117-2121.

Jackson RJ, Hellen CU, Pestova TV (2010) The mechanism of eukaryotic translation initiation and principles of its regulation. Nat Rev Mol Cell Biol 11:113-127.

Junn E, Lee KW, Jeong BS, Chan TW, Im JY, Mouradian MM (2009) Repression of alpha-synuclein expression and toxicity by microRNA-7. Proc Natl Acad Sci U S A 106:13052-13057.

Karanth S, Yang G, Yeh J, Richardson PM (2006) Nature of signals that initiate the immune response during Wallerian degeneration of peripheral nerves. Exp Neurol 202:161-166.

Kawase-Koga Y, Otaegi G, Sun T (2009) Different timings of Dicer deletion affect neurogenesis and gliogenesis in the developing mouse central nervous system. Dev Dyn 238:2800-2812.

Kedersha N, Stoecklin G, Ayodele M, Yacono P, Lykke-Andersen J, Fritzler MJ, Scheuner D, Kaufman RJ, Golan DE, Anderson P (2005) Stress granules and processing bodies are dynamically linked sites of mRNP remodeling. J Cell Biol 169:871-884.

Keenan TW, Winter S, Rackwitz HR, Heid HW (2000) Nuclear coactivator protein p100 is present in endoplasmic reticulum and lipid droplets of milk secreting cells. Biochim Biophys Acta 1523:84-90.

Kim AH, Reimers M, Maher B, Williamson V, McMichael O, McClay JL, van den Oord EJ, Riley BP, Kendler KS, Vladimirov VI (2010) MicroRNA expression profiling in the prefrontal cortex of individuals affected with schizophrenia and bipolar disorders. Schizophr Res 124:183-191.

Kim J, Inoue K, Ishii J, Vanti WB, Voronov SV, Murchison E, Hannon G, Abeliovich A (2007) A MicroRNA feedback circuit in midbrain dopamine neurons. Science 317:1220-1224.

Kiriakidou M, Tan GS, Lamprinaki S, De Planell-Saguer M, Nelson PT, Mourelatos Z (2007) An mRNA m7G cap binding-like motif within human Ago2 represses translation. Cell 129:1141-1151.

Kobayashi T, Lu J, Cobb BS, Rodda SJ, McMahon AP, Schipani E, Merkenschlager M, Kronenberg HM (2008) Dicer-dependent pathways regulate chondrocyte proliferation and differentiation. Proc Natl Acad Sci U S A 105:1949-1954.

Kole AJ, Swahari V, Hammond SM, Deshmukh M (2011) miR-29b is activated during neuronal maturation and targets BH3-only genes to restrict apoptosis. Genes Dev 25:125-130.

Korhonen HM, Meikar O, Yadav RP, Papaioannou MD, Romero Y, Da Ros M, Herrera PL, Toppari J, Nef S, Kotaja N (2011) Dicer is required for haploid male germ cell differentiation in mice. PLoS One 6:e24821.

Koritzinsky M, Magagnin MG, van den Beucken T, Seigneuric R, Savelkouls K, Dostie J, Pyronnet S, Kaufman RJ, Weppler SA, Voncken JW, Lambin P, Koumenis C, Sonenberg N, Wouters BG (2006) Gene expression during acute and prolonged hypoxia is regulated by distinct mechanisms of translational control. Embo J 25:1114-1125.

Koturbash I, Zemp FJ, Pogribny I, Kovalchuk O (2011) Small molecules with big effects: the role of the microRNAome in cancer and carcinogenesis. Mutat Res 722:94-105.

Krarup C, Archibald SJ, Madison RD (2002) Factors that influence peripheral nerve regeneration: an electrophysiological study of the monkey median nerve. Ann Neurol 51:69-81.

Kuo LT, Tsai SY, Groves MJ, An SF, Scaravilli F (2011) Gene expression profile in rat dorsal root ganglion following sciatic nerve injury and systemic neurotrophin-3 administration. J Mol Neurosci 43:503-515.

Kusuda R, Cadetti F, Ravanelli MI, Sousa TA, Zanon S, De Lucca FL, Lucas G (2011) Differential expression of microRNAs in mouse pain models. Mol Pain 7:17.

Kye MJ, Liu T, Levy SF, Xu NL, Groves BB, Bonneau R, Lao K, Kosik KS (2007) Somatodendritic microRNAs identified by laser capture and multiplex RT-PCR. Rna 13:1224-1234.

Lee SK, Hollenbeck PJ (2003) Organization and translation of mRNA in sympathetic axons. J Cell Sci 116:4467-4478.

Lee Y, Ahn C, Han J, Choi H, Kim J, Yim J, Lee J, Provost P, Radmark O, Kim S, Kim VN (2003) The nuclear RNase III Drosha initiates microRNA processing. Nature 425:415-419.

Lee Y, Hur I, Park SY, Kim YK, Suh MR, Kim VN (2006) The role of PACT in the RNA silencing pathway. Embo J 25:522-532.

Lei P, Li Y, Chen X, Yang S, Zhang J (2009) Microarray based analysis of microRNA expression in rat cerebral cortex after traumatic brain injury. Brain research 1284:191-201.

Leung AK, Calabrese JM, Sharp PA (2006) Quantitative analysis of Argonaute protein reveals microRNA-dependent localization to stress granules. Proc Natl Acad Sci U S A 103:18125-18130.

Li C, Nie H, Wang M, Su L, Li J, Yu B, Wei M, Ju J, Yu Y, Yan M, Gu Q, Zhu Z, Liu B (2012) MicroRNA-409-3p regulates cell proliferation and apoptosis by targeting PHF10 in gastric cancer. Cancer Lett.

Li Q, Bian S, Hong J, Kawase-Koga Y, Zhu E, Zheng Y, Yang L, Sun T (2011) Timing specific requirement of microRNA function is essential for embryonic and postnatal hippocampal development. PLoS One 6:e26000.

Liang R, Khanna A, Muthusamy S, Li N, Sarojini H, Kopchick JJ, Masternak MM, Bartke A, Wang E (2011) Post-transcriptional regulation of IGF1R by key microRNAs in long-lived mutant mice. Aging Cell 10:1080-1088.

Lie DC, Colamarino SA, Song HJ, Desire L, Mira H, Consiglio A, Lein ES, Jessberger S, Lansford H, Dearie AR, Gage FH (2005) Wnt signalling regulates adult hippocampal neurogenesis. Nature 437:1370-1375.

Lim LP, Lau NC, Garrett-Engele P, Grimson A, Schelter JM, Castle J, Bartel DP, Linsley PS, Johnson JM (2005) Microarray analysis shows that some microRNAs downregulate large numbers of target mRNAs. Nature 433:769-773.

Liu K, Liu Y, Mo W, Qiu R, Wang X, Wu JY, He R (2011) MiR-124 regulates early neurogenesis in the optic vesicle and forebrain, targeting NeuroD1. Nucleic Acids Res 39:2869-2879.

Liu N-K, Wang X-F, Lu Q-B, Xu X-M (2009) Altered microRNA expression following traumatic spinal cord injury. Experimental Neurology 219:424-429.

Liu R-Y, Schmid R-S, Snider WD, Maness PF (2002) NGF Enhances Sensory Axon Growth Induced by Laminin but Not by the L1 Cell Adhesion Molecule. Molecular and Cellular Neuroscience 20:2-12.

Lucas FR, Salinas PC (1997) WNT-7a induces axonal remodeling and increases synapsin I levels in cerebellar neurons. Dev Biol 192:31-44.

Lugli G, Larson J, Martone ME, Jones Y, Smalheiser NR (2005) Dicer and eIF2c are enriched at postsynaptic densities in adult mouse brain and are modified by neuronal activity in a calpain-dependent manner. J Neurochem 94:896-905.

Lugli G, Torvik VI, Larson J, Smalheiser NR (2008) Expression of microRNAs and their precursors in synaptic fractions of adult mouse forebrain. J Neurochem 106:650-661.

Lykke-Andersen J (2002) Identification of a human decapping complex associated with hUpf proteins in nonsense-mediated decay. Mol Cell Biol 22:8114-8121.

Magill ST, Cambronne XA, Luikart BW, Lioy DT, Leighton BH, Westbrook GL, Mandel G, Goodman RH (2010) microRNA-132 regulates dendritic growth and arborization of newborn neurons in the adult hippocampus. Proc Natl Acad Sci U S A 107:20382-20387.

Makwana M, Raivich G (2005) Molecular mechanisms in successful peripheral regeneration. Febs J 272:2628-2638.

Malkinson G, Spira ME (2010) Clustering of excess growth resources within leading growth cones underlies the recurrent "deposition" of varicosities along developing neurites. Exp Neurol 225:140-153.

Mao B, Wu W, Davidson G, Marhold J, Li M, Mechler BM, Delius H, Hoppe D, Stannek P, Walter C, Glinka A, Niehrs C (2002) Kremen proteins are Dickkopf receptors that regulate Wnt/beta-catenin signalling. Nature 417:664-667.

Martin J, Jenkins RH, Bennagi R, Krupa A, Phillips AO, Bowen T, Fraser DJ (2011) Post-transcriptional regulation of Transforming Growth Factor Beta-1 by microRNA-744. PLoS One 6:e25044.

Martino S, di Girolamo I, Orlacchio A, Datti A (2009) MicroRNA implications across neurodevelopment and neuropathology. J Biomed Biotechnol 2009:654346.

Martins M, Rosa A, Guedes LC, Fonseca BV, Gotovac K, Violante S, Mestre T, Coelho M, Rosa MM, Martin ER, Vance JM, Outeiro TF, Wang L, Borovecki F, Ferreira JJ, Oliveira SA (2011) Convergence of miRNA expression profiling, alpha-synuclein interacton and GWAS in Parkinson's disease. PLoS One 6:e25443.

McCoy CE (2012) The role of miRNAs in cytokine signaling. Front Biosci 17:2161-2171.

McCurley AT, Callard GV (2010) Time Course Analysis of Gene Expression Patterns in Zebrafish Eye During Optic Nerve Regeneration. J Exp Neurosci 2010:17-33.

McMurray R, Islamov R, Murashov AK (2003) Raloxifene analog LY117018 enhances the regeneration of sciatic nerve in ovariectomized female mice. Brain Res 980:140-145.

Meister G, Tuschl T (2004) Mechanisms of gene silencing by double-stranded RNA. Nature 431:343-349.

Miletic G, Hanson EN, Miletic V (2004) Brain-derived neurotrophic factor-elicited or sciatic ligation-associated phosphorylation of cyclic AMP response element binding protein in the rat spinal dorsal horn is reduced by block of tyrosine kinase receptors. Neurosci Lett 361:269-271.

Miller BH, Zeier Z, Xi L, Lanz TA, Deng S, Strathmann J, Willoughby D, Kenny PJ, Elsworth JD, Lawrence MS, Roth RH, Edbauer D, Kleiman RJ, Wahlestedt C (2012) MicroRNA-132 dysregulation in schizophrenia has implications for both neurodevelopment and adult brain function. Proc Natl Acad Sci U S A 109:3125-3130.

Mudhasani R, Puri V, Hoover K, Czech MP, Imbalzano AN, Jones SN (2011) Dicer is required for the formation of white but not brown adipose tissue. J Cell Physiol 226:1399-1406.

Murashov AK, Chintalgattu V, Islamov RR, Lever TE, Pak ES, Sierpinski PL, Katwa LC, Van Scott MR (2007) RNAi pathway is functional in peripheral nerve axons. Faseb J 21:656-670.

Murashov AK, Pak ES, Hendricks WA, Owensby JP, Sierpinski PL, Tatko LM, Fletcher PL (2005) Directed differentiation of embryonic stem cells into dorsal interneurons. FASEB J 19:252-254.

Nagalakshmi VK, Ren Q, Pugh MM, Valerius MT, McMahon AP, Yu J (2011) Dicer regulates the development of nephrogenic and ureteric compartments in the mammalian kidney. Kidney Int 79:317-330.

Nakamura T, Matsumoto K (2008) The functions and possible significance of Kremen as the gatekeeper of Wnt signalling in development and pathology. J Cell Mol Med 12:391-408.

Napoli C, Lemieux C, Jorgensen R (1990) Introduction of a Chimeric Chalcone Synthase Gene into Petunia Results in Reversible Co-Suppression of Homologous Genes in trans. Plant Cell 2:279-289.

Natera-Naranjo O, Aschrafi A, Gioio AE, Kaplan BB (2010) Identification and quantitative analyses of microRNAs located in the distal axons of sympathetic neurons. Rna 16:1516-1529.

Navarro X, Vivo M, Valero-Cabre A (2007) Neural plasticity after peripheral nerve injury and regeneration. Prog Neurobiol 82:163-201.

Ngeow WC (2010) Scar less: a review of methods of scar reduction at sites of peripheral nerve repair. Oral Surg Oral Med Oral Pathol Oral Radiol Endod 109:357-366.

Nix WA, Hopf HC (1983) Electrical stimulation of regenerating nerve and its effect on motor recovery. Brain Res 272:21-25.

Noble J, Munro CA, Prasad VS, Midha R (1998) Analysis of upper and lower extremity peripheral nerve injuries in a population of patients with multiple injuries. J Trauma 45:116-122.

O'Rourke JR, Georges SA, Seay HR, Tapscott SJ, McManus MT, Goldhamer DJ, Swanson MS, Harfe BD (2007) Essential role for Dicer during skeletal muscle development. Dev Biol 311:359-368.

Ofir M, Hacohen D, Ginsberg D (2011) MiR-15 and miR-16 are direct transcriptional targets of E2F1 that limit E2F-induced proliferation by targeting cyclin E. Mol Cancer Res 9:440-447.

Okada M, Nakagawa T, Minami M, Satoh M (2002) Analgesic effects of intrathecal administration of P2Y nucleotide receptor agonists UTP and UDP in normal and neuropathic pain model rats. J Pharmacol Exp Ther 303:66-73.

Olde Loohuis NF, Kos A, Martens GJ, Van Bokhoven H, Nadif Kasri N, Aschrafi A (2012) MicroRNA networks direct neuronal development and plasticity. Cell Mol Life Sci 69:89-102.

Packer AN, Xing Y, Harper SQ, Jones L, Davidson BL (2008) The bifunctional microRNA miR-9/miR-9* regulates REST and CoREST and is downregulated in Huntington's disease. J Neurosci 28:14341-14346.

Park C, Yan W, Ward SM, Hwang SJ, Wu Q, Hatton WJ, Park JK, Sanders KM, Ro S (2011) MicroRNAs dynamically remodel gastrointestinal smooth muscle cells. PLoS One 6:e18628.

Parker R, Sheth U (2007) P bodies and the control of mRNA translation and degradation. Mol Cell 25:635-646.

Pauley KM, Eystathioy T, Jakymiw A, Hamel JC, Fritzler MJ, Chan EK (2006) Formation of GW bodies is a consequence of microRNA genesis. EMBO Rep 7:904-910.

Peng KA, Masliah E (2010) Lentivirus-expressed siRNA vectors against Alzheimer disease. Methods Mol Biol 614:215-224.

Pereira JA, Baumann R, Norrmen C, Somandin C, Miehe M, Jacob C, Luhmann T, Hall-Bozic H, Mantei N, Meijer D, Suter U (2010) Dicer in Schwann Cells Is Required for Myelination and Axonal Integrity. Journal of Neuroscience 30:6763-6775.

Peters L, Meister G (2007) Argonaute proteins: mediators of RNA silencing. Mol Cell 26:611-623.

Pinter R, Hindges R (2010) Perturbations of microRNA function in mouse dicer mutants produce retinal defects and lead to aberrant axon pathfinding at the optic chiasm. Plos One 5:e10021.

Purro SA, Ciani L, Hoyos-Flight M, Stamatakou E, Siomou E, Salinas PC (2008) Wnt regulates axon behavior through changes in microtubule growth directionality: a new role for adenomatous polyposis coli. The Journal of neuroscience : the official journal of the Society for Neuroscience 28:8644-8654.

Raivich G, Makwana M (2007) The making of successful axonal regeneration: genes, molecules and signal transduction pathways. Brain Res Rev 53:287-311.

Rana TM (2007) Illuminating the silence: understanding the structure and function of small RNAs. Nat Rev Mol Cell Biol 8:23-36.

Rao PK, Toyama Y, Chiang HR, Gupta S, Bauer M, Medvid R, Reinhardt F, Liao R, Krieger M, Jaenisch R, Lodish HF, Blelloch R (2009) Loss of cardiac microRNA-mediated regulation leads to dilated cardiomyopathy and heart failure. Circ Res 105:585-594.

Raoul C, Abbas-Terki T, Bensadoun JC, Guillot S, Haase G, Szulc J, Henderson CE, Aebischer P (2005) Lentiviral-mediated silencing of SOD1 through RNA interference retards disease onset and progression in a mouse model of ALS. Nat Med 11:423-428.

Redell JB, Liu Y, Dash PK (2009) Traumatic brain injury alters expression of hippocampal microRNAs: potential regulators of multiple pathophysiological processes. J Neurosci Res 87:1435-1448.

Redshaw N, Wheeler G, Hajihosseini MK, Dalmay T (2009) microRNA-449 is a putative regulator of choroid plexus development and function. Brain Res 1250:20-26.

Ritchie W, Rajasekhar M, Flamant S, Rasko JE (2009) Conserved expression patterns predict microRNA targets. PLoS Comput Biol 5:e1000513.

Sahores M, Gibb A, Salinas PC (2010) Frizzled-5, a receptor for the synaptic organizer Wnt7a, regulates activity-mediated synaptogenesis. Development 137:2215-2225.

Santarelli DM, Beveridge NJ, Tooney PA, Cairns MJ (2011) Upregulation of dicer and microRNA expression in the dorsolateral prefrontal cortex Brodmann area 46 in schizophrenia. Biol Psychiatry 69:180-187.

Sanuki R, Onishi A, Koike C, Muramatsu R, Watanabe S, Muranishi Y, Irie S, Uneo S, Koyasu T, Matsui R, Cherasse Y, Urade Y, Watanabe D, Kondo M, Yamashita T, Furukawa T (2011) miR-124a is required for hippocampal axogenesis and retinal cone survival through Lhx2 suppression. Nat Neurosci 14:1125-1134.

Sasaki T, Shiohama A, Minoshima S, Shimizu N (2003) Identification of eight members of the Argonaute family in the human genome small star, filled. Genomics 82:323-330.

Saugstad JA (2010) MicroRNAs as effectors of brain function with roles in ischemia and injury, neuroprotection, and neurodegeneration. J Cereb Blood Flow Metab 30:1564-1576.

Sayed D, Rane S, Lypowy J, He M, Chen IY, Vashistha H, Yan L, Malhotra A, Vatner D, Abdellatif M (2008) MicroRNA-21 targets Sprouty2 and promotes cellular outgrowths. Mol Biol Cell 19:3272-3282.

Schacher S, Wu F (2002) Synapse formation in the absence of cell bodies requires protein synthesis. J Neurosci 22:1831-1839.

Schaefer A, O'Carroll D, Tan CL, Hillman D, Sugimori M, Llinas R, Greengard P (2007) Cerebellar neurodegeneration in the absence of microRNAs. J Exp Med 204:1553-1558.

Schmidhammer R, Hausner T, Hopf R, Zandieh S, Redl H (2007) In peripheral nerve regeneration environment enriched with activity stimulating factors improves functional recovery. Acta Neurochir Suppl 100:161-167.

Scholzke MN, Schwaninger M (2007) Transcriptional regulation of neurogenesis: potential mechanisms in cerebral ischemia. J Mol Med (Berl) 85:577-588.

Schratt GM, Tuebing F, Nigh EA, Kane CG, Sabatini ME, Kiebler M, Greenberg ME (2006) A brain-specific microRNA regulates dendritic spine development. Nature 439:283-289.

Schuning J, Scherens A, Haussleiter IS, Schwenkreis P, Krumova EK, Richter H, Maier C (2009) Sensory changes and loss of intraepidermal nerve fibers in painful unilateral nerve injury. Clin J Pain 25:683-690.

Sempere LF, Freemantle S, Pitha-Rowe I, Moss E, Dmitrovsky E, Ambros V (2004) Expression profiling of mammalian microRNAs uncovers a subset of brain-expressed microRNAs with possible roles in murine and human neuronal differentiation. Genome Biol 5:R13.

Sen GL, Blau HM (2005) Argonaute 2/RISC resides in sites of mammalian mRNA decay known as cytoplasmic bodies. Nat Cell Biol 7:633-636.

She M, Decker CJ, Svergun DI, Round A, Chen N, Muhlrad D, Parker R, Song H (2008) Structural basis of dcp2 recognition and activation by dcp1. Mol Cell 29:337-349.

Shen H, Yuan Y, Ding F, Liu J, Gu X (2008) The protective effects of Achyranthes bidentata polypeptides against NMDA-induced cell apoptosis in cultured hippocampal neurons through differential modulation of NR2A- and NR2B-containing NMDA receptors. Brain Res Bull 77:274-281.

Sheth U, Parker R (2003) Decapping and decay of messenger RNA occur in cytoplasmic processing bodies. Science 300:805-808.

Shi Y, Zhao X, Hsieh J, Wichterle H, Impey S, Banerjee S, Neveu P, Kosik KS (2010) MicroRNA regulation of neural stem cells and neurogenesis. J Neurosci 30:14931-14936.

Sibley CR, Seow Y, Saayman S, Dijkstra KK, El Andaloussi S, Weinberg MS, Wood MJ (2012) The biogenesis and characterization of mammalian microRNAs of mirtron origin. Nucleic Acids Res 40:438-448.

Siegel G, Obernosterer G, Fiore R, Oehmen M, Bicker S, Christensen M, Khudayberdiev S, Leuschner PF, Busch CJ, Kane C, Hubel K, Dekker F, Hedberg C, Rengarajan B, Drepper C, Waldmann H, Kauppinen S, Greenberg ME, Draguhn A, Rehmsmeier M, Martinez J, Schratt GM (2009) A functional screen implicates microRNA-138-dependent regulation of the depalmitoylation enzyme APT1 in dendritic spine morphogenesis. Nat Cell Biol 11:705-716.

Siomi H, Ishizuka A, Siomi MC (2004) RNA interference: a new mechanism by which FMRP acts in the normal brain? What can Drosophila teach us? Ment Retard Dev Disabil Res Rev 10:68-74.

Skaper SD (2005) Neuronal growth-promoting and inhibitory cues in neuroprotection and neuroregeneration. Ann N Y Acad Sci 1053:376-385.

Smalheiser NR (2008) Synaptic enrichment of microRNAs in adult mouse forebrain is related to structural features of their precursors. Biol Direct 3:44.

Smith B, Treadwell J, Zhang D, Ly D, McKinnell I, Walker PR, Sikorska M (2010) Large-scale expression analysis reveals distinct microRNA profiles at different stages of human neurodevelopment. PLoS One 5:e11109.

Snider WD, Zhou FQ, Zhong J, Markus A (2002) Signaling the pathway to regeneration. Neuron 35:13-16.

Solberg N, Machon O, Krauss S (2008) Effect of canonical Wnt inhibition in the neurogenic cortex, hippocampus, and premigratory dentate gyrus progenitor pool. Dev Dyn 237:1799-1811.

Song G, Wang L (2009) A conserved gene structure and expression regulation of miR-433 and miR-127 in mammals. PLoS One 4:e7829.

Song MG, Li Y, Kiledjian M (2010) Multiple mRNA decapping enzymes in mammalian cells. Mol Cell 40:423-432.

Stefani G, Slack FJ (2008) Small non-coding RNAs in animal development. Nat Rev Mol Cell Biol 9:219-230.

Stoll G, Muller HW (1999) Nerve injury, axonal degeneration and neural regeneration: basic insights. Brain Pathol 9:313-325.

Strickland IT, Richards L, Holmes FE, Wynick D, Uney JB, Wong LF (2011) Axotomy-induced miR-21 promotes axon growth in adult dorsal root ganglion neurons. PLoS One 6:e23423.

Sun WJ, Sun CK, Zhao H, Lin H, Han QQ, Wang JY, Ma H, Chen B, Xiao ZF, Dai JW (2009) Improvement of Sciatic Nerve Regeneration Using Laminin-Binding Human NGF-beta. Plos One 4:-.

Sundstrom JF, Vaculova A, Smertenko AP, Savenkov EI, Golovko A, Minina E, Tiwari BS, Rodriguez-Nieto S, Zamyatnin AA, Jr., Valineva T, Saarikettu J, Frilander MJ, Suarez MF, Zavialov A, Stahl U, Hussey PJ, Silvennoinen O, Sundberg E, Zhivotovsky B, Bozhkov PV (2009) Tudor staphylococcal nuclease is an evolutionarily conserved component of the programmed cell death degradome. Nat Cell Biol 11:1347-1354.

Takimoto K, Wakiyama M, Yokoyama S (2009) Mammalian GW182 contains multiple Argonaute-binding sites and functions in microRNA-mediated translational repression. Rna 15:1078-1089.

Talebizadeh Z, Butler MG, Theodoro MF (2008) Feasibility and relevance of examining lymphoblastoid cell lines to study role of microRNAs in autism. Autism Res 1:240-250.

Tan Y, Zhang B, Wu T, Skogerbo G, Zhu X, Guo X, He S, Chen R (2009) Transcriptional inhibiton of Hoxd4 expression by miRNA-10a in human breast cancer cells. BMC Mol Biol 10:12.

Tanaka T, Sugaya S, Kita K, Arai M, Kanda T, Fujii K, Imazeki F, Sugita K, Yokosuka O, Suzuki N (2012) Inhibition of cell viability by human IFN-beta is mediated by microRNA-431. Int J Oncol 40:1470-1476.

Teixeira D, Sheth U, Valencia-Sanchez MA, Brengues M, Parker R (2005) Processing bodies require RNA for assembly and contain nontranslating mRNAs. Rna 11:371-382.

Tijsen AJ, Creemers EE, Moerland PD, de Windt LJ, van der Wal AC, Kok WE, Pinto YM (2010) MiR423-5p as a circulating biomarker for heart failure. Circ Res 106:1035-1039.

Tsujino H, Kondo E, Fukuoka T, Dai Y, Tokunaga A, Miki K, Yonenobu K, Ochi T, Noguchi K (2000) Activating transcription factor 3 (ATF3) induction by axotomy in sensory and motoneurons: A novel neuronal marker of nerve injury. Mol Cell Neurosci 15:170-182.

van Meeteren NL, Brakkee JH, Hamers FP, Helders PJ, Gispen WH (1997) Exercise training improves functional recovery and motor nerve conduction velocity after sciatic nerve crush lesion in the rat. Arch Phys Med Rehabil 78:70-77.

Verma P, Chierzi S, Codd AM, Campbell DS, Meyer RL, Holt CE, Fawcett JW (2005) Axonal protein synthesis and degradation are necessary for efficient growth cone regeneration. The Journal of neuroscience : the official journal of the Society for Neuroscience 25:331-342.

Verrier JD, Semple-Rowland S, Madorsky I, Papin JE, Notterpek L (2010) Reduction of Dicer impairs Schwann cell differentiation and myelination. J Neurosci Res 88:2558-2568.

Visvanathan J, Lee S, Lee B, Lee JW, Lee SK (2007) The microRNA miR-124 antagonizes the anti-neural REST/SCP1 pathway during embryonic CNS development. Genes Dev 21:744-749.

Vogelaar CF, Gervasi NM, Gumy LF, Story DJ, Raha-Chowdhury R, Leung KM, Holt CE, Fawcett JW (2009) Axonal mRNAs: characterisation and role in the growth and regeneration of dorsal root ganglion axons and growth cones. Mol Cell Neurosci 42:102-115.

Vogelaar CF, Vrinten DH, Hoekman MF, Brakkee JH, Burbach JP, Hamers FP (2004) Sciatic nerve regeneration in mice and rats: recovery of sensory innervation is followed by a slowly retreating neuropathic pain-like syndrome. Brain Res 1027:67-72.

von Schack D, Agostino MJ, Murray BS, Li Y, Reddy PS, Chen J, Choe SE, Strassle BW, Li C, Bates B, Zhang L, Hu H, Kotnis S, Bingham B, Liu W, Whiteside GT, Samad TA, Kennedy JD, Ajit SK (2011) Dynamic changes in the microRNA expression profile reveal multiple regulatory mechanisms in the spinal nerve ligation model of neuropathic pain. PLoS One 6:e17670.

Waetzig V, Herdegen T (2005) MEKK1 controls neurite regrowth after experimental injury by balancing ERK1/2 and JNK2 signaling. Mol Cell Neurosci 30:67-78.

Wang G, van der Walt JM, Mayhew G, Li YJ, Zuchner S, Scott WK, Martin ER, Vance JM (2008a) Variation in the miRNA-433 binding site of FGF20 confers risk for Parkinson disease by overexpression of alpha-synuclein. Am J Hum Genet 82:283-289.

Wang K, Zhang Y, Li X, Chen L, Wang H, Wu J, Zheng J, Wu D (2008b) Characterization of the Kremen-binding site on Dkk1 and elucidation of the role of Kremen in Dkk-mediated Wnt antagonism. J Biol Chem 283:23371-23375.

Wang T, Li M, Guan J, Li P, Wang H, Guo Y, Shuai S, Li X (2011) MicroRNAs miR-27a and miR-143 Regulate Porcine Adipocyte Lipid Metabolism. Int J Mol Sci 12:7950-7959.

Wang WX, Rajeev BW, Stromberg AJ, Ren N, Tang G, Huang Q, Rigoutsos I, Nelson PT (2008c) The expression of microRNA miR-107 decreases early in Alzheimer's disease and may accelerate disease progression through regulation of beta-site amyloid precursor protein-cleaving enzyme 1. J Neurosci 28:1213-1223.

Wang Y, Thekdi N, Smallwood PM, Macke JP, Nathans J (2002a) Frizzled-3 is required for the development of major fiber tracts in the rostral CNS. The Journal of neuroscience : the official journal of the Society for Neuroscience 22:8563-8573.

Wang Y, Zhang J, Mori S, Nathans J (2006) Axonal growth and guidance defects in Frizzled3 knock-out mice: a comparison of diffusion tensor magnetic resonance imaging, neurofilament staining, and genetically directed cell labeling. The Journal of neuroscience : the official journal of the Society for Neuroscience 26:355-364.

Wang Z, Jiao X, Carr-Schmid A, Kiledjian M (2002b) The hDcp2 protein is a mammalian mRNA decapping enzyme. Proc Natl Acad Sci U S A 99:12663-12668.

Wayman GA, Impey S, Marks D, Saneyoshi T, Grant WF, Derkach V, Soderling TR (2006) Activity-dependent dendritic arborization mediated by CaM-kinase I activation and enhanced CREB-dependent transcription of Wnt-2. Neuron 50:897-909.

Wexler EM, Paucer A, Kornblum HI, Palmer TD, Geschwind DH (2009) Endogenous Wnt signaling maintains neural progenitor cell potency. Stem Cells 27:1130-1141.

Wheeler G, Ntounia-Fousara S, Granda B, Rathjen T, Dalmay T (2006) Identification of new central nervous system specific mouse microRNAs. FEBS Lett 580:2195-2200.

Williams AH, Valdez G, Moresi V, Qi X, McAnally J, Elliott JL, Bassel-Duby R, Sanes JR, Olson EN (2009) MicroRNA-206 delays ALS progression and promotes regeneration of neuromuscular synapses in mice. Science 326:1549-1554.

Willis DE, Twiss JL (2006) The evolving roles of axonally synthesized proteins in regeneration. Curr Opin Neurobiol 16:111-118.

Witzel C, Rohde C, Brushart TM (2005) Pathway sampling by regenerating peripheral axons. J Comp Neurol 485:183-190.

Wu D, Raafat A, Pak E, Clemens S, Murashov AK (2012) Dicer-microRNA pathway is critical for peripheral nerve regeneration and functional recovery in vivo and regenerative axonogenesis in vitro. Exp Neurol 233:555-565.

Wu D, Raafat M, Pak E, Hammond S, Murashov AK (2011a) MicroRNA machinery responds to peripheral nerve lesion in an injury-regulated pattern. Neuroscience 190:386-397.

Wu L, Zhou H, Lin H, Qi J, Zhu C, Gao Z, Wang H (2011b) Circulating microRNAs are elevated in plasma from severe pre-eclamptic pregnancies. Reproduction.

Xia H, Mao Q, Paulson HL, Davidson BL (2002) siRNA-mediated gene silencing in vitro and in vivo. Nat Biotechnol 20:1006-1010.

Xiao GR, Hao H, Zhao QL, Yan HY, Shan QH (2007) [Observation on therapeutic effect of electroacupuncture combined with functional training for treatment of peripheral nerve incomplete injury of upper limbs]. Zhongguo Zhen Jiu 27:329-332.

Yamazaki T, Sabit H, Oya T, Ishii Y, Hamashima T, Tokunaga A, Ishizawa S, Jie S, Kurashige Y, Matsushima T, Furuta I, Noguchi M, Sasahara M (2009) Activation of MAP kinases, Akt and PDGF receptors in injured peripheral nerves. J Peripher Nerv Syst 14:165-176.

Yang C, Cai J, Wang Q, Tang H, Cao J, Wu L, Wang Z (2012) Epigenetic silencing of miR-130b in ovarian cancer promotes the development of multidrug resistance by targeting colony-stimulating factor 1. Gynecol Oncol 124:325-334.

Yang JS, Lai EC (2010) Dicer-independent, Ago2-mediated microRNA biogenesis in vertebrates. Cell Cycle 9:4455-4460.

Yang WH, Yu JH, Gulick T, Bloch KD, Bloch DB (2006) RNA-associated protein 55 (RAP55) localizes to mRNA processing bodies and stress granules. RNA 12:547-554.

Yi R, O'Carroll D, Pasolli HA, Zhang Z, Dietrich FS, Tarakhovsky A, Fuchs E (2006) Morphogenesis in skin is governed by discrete sets of differentially expressed microRNAs. Nat Genet 38:356-362.

Yi YH, Sun XS, Qin JM, Zhao QH, Liao WP, Long YS (2010) Experimental identification of microRNA targets on the 3' untranslated region of human FMR1 gene. J Neurosci Methods 190:34-38.

Yoo S, van Niekerk EA, Merianda TT, Twiss JL (2009) Dynamics of axonal mRNA transport and implications for peripheral nerve regeneration. Exp Neurol.

Yu B, Zhou S, Qian T, Wang Y, Ding F, Gu X (2011a) Altered microRNA expression following sciatic nerve resection in dorsal root ganglia of rats. Acta Biochim Biophys Sin (Shanghai) 43:909-915.

Yu B, Zhou S, Wang Y, Ding G, Ding F, Gu X (2011b) Profile of microRNAs following rat sciatic nerve injury by deep sequencing: implication for mechanisms of nerve regeneration. PLoS One 6:e24612.

Yu YM, Gibbs KM, Davila J, Campbell N, Sung S, Todorova TI, Otsuka S, Sabaawy HE, Hart RP, Schachner M (2011c) MicroRNA miR-133b is essential for functional recovery after spinal cord injury in adult zebrafish. Eur J Neurosci 33:1587-1597.

Yun B, Anderegg A, Menichella D, Wrabetz L, Feltri ML, Awatramani R (2010) MicroRNA-deficient Schwann cells display congenital hypomyelination. J Neurosci 30:7722-7728.

Zehir A, Hua LL, Maska EL, Morikawa Y, Cserjesi P (2010) Dicer is required for survival of differentiating neural crest cells. Dev Biol 340:459-467.

Zhang HY, Zheng SJ, Zhao JH, Zhao W, Zheng LF, Zhao D, Li JM, Zhang XF, Chen ZB, Yi XN (2011) MicroRNAs 144, 145, and 214 are down-regulated in primary neurons responding to sciatic nerve transection. Brain Res 1383:62-70.

Zhao J, Lee MC, Momin A, Cendan CM, Shepherd ST, Baker MD, Asante C, Bee L, Bethry A, Perkins JR, Nassar MA, Abrahamsen B, Dickenson A, Cobb BS, Merkenschlager M, Wood JN (2010) Small RNAs control sodium channel expression, nociceptor excitability, and pain thresholds. J Neurosci 30:10860-10871.

Zhou S, Yu B, Qian T, Yao D, Wang Y, Ding F, Gu X (2011) Early changes of microRNAs expression in the dorsal root ganglia following rat sciatic nerve transection. Neurosci Lett 494:89-93.

Zigmond RE (2011) gp130 cytokines are positive signals triggering changes in gene expression and axon outgrowth in peripheral neurons following injury. Front Mol Neurosci 4:62.

APPENDIX A: Animal Care and Use Committee Protocol Approval

East Carolina University

1907-2007 CENTENNIAL

Animal Care and Use Committee
212 Ed Warren Life Sciences Building
East Carolina University
Greenville, NC 27834

252-744-2436 office
252-744-2355 fax

February 16, 2010

Alex Murashov, M.D., Ph.D.
Department of Physiology
Brody 6N-98
ECU Brody School of Medicine

Dear Dr. Murashov:

Your Animal Use Protocol entitled, "The Significance of MicroRNA Pathway in Peripheral Nerve Regeneration Following Sciatic Nerve Injury," (AUP #Q286) was reviewed by this institution's Animal Care and Use Committee on 2/16/10. The following action was taken by the Committee:

"Approved as submitted"

Please contact Dale Aycock at 744-2997 prior to biohazard use

A copy is enclosed for your laboratory files. Please be reminded that all animal procedures must be conducted as described in the approved Animal Use Protocol. Modifications of these procedures cannot be performed without prior approval of the ACUC. The Animal Welfare Act and Public Health Service Guidelines require the ACUC to suspend activities not in accordance with approved procedures and report such activities to the responsible University Official (Vice Chancellor for Health Sciences or Vice Chancellor for Academic Affairs) and appropriate federal Agencies.

Sincerely yours,

Robert G. Carroll, Ph.D.

Robert G. Carroll, Ph.D.
Chairman, Animal Care and Use Committee

RGC/jd

enclosure